LOW-TEMPERATURE HOMOGENEOUS OXIDATION OF ALKANES USING HYDROGEN PEROXIDE

By

MICHAEL A. GONZALEZ

A DISSERTATION PRESENTED TO THE GRADUATE SCHOOL
OF THE UNIVERSITY OF FLORIDA IN PARTIAL FULFILLMENT
OF THE REQUIREMENTS FOR THE DEGREE OF
DOCTOR OF PHILOSOPHY

UNIVERSITY OF FLORIDA

1998

To my dear wife, Stacy Michelle, for all your support and belief in me. You complete me.

ACKNOWLEDGMENTS

No one has ever said life way easy, but it has been said that it can be extremely rewarding. My decision to attend college and graduate school has made my life very fulfilling, and I have only lived less than one-third of it. Although college and graduate school has been filled with late night study sessions, overnighters at the lab and numerous classes (as well as migraines), I would do it all again if given the opportunity.

My undergraduate freshman year at the University of Texas El Paso (UTEP) was a time of indecisiveness and uncertainty about my future career aspirations. In my sophomore year all these worries had changed for the better, this was the result of receiving a scholarship and being given the opportunity to conduct undergraduate research in the area of inorganic structural and polymeric chemistry. For this I would like to thank Dr. Phillip Goodell, Dr. L.W. ter Haar and the Research Careers for Minority Students (RCMS) committee for the opportunity to allow me to demonstrate my academic and research wares. My adventures at UTEP would not have been possible without the aid of Tony "Hubcap" Sanchez, Manuel "Manny" Garbalena, Anthony "Skate" Guarnero, Joseph "Little Joe" Janisheck and Gerardo "Ardo" Fuentes. To my friends I say thanks for the memories and the friendship; you will never be forgotten.

From Texas my quest for higher learning landed me in sunny Florida, where graduate life began at the University of Florida. I chose to work for Dr. Russell "Doc" Drago, the second best decision I have made in my life. Doc is the reason I remain in chemistry; he is the most intelligent person I know, and his fervor for chemistry is undaunting. I can only hope to achieve this level in my chemistry career. "Doc, thank you for all your patience and instilling a portion of your scientific knowledge in me." I would also like to offer thanks to Ruth Drago, she has made my four-year stay memorable. I would like to thank her and Doc for taking Stacy, Mikey and me into their "scientific" as well as personal family and making us feel like family. This, in turn, made our transition to Florida effortless.

My graduate school life was also made memorable by the friendships I formed with members of the Drago group, both past and present. To the past members, Mike "Bevis" Robbins, Todd "I can fix it" Lafrenz, Phil Kaufman, Garth "Ogre" Dahlen, Chris Chronister, Don Ferris "Bueller" and Mike Naughton, I offer my thanks for showing me how to survive in graduate school on both an academic and personal level. The current Drago group members, especially the oxidation sub-group, are the greatest. Ken "Kato" Lo, has been a great friend and always listened to me, plus I will never forget our Friday lunches. Alfredo "Alf" Mateus was a great help with understanding heterogeneous oxidation chemistry. Without Ben "Hubcap" Gordon I would not have completed the last three months of research. Cheng "Tiger" Xu helped me understand the iron-oxo system. I also want to thank Steve "Jorg" Joerg for bailing me out of trouble, answering my philosophical and ethical questions, and running my NMR's. I would also like to thank Krystoff Jurzyk and Nick "Corn on the" Kob for insight on high temperature

heterogeneous chemistry. I would also like to say thanks to Maribel and Diane for their help in office matters.

The biggest thanks go to Stacy, my best decision, for standing by me, believing in me and giving me the best things in life a person could ask for: love and a child. I thank her for putting up with me on late nights of writing research summaries, being at the lab and tutoring. This dissertation is as much hers as it is mine.

I thank my parents for their love and support. Dad always told me to set high goals and never settle for second best. And mother was always there when I needed an ear, and for this I say thanks.

No one knows what the future holds, but with my wife, family and friends, I know I can approach it and control my own destiny.

TABLE OF CONTENTS

page

LIST OF TABLES

LIST OF FIGURES

Abstract of Dissertation Presented to the Graduate School
of the University of Florida in Partial Fulfillment of the
Requirements for the Degree of Doctor of Philosophy

LOW-TEMPERATURE HOMOGENEOUS OXIDATION OF ALKANES USING HYDROGEN PEROXIDE

By

Michael A. Gonzalez

May 1998

Chairman: Dr. Russell S. Drago
Major Department: Chemistry

The activation of saturated hydrocarbons by metal complexes in the liquid phase became an active research area towards the end of the 1960. Stringent conditions such as the use of powerful oxidants, corrosive superacids, elevated pressures and high temperatures are used for the selective oxidation of low molecular weight paraffins. As products from these oxidations gain increased industrial importance, environmentally friendly and cost-efficient catalysts and processes are sought.

Natural gas reserves, which are approximately 90% methane, are abundant and a source of a valuable feedstock. The direct oxidation of methane to methanol provides the first step towards a route to an alternative large-scale transportation fuel replacing dwindling petroleum reserves. For this reason, the development of a direct one-step process for the oxidation of methane to methanol becomes of interest. Also of

importance is the ability to synthesize valuable organic compounds selectively (alcohols, aldehydes, ketones and carboxylic acids) from higher alkane feed stocks.

Previous reports from this laboratory have demonstrated the use of the *cis*-$[Ru(dmp)_2(H_2O)_2](PF_6)_2$ precursor, where dmp is 2,9-dimethyl-1,10-phenanthroline, for the activation of methane in acetonitrile. The nitrogen-based dmp ligand not only increases the electrophillicity of the metal center, but also imparts a steric hindrance about the metal, forcing a *cis* geometry, allowing the catalyst to be a more potent oxidant. Using the properties from this complex, a number of derivatives have been successfully synthesized and characterized.

The synthesis and characterization of each newly synthesized catalyst: *cis*-$[Ru(dmp)_2(H_2O)_2](CF_3SO_3)_2$, *cis*-$[Fe(dmp)_2(H_2O)_2](CF_3SO_3)_2$ and $[Fe(dmp)Cl_2]$, as well as the ability of each to hydroxylate C_2-C_5 alkanes in acetonitrile and methane in a glacial acetic acid/acetic anhydride solvent mixture at 75°C and 40 psi are presented. Also investigated is the ability to modify and increase the selectivity to the alcohol product upon addition of a metal chloride, and the effect of temperature on each catalyst precursor. Preliminary mechanistic data suggesting a pathway for methane and higher alkane oxidation are also presented.

CHAPTER 1
GENERAL INTRODUCTION TO ACTIVATION OF ALKANES

Importance of Homogeneous Catalysis

The end of the 1960s confronted the field of homogeneous catalysis with a potential problem. This obstacle was the inability for a soluble transition-metal complex to effectively activate a saturated hydrocarbon in the liquid phase.[1] As large resources of natural gas were discovered, the need for improvements to the current homogeneous catalytic systems became apparent, as well as the demand for alternative catalysts.

One solution to this issue was the development of new classes of metal complexes, which were capable of undergoing an oxidative addition across the C-H bond of a paraffin (Equation 1-1). The application of this catalyst would allow for alkanes to be utilized as feedstocks in a number of industrial chemical reactions. This oxidative addition process produces the desired oxidized products in selectivity ratios, which are more favorable than those achieved using typical free radical reagents.[2,3,4]

(Equation 1-1) $M + R\text{-}H \longrightarrow R\text{-}M\text{-}H$

As advances in coordination chemistry and catalysis were developed, reports of activating hydrogen, olefins, aromatics, carbon monoxide, and molecular nitrogen with soluble transition-metal complexes became commonplace.[1] The term activation is used

to imply "the molecule or its part becoming a ligand in the coordination sphere of the complex and, as a result, undergoing a subsequent chemical transformation"(p. 2).[1]

The primary deterrent one is confronted with in the activation of alkanes is the chemical inertness these molecules possess. Alkanes are benign, to the point they can be safely used as a non-interacting solvent. Therefore, any such activation of an alkane would require notably stringent conditions. These conditions typically require active particles, which include strong oxidants, superacids, free atoms, radicals, carbenes, high temperatures (500-1000°C) and other sources of energy (i.e. radiation chemistry). As environmental and monetary constraints become more significant, a more desirable oxidation technology needed to be sought.[2,3,4]

Interest in the activation of methane, a primary component in natural gas, also heightened prompting the development of a new catalyst that was able to impart selectivity in its oxidized product under relatively mild conditions. The typically inert methane molecule, along with its alkane counterparts, required designing a catalyst that was able to effectively activate these substrates which did not contain double or triple bonds or lone electron pairs and possessing relatively strong covalent C-H and C-C σ–bonds.[1]

Shilov[1] had presented evidence for the activation of alkanes; he expressed that if other more selective reactions of alkanes under "comparatively mild conditions" exist, there is an inherent ability to oxidize the alkanes in question. The statements that follow provide a basis for his proclamation:

- Numerous examples of homogeneous H_2 activation are reported.[2] One example is the H-D exchange for hydrogenation. Yet, the σ bond in molecular hydrogen is not weaker than the σ C-H bond in alkanes.
- Many metal complexes (ML_n or M) are capable of reacting with substrates containing "activated" C-H bonds.[2] One example is the C-H bond in aromatics or in the α-position to double bonds. As the C-H bond is broken, formation of a M-C bond results. However, the C-H bond energy which is greater in aromatics than alkanes does not hinder the reaction.
- Also demonstrated is the involvement of a "nonactivated" aliphatic C-H bond within the coordination sphere. This occurs when a suitable position on the ligand of the complex becomes available.[2] This results in a process defined as "cyclometallation" and provides evidence for the possibility of a reaction occurring with alkanes, possibly at elevated temperatures.
- Hydroxylation of C-H bonds in saturated hydrocarbons catalyzed by metal enzymes is known.[2] One published example is the oxidation of methane to methanol (primarily) by methane monooxygenase.

General Classification of Homogeneous Oxidation Reactions

This research is directed towards developing a series of homogeneous catalysts able to activate saturated hydrocarbons, olefins and aromatics with mild oxidants. In order to do so, an understanding of the fundamental chemical reactions must be understood. These liquid phase (homogeneous) transition metal catalyzed oxidations can be categorized into three areas.[5] These categories include the following:

1. Free Radical Autoxidation

The Mid-Century/Amoco process for the conversion of *p*-xylene to terepthalic acid is one example of this category. This reaction is exhibited in Equation 1-2.

(Equation 1-2)

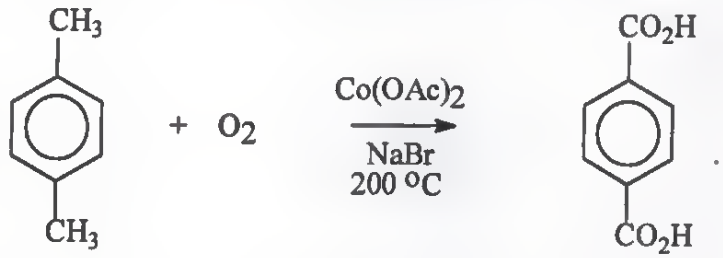

In this process air (20psi) is utilized as the oxidant, with a bromide-promoted cobalt salt as the catalyst in an acetic acid solvent. The primary oxidation step, i.e. *p*-xylene to *p*-toluic acid, occurs quite readily in the presence of a small amount of the cobalt salt. The secondary oxidation step, formation of the di-acid, necessitates the presence of higher concentrations of the catalyst and/or addition of the bromide promoter.[2]

Oxidations of alkyl aromatics involving a cobalt (III) catalyst appear to proceed almost exclusively via an electron transfer mechanism.[1] The reaction of the alkyl aromatic with Co(III) results in formation of $[ArCH_3]^{+\bullet}$ and a Co(III) radical. Loss of a proton results in producing $ArCH_2\bullet$ and $H^{+}\bullet$. In the presence of air or oxygen, a peroxy species is formed producing $ArCH_2O_2\bullet$, which then reacts to produce the normal oxidation products. The Co(II)• catalyst can be regenerated either by reacting with O_2, combined with $ArCH_2O_2\bullet$, or by reacting with the hydroperoxy species, $ArCH_2O_2H$, to produce ArCHO, Co(III) and OH•.[2]

The corresponding aromatic acids are produced by subsequent aldehyde oxidation via a peroxy acid intermediate. The addition of the bromide allows for formation of bromine atoms (Br•) via electron transfer oxidation of bromide by Co(III). The bromine atom has been demonstrated to be extremely efficient at hydrogen atom abstraction, which can allow for rapid formation of the benzyl radical, thus initiating the autoxidation sequence.[1]

2. Nucleophillic Attack on Coordinated Substrates

An example of this classification is the Wacker Process for oxidizing ethylene to vinyl acetate. This reaction is provided in Equation 1-3.

(Equation 1-3) $H_2C{=}CH_2 + \frac{1}{2}\, O_2 + HOAc \longrightarrow H_2C{=}CHOAc + H_2O$

$PdCl_2$ and $CuCl_2$ are two catalysts necessary for the above reaction to proceed in an acetic acid (CH_3COOH) solvent. The initial stage of the oxidation involves the π-coordination of the ethene substrate with concurrent or subsequent loss of chloride to form a sixteen-valence electron palladium (II) anion, which in turn undergoes a ligand replacement reaction to yield the neutral palladium (II) aquo species. Coordination of ethene to the palladium (II) metal center results in a decrease in the double bond electron density, allowing it to become more susceptible to nucleophillic attack by either OH^- or H_2O_2.[2]

The palladium metal is re-oxidized to palladium chloride by the co-catalyst, either $CuCl_2$ or $FeCl_3$, as described above. In this case, the co-catalyst, $CuCl_2$ is the reduction

product of CuCl that is readily oxidized with either air or oxygen. Therefore, this catalyst combination gives rise to a catalytic system which allows for air or oxygen oxidation of ethene to ethanal.[2]

3. Metal-Catalyzed Oxygen Atom Transfer Reactions from Coordinated Hydroperoxides or Metal-Oxo Species to Organic Substrates

The reaction of propylene with alkylhydroperoxides to yield propylene oxide falls within this category. This reaction is illustrated in Equation 1-4.

(Equation 1-4)

This process involves the reaction of a homogeneous metal catalyst, molybdenum, with an organic hydroperoxide and an alkene. As a result this reaction produces an epoxide product in a relatively high yield. This oxidation process proceeds with the hydroperoxide becoming "activated by coordination" to the metal center. As a result, the peroxide's oxygen experiences a decrease in electron density, rendering it susceptible to nucleophillic attack by the alkene. Additional metal catalysts for this reaction are those belonging to the second row, positioned early in the series and possessing high attainable oxidation states. Metals with these characteristics include Mo(VI), W(VI) and Ti(VI).[2]

Transfer of the oxygen from the metal hydroperoxide complex to the alkene is suggested to occur via a cyclic transition state, as detailed in Equation 1-5.

(Equation 1-5) 

The success of the Mo(VI), W(VI) and Ti(VI) catalysts for this type of oxidation reaction is attributed to their being weak oxidants with poor one electron redox potentials: ~0.21, -0.03 and -0.37eV respectively. Therefore, they are poor catalysts for homolytic hydroperoxide decomposition, as exhibited in Equation 1-6, which is detrimental to the desired epoxidation reaction.[1]

(Equation 1-6) $[M^{n+}RO_2H] \longrightarrow M^{(n-1)+} + RO_2\bullet + H^+\bullet$

It is important to emphasize that only the autoxidation, category number 1, utilizes the direct reaction of molecular oxygen with the organic substrate.[6]

Homogeneous catalysis is now a relatively mature field with a number of diverse reactions being investigated for informative studies as well as mechanism and theoretical analysis. Along with the growth in this field, a relationship to other important areas has been firmly established. These areas include heterogeneous catalysis, organometallic chemistry and bio-catalysis.

Homogeneous catalysis is a resource, which is virtually untapped, and its importance cannot be overestimated. In the age of industry becoming oriented towards specialty chemicals, methods to catalyze functional group transformation, hydrocarbon

activation, polymerization and asymmetrical catalysis, the need and importance for effective homogeneous catalytic systems will continue to grow.

The activation of C-H bonds in alkanes by transition metal complexes, not long ago thought to be the most difficult challenges facing chemists, is now almost commonplace. Many, examples, often under remarkably mild conditions, have appeared.[1,3,7] Problems arise in the transformation of these fundamentals into the practical alkane conversion process. These reasons include thermodynamics, a reaction being uphill at ambient conditions, catalyst stability, and catalyst incompatibility with O_2 to activate alkanes. Other problems include the issue of selectivity. Regioselectivity is an obvious problem, one such case is if terminal alcohols are preferred over their isomeric products. More important, the products (alcohols and aldehydes) tend to be considerably more reactive than the starting alkane. This then places a limit on the achievable yield of the desired hydroxylated product.

General Classification of Alkane Activation Reactions

Three categories of remarkably facile alkane activation can be described: oxidative addition (Equation 1-7), σ-bond metathesis (Equation 1-8) and electrophillic substitution (Equation 1-9).[1,3,7]

(Equation 1-7) $L_nM + R\text{-}H \longrightarrow L_nM(H)(R)$

(Equation 1-8) $L_nM\text{-}X + R\text{-}H \longrightarrow LnM\text{-}R + H\text{-}X$

(Equation 1-9) $L_nM^{y+} + R\text{-}H \longrightarrow L_nM\text{-}R^{(y-1)+} + H^+$

The first in this classification of reactions, oxidative addition reactions, has been found to occur in low valent electron rich, coordinatively unsaturated metal centers towards the right end of the transition metal series (Groups VI-X).[3]

Sigma-bond metathesis reactions, the second classification, are observed for complexes containing Group III transition metals (including lanthanides and actinides), as well as metals belonging to Group IV. Also exhibited in this category are examples of intramolecular reactions with metals belonging to Group V. These reactions lead to stable organometallic products; however, very limited examples of alkane functionalization have been achieved. Each of the active species involved is highly sensitive to O_2 and the oxygenated products that are produced.[3]

Finally, electrophillic substitution reactions have been observed with the "traditional" or "classic" coordination complexes. An example of a such complex is $PtCl_x(H_2O)_{4-x}^{(x-2)-}$.[8,9] In the duration of the mechanistic process, a stable organometallic species is not obtained, but net functionalization of the alkane is achieved. This category of catalysis appears attractive in that the species involved will utilize dioxygen. This property allows in principle for the closing of the catalytic cycle.

Examples of Alkane Activation by Homogeneous Catalysts

Many examples of homogeneous catalytic reactions are published in literature, although this number is too large to provide one example for each area of activation. Two important examples are exhibited to provide a general idea of the catalytic chemistry being performed on the industrial and laboratory scale with homogeneous catalysts.

The hydroformylation or Oxo reaction discovered in 1938 by Roelen is utilized on a large industrial scale.[10,11,12] This process employs a homogeneous catalyst based on cobalt[10,11,12] or rhodium.[13] Most commonly the $HCo(CO)_4$ pre-catalyst is employed, the product generated by the *in-situ* hydrogenation of $CO_2(CO)_8$.

In 1961, Heck and Breslow[14] proposed the mechanism for the cobalt-based Hydroformylation process, as illustrated in Figure 1-1. Five elementary processes comprise the complete mechanism.

The first step involves the dissociation of the carbonyl ligand from $HCo(CO)_4$ to produce the catalytically active species tricarbonylhydridocobalt, $[HCo(CO)_3]$. This is followed by the combination of the active catalyst with the olefin to generate a π–olefin complex. The migratory insertion of the olefin into the Co-H bond is the third step, proceed by the alkyl undergoing a migratory insertion into the Co-CO bond. In the final step an H_2 induced aldehyde elimination occurs, producing the desired oxidized product and regeneration of the active catalyst.

Another cobalt based catalytic system is the reductive carbonylation of methanol (Equation 1-10). This example illustrates how cobalt-based catalysts have dominated this area of industrial chemistry for the past fifty years.[15-22] Alternative metals are capable of catalyzing the identical reaction; however, these are generally inferior to those of the cobalt-based systems.

(Equation 1-10) $CH_3OH + CO + H_2 \longrightarrow CH_3CHO + H_2O$

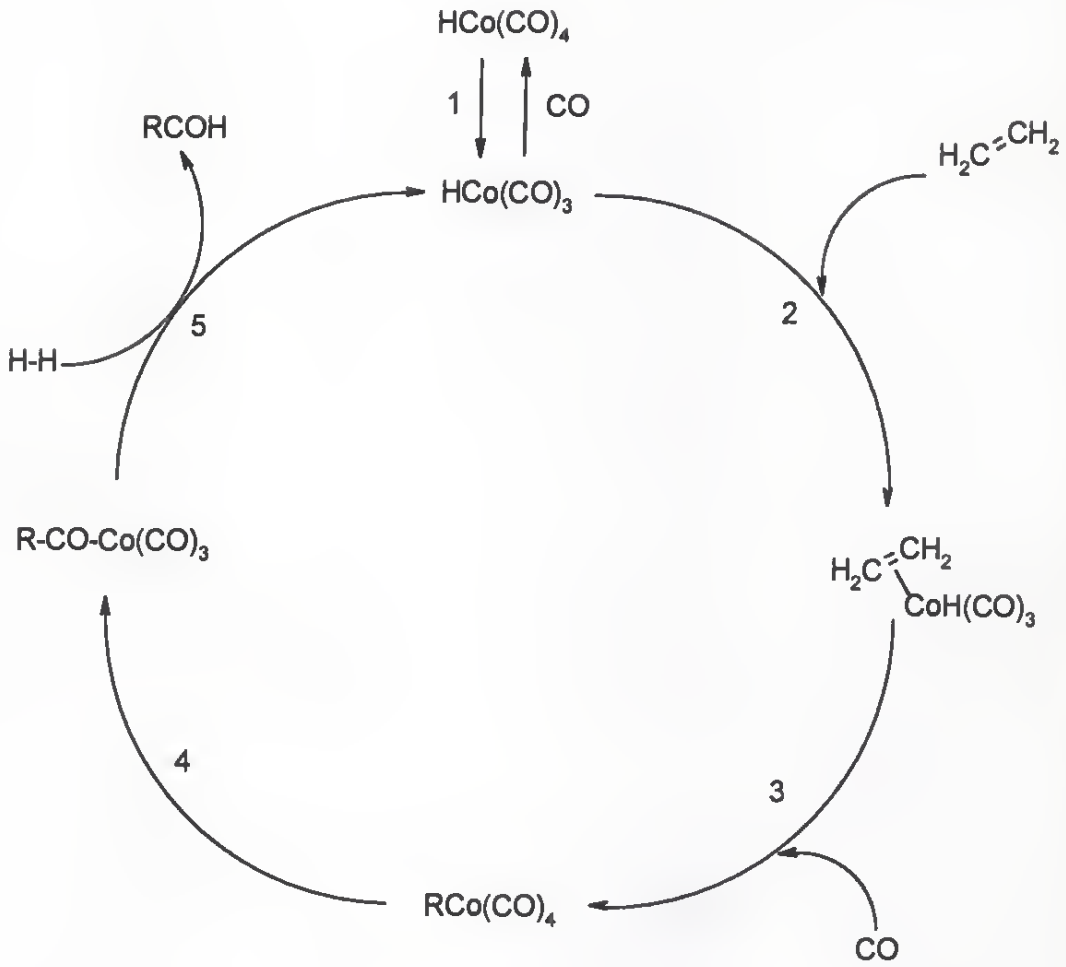

Figure 1-1: Catalytic Cycle for the Hydroformylation Reaction

Improvements to the cobalt-based catalyst have been achieved through the use of co-catalysts and promoters. Such promoters employed include iodide, phosphines and transition metals.[18] Iodide, by far the most important of this group, is almost always utilized as a promoter. Despite advances in catalyst performance, high pressure and temperatures are required. Conditions for these catalysts are typically operated at pressures of 4000-8000 psi and temperatures of 175-200°C. The increased pressures required can pose obvious difficulties for reactor design and operation, as well as for safety considerations. The elevated temperatures required can lead to the formation of heavy by-products via the Aldol condensation reaction of acetaldehyde.[19,20]

It is shown both rhodium and cobalt are capable of catalyzing a variety of carbonylation reactions.[23,24] Rhodium catalysts have been demonstrated to be significantly more active than their cobalt counterparts and allow reactions to proceed at much lower extremes of temperature and pressure. However, iodide is necessary as a promoter. In the presence of this promoter and CO, rhodium is an extremely proficient catalyst for the carbonylation of methanol to acetic acid. This process is known as the Monsanto Acetic Acid Process.[25-28]

Designing a Homogeneous Catalyst

The focal point of our research is directed towards designing and developing a catalyst able to undergo chemistry involving a transition-metal catalyzed oxygen atom transfer from a metal-oxo complexes or species. The activation of alkanes, primarily methane, utilizing this newly developed metal-oxo complex is our primary goal. The development of this catalyst can be hindered due to the following conditions:

1. The role of the transition metal complex for activation of molecular oxygen can be complicated by numerous competing reaction pathways which are present.
2. In order to selectively oxidize a variety of substrates, a number of different conditions may be required.
3. The lack of any obvious pattern or role portrayed by the metal, as well as lack of a detailed reaction mechanism.

A catalyst can either be homogeneous or heterogeneous in nature. A homogeneous catalyst was selected on the basis of its advantages in a reaction mixture and underlying chemistry. The advantages and disadvantages of utilizing a homogeneous catalyst are listed in Table 1-1 and Table 1-2 respectively.

Five Classes of Metal-Oxo Reactions

Oxidation pathways have been exhibited to occur in a number of general reaction pathways. Drago[29] has formulated five classes of metal-oxo reactions, which are based on the role of the transition metal complex. In order to effectively categorize these reactions, the mechanism for substrate oxidation was omitted. The five classes are listed below and each reaction mechanism summarized. An example of each reaction class is also provided.

Class I: Metal Bound O_2

(Equation 1-11) $M + O_2 \longrightarrow M\text{-}O\text{-}O$

(Equation 1-12) $M\text{-}O\text{-}O + RH \longrightarrow M\text{-}O\text{-}O\text{-}H + R\cdot$

Table 1-1: Advantages of Homogeneous Catalysts

Advantage	Description
Homogeneity	Uniform active structure
Efficiency	Theoretically all the atoms or molecules of the catalyst are available for reactants
Reproducibility	A result of well-controlled active sites
High Selectivity	Often more specific than a heterogeneous catalyst even for asymmetric induction
Mild Reaction Conditions	High activity often achieved under mild conditions
Controllability	If chemical information is readily available, modification allowing the control of electronic and steric properties of the metal center can be attained.
Reaction Mechanism	Investigation of the molecular reaction can be performed.

Table 1-2: Disadvantages of a Homogeneous Catalyst

Advantage	Description
Separation	The separating of an expensive catalyst from the reaction mixture poses a problem and can be costly, and may also require special treatment, which usually destroys the catalyst.
Solubility	The range of solvents suitable for a homogeneous catalyst is often limited by the solubility of the catalyst; a compatible solvent is not necessarily the most suitable for a high reaction rate.

(Equation 1-13) $M\text{-}O\text{-}O\text{-}H + R\cdot \longrightarrow M + ROOH$

(Equation 1-14) $ROOH \longrightarrow ROH \text{ or } R{=}O$

Molecular oxygen is coordinated to the metal (Equation 1-11) to increase its basicity and radical reactivity. The substrate then undergoes hydrogen atom abstraction by the metal-peroxo species to generate a metal hydroperoxo species and an alkyl radical (Equation 1-12). The metal hydroperoxo species and the alkyl radical then undergo recombination (Equation 1-13) to generate an alkylhydroperoxide species and the reduced metal species. The final step (Equation 1-14) involves decomposition of the alkylhydroperoxide to yield the corresponding alcohol and ketone. Cobalt (II) coordination compounds that reversibly bind dioxygen are examples of this group.

Class II: Metal-Oxo via O_2

(Equation 1-15) $M + O_2 \longrightarrow M\text{-}O\text{-}O$

(Equation 1-16) $M\text{-}O\text{-}O + M \longrightarrow M\text{-}O\text{-}O\text{-}M$

(Equation 1-17) $M^{n+}\text{-}O\text{-}O\text{-}M^{n+} \longrightarrow 2\, M^{n+2}(O)$

(Equation 1-18) $M{=}O + S \longrightarrow SO + M$

Once again the metal coordinates dioxygen (Equation 1-15); however, in this series another metal enters the coordination sphere and forms a μ-peroxo dimer (Equation 1-16). This μ-peroxo dimer then undergoes cleavage to form two high-valent metal-oxo complexes (Equation 1-17). The metal-oxo complex is then able to undergo oxygen atom

transfer or another similar type reaction (Equation 1-18), thus regenerating the lower oxidation-state of the metal and producing the oxidized species of the substrate. Metal oxidation states normally involved in this cycle are two to four, three to five or four to six. One system to be discussed, *cis*-$[Ru(dmp)_2(H_2O)_2]^{2+}$, is an example of this category.

Class III: Metal-Oxo via Peroxides

(Equation 1-19) $M^{n+} + H_2O_2 \longrightarrow M^{n+2}(O) + H_2O$

(Equation 1-20) $M^{n+2}(O) + S \longrightarrow SO + M^{n+}$

This class of reactions takes advantage of the more powerful oxidizing ability of hydrogen peroxide to oxidize lower-valent metal complexes to metal-oxo complexes. The low-valent metal complex is oxidized with hydrogen peroxide (Equation 1-19) to a higher valency producing a metal-oxo complex and a benign by-product, water. The metal-oxo species is then able to undergo oxygen atom transfer or a similar reaction (Equation 1-20), thus regenerating the lower oxidation-state of the metal and producing the oxidized species of the substrate. A candidate for this class is a monooxygenase enzyme, which involve metal-oxo oxidants.

Class IV: Metal-Peroxo Systems

IVa- Metal Catalyzed Peroxide Decomposition

(Equation 1-21) $M^{n+} + H_2O_2 \longrightarrow M^{n+1} + OH^- + OH\cdot$

(Equation 1-22) $M^{n} + H_2O_2 \longrightarrow M^{n+} + H^+ + HO_2\cdot$

IVb: Metal-Peroxo Formation

(Equation 1-23) $M{=}O + H_2O_2 \longrightarrow MO_2 + H_2O$

(Equation 1-24) $MO_2 + S \longrightarrow SO + M{=}O$

Metal peroxo complexes are the reactive intermediates for this group. Several reactions with substrates yield further divisions of this class. In class IVa, the metal complex reacts with hydrogen peroxide to generate radical species, which are the result of peroxide decomposition (Equations 1-23 and 1-24). An example of this class is Haber-Weiss and Fenton Chemistry. The radial species, the active oxidant, are then able to oxidize the substrate. Class IVb is the result of the bound metal peroxo or alkylperoxo complex attacking the substrate. The metal peroxo is generated by the reaction of a metal-oxo species with hydrogen peroxide. The alkylhydroperoxo species is generated in the same fashion as illustrated in Equation 1-22. Asymmetric epoxidation of alkenes with alkylperoxides are examples of this class of chemistry.

Class V: Metal Centered Oxidizing Agents

- Metal center is active electron acceptor in the oxidation.
- Often involves coordination of substrate to metal center, "activation".
- The Wacker process, Equation 1-3, is an example of this class.
- The reduced complex is re-oxidized by O_2 or peroxide.

The approach taken in this research is to develop a catalyst that possesses properties pertaining to either Class II or III. The developed catalyst could also possess a mechanism of regeneration with dioxygen to generate a high-valent metal-oxo complex, as in Class V, necessary for alkane oxidation. This catalyst must be able to perform the key step, that being the generation of a strongly oxidizing high-valent metal center.[30]

The desired reaction pathway, illustrated in Figure 1-2, exhibits the need for a metal center, which can be activated by hydrogen peroxide or molecular oxygen to form the mono-oxo species. This activated complex may be a powerful enough oxidant to activate the substrate or be further oxidized by hydrogen peroxide or dioxygen to generate a di-oxo species, a complex with greater oxidizing strength than the mono-oxo species. Upon delivery of its one or two oxygen atoms, the reduced metal center could be re-oxidized by hydrogen peroxide or oxygen to regenerate the mono or di-oxo species, thereby closing the catalytic cycle

Homolytic or Heterolytic Pathway?

There are two pathways, which exist for a metal center to be activated by dioxygen or hydrogen peroxide. These pathways are known as homolytic and heterolytic oxidation. The former[31] normally involves the following transition metal couples: V^{V}/V^{IV}, Cr^{VI}/Cr^{V}, Mn^{III}/Mn^{II}, Fe^{III}/Fe^{II}, Co^{III}/Co^{II} and Cu^{II}/Cu^{I}. Characteristics of this reaction include the production of a free radical intermediate, oxidation occurring in the outer-sphere via bimolecular steps, non-coordination of the substrate. Oxidation products are generally not very selective or stereospecific, and the metal center undergoes a one-electron oxidation and reduction step. Examples of relevant oxidations employing this

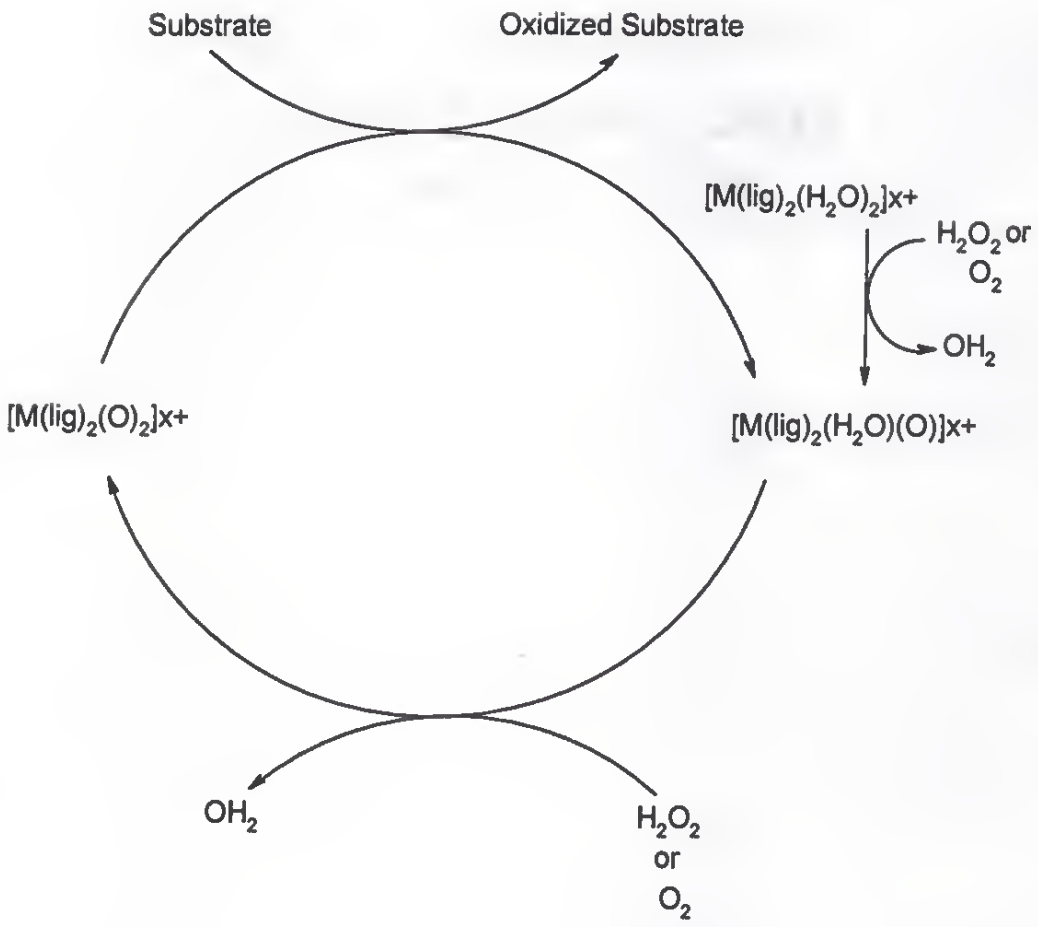

Figure 1-2: Desired Reaction Pathway for Substrate Oxidation

oxidation pathway include the non-stereoselective epoxidation of olefins occurring with transition metal complexes of vanadium, manganese and iron and the hydroxylation of alkanes and arenes occurring with the transition metal complexes of vanadium, chromium, manganese, iron, cobalt and copper.

The latter, heterolytic oxidations,[31] involves the following transition metals: Ti^{V}, V^{V}, Cr^{VI}, Mo^{VI}, Mo^{IV}, Mn^{VII}. Ru^{VII}, Os^{VI-VII}, Rh^{III}/Rh^{I}, Ir^{III}/Ir^{I}, Pd^{II}/Pd^{O}, Pt^{II}/Pt^{O}. Characteristics of this reaction pathway include the inability to produce a free radical intermediate, the reaction occurring in the coordination sphere of the metal, substrate coordination resulting in activation, high selectivity and stereospecificity of the oxidized products and no net change in the oxidation state of the metal. However if a change in the oxidation state occurs, it is via a two electron step, i.e. M^{2+} to M^{4+}. Examples of heterolytic oxidations include the stereoselective epoxidation of olefins with transition metal complexes of titanium, vanadium and tungsten and the ketonization of olefins with transition metal complexes of rhenium, iridium, palladium and platinum. Mimoun[30] has also categorized a reaction coordinate pathway involving metal-oxygen species, which is illustrated in Figure 1-3.

Effect of Ligand on Metal Center

Numerous and thorough studies for polypyridyl ligands with ruthenium metal centers by Drago[31], Meyer[32], Takeuchi[33] and Che[34] have been performed. These studies have revealed certain features that make these complexes capable of catalyzing oxidations of hydrocarbons with molecular oxygen. These complexes display a series of reversible

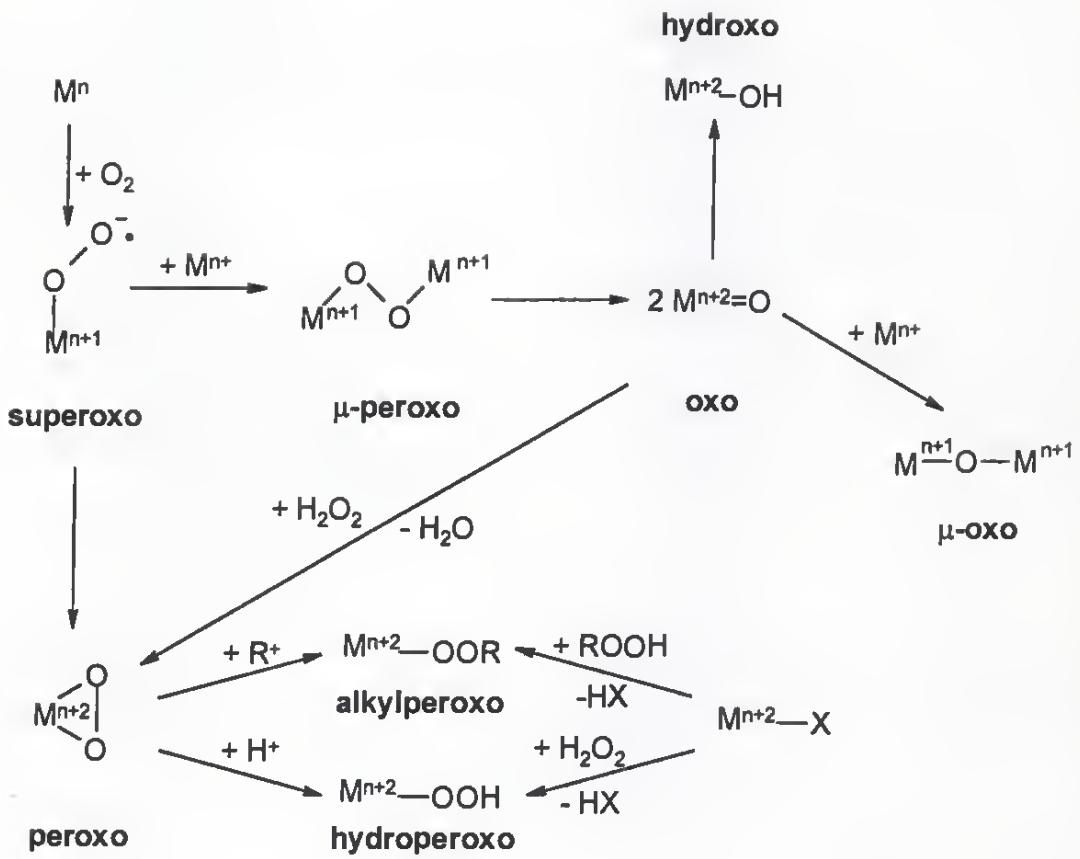

Figure 1-3: Detailed Reaction Pathways of Metal-Oxygen Species

and accessible oxidation states (i.e. from 2^+ to 6^+) to reduce dioxygen completely.

The poylpyridyl ligand provides the stability for the metal center to achieve higher oxidation states and impart stability to the complex. It also forms stable ruthenium oxo-species, $\{Ru(O)\}^{2+}$ and $\{Ru(O)_2\}^{2+}$, which are known to be excellent metal oxygen atom-transfer reagents towards a variety of substrates. The activation of methane and other saturated alkanes is the field where the majority of our interest lies.

H_2O_2 as an Oxidant

The need for an inexpensive, environmentally friendly and benign by-product oxidant is of top concern. Many oxidants are available which include dioxygen, hydrogen peroxide, alkyl hydroperoxides, peracids, sodium sulfate, oxone, nitric acid, dichromate, bromine, manganate and Caro's acid (H_2SO_5). However, the last five are costly, and involve expensive disposal problems. Nitric acid also produces noxious NO_x compounds as by-products.

Peroxygen reagents have been utilized in chemical synthesis for a number of years.[35] As the public, chemical producers, and governmental agencies direct their efforts towards "greener" pathways, the interest in the use of peroxygen oxidants has increased. A reagent, hydrogen peroxide (H_2O_2), can offer environmental and economic benefits.

Hydrogen peroxide is available for chemical synthesis as an aqueous solution in concentrations ranging from 35% to 90% by weight. Stabilizers are normally present in the part per million levels to prevent decomposition. With no additional additives being present, a minimization in unwanted side reactions is an additional advantage.

Hydrogen peroxide can also be stabilized for extended periods of times under a variety of conditions. As an aqueous solution, hydrogen peroxide will lose less than one percent of its active oxygen content per year, when stored in compatible containers at ambient temperatures. This stability allows hydrogen peroxide to be a more efficient oxidant than dichromate or permanganate on a weight for weight basis.

Reactions involving hydrogen peroxide are traditionally performed under mild conditions of temperature and pressure, preventing an increase in peroxide decomposition. By performing under these conditions the need for a large capital investment is eliminated as well as a decrease in safety concerns. Reactions, which use hydrogen peroxide as an oxidant, can also proceed in either an aqueous, organic or neat solvent. This allows for reaction and reactor design to be engineered allowing one to avoid the use of solvents, thus eliminating costly start-up expenses and production of waste streams.[36]

The major benefit of using hydrogen peroxide is its environmental acceptability. When the oxidizing power of the peroxide is spent, only water remains as the by-product, eliminating the need for expensive effluent disposal and treatment. Hydrogen peroxide is also relatively inexpensive as a reagent, when compared on the basis of oxidizing power and by-product production. Although chlorine and oxygen oxidants are less expensive, since these are gases, phase separation concerns are raised as well as the inability to achieve selectivity towards oxidation products.

Hydrogen peroxide can be utilized in a variety of methods: direct activation, catalytic activation and activation via peroxides. All require the use of hydrogen peroxide to be activated to an even more potent oxidant. Figure 1-4 summarizes methods

for activating hydrogen peroxide. Our use of hydrogen peroxide falls under the area of catalytic activation. Hydrogen peroxide is activated with a metal complex by forming a metal-oxo or metal-peroxo species.[36]

The Einchem Corporation has demonstrated the feasibility of using hydrogen peroxide as an oxidant on a commercial scale. Einchem has developed a heterogeneous titanium silicate zeolite catalyst, commercial tradename of TS-1.[37] This catalyst, totally heterogeneous in nature, has a wide synthetic use for hydrogen peroxide oxidations. Einchem has commercialized this catalyst for the hydroxylation of phenol to hydroquinone and catechol.

The catalysts used in this research will employ hydrogen peroxide and dioxygen. Hydrogen peroxide was chosen as the primary oxidant for hydrocarbons because of its ease of handling and oxidizing strength. Dioxygen is the desired oxidant but hydrogen peroxide can be used safely with hydrocarbons, while dioxygen requires one to remain within the explosion limits.

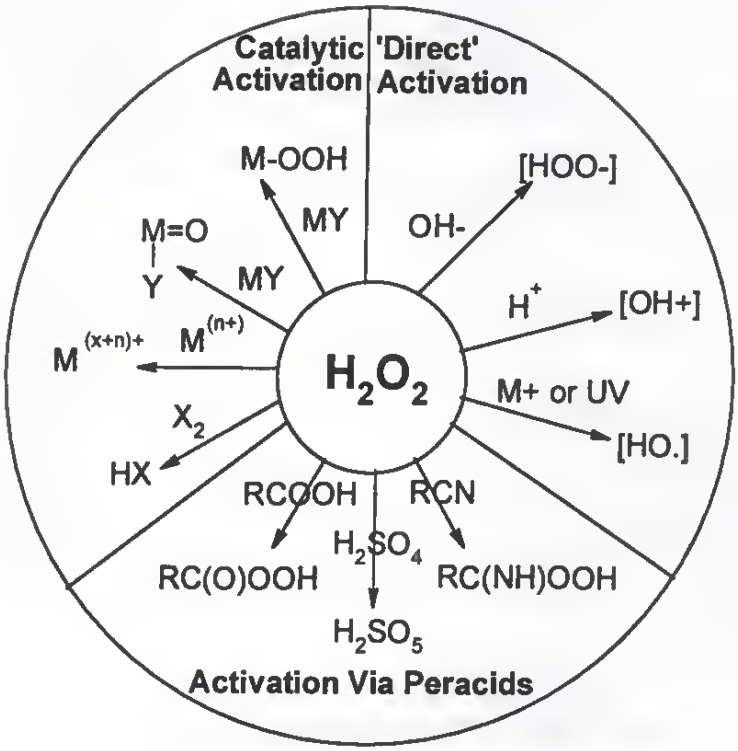

Figure 1-4: Methods for Activating Hydrogen Peroxide

CHAPTER 2
HOMOGENEOUS CATALYZED PARTIAL OXIDATION OF METHANE WITH HYDROGEN PEROXIDE AND OXYGEN

Introduction

Cis-ruthenium oxo complexes were previously reported to be effective catalysts to activate hydrogen peroxide and molecular oxygen for the selective oxidation of alkenes[38] and alkanes.[39,40] The sterically hindered complex *cis*-$[Ru(dmp)_2(H_2O)_2](PF_6)_2$ (**II**), where dmp is 2,9-dimethyl-1,10-phenanthroline (Figure 2-1), is a precursor that can be oxidized with hydrogen peroxide to form *cis*-$[Ru(dmp)_2(O)(H_2O)](PF_6)_2$ or *cis*-$[Ru(dmp)_2(O)_2](PF_6)_2$ as shown in Equations 2-1 and 2-2.

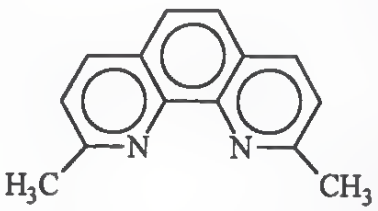

Figure 2-1: Structure for 2,9-dimethyl-1,10-phenanthroline

Unsuccessful attempts to isolate these oxo complexes led to their characterization based

(Equation 2-1) *cis*-$[Ru^{II}(dmp)_2(S)_2](PF_6)_2$ ⟶ *cis*-$[Ru^{IV}(dmp)_2(S)(O)](PF_6)_2$

(Equation 2-2) *cis*-$[Ru^{IV}(dmp)_2(S)(O)](PF_6)_2$ ⟶ *cis*-$[Ru^{VI}(dmp)_2(O)_2](PF_6)_2$

on isobestic points in the electronic spectra and changes in solution NMR as hydrogen peroxide is added to **II**. The electronic spectra of the oxidized complex are similar to those of analogous ruthenium-oxo complexes.[41] *Cis*-$\{Ru(O)_2\}^{2+}$ complexes isomerize to the *trans*-complexes which are weaker oxidants than the cis analogues.[41,42,43,44,45] The novel aspect of the dmp ligand is its steric requirement which prevents isomerization of the *cis*-$[Ru(O)_2]^{2+}$ complex and inhibits formation of both tris complexes and stable μ-oxo dinuclear species. The intra-ligand repulsions and neutral ligand charge also make the high oxidation state ruthenium center electropositive.[41]

Preliminary results describe the use of this complex to catalyze the oxidation of alkanes using H_2O_2 as the oxidant.[40] Figure 2-2 summarizes the proposed[46] catalytic cycle for alkane oxidation via *cis*-$[Ru(dmp)_2(O)_2]^{2+}$. The *cis*-$[Ru(II)(dmp)_2(H_2O)_2]^{2+}$ precursor is oxidized rapidly by H_2O_2 to form the (III),(IV) and (VI) oxidation state complexes. In alkane oxidations, *cis*-$[Ru(III)(dmp)_2(H_2O)(OH)]^{2+}$ reacts with dioxygen to produce the *cis*-$[Ru(IV)(dmp)_2(H_2O)(O)]^{2+}$ but *cis*-$[Ru(II)(dmp)_2(H_2O)_2]^{2+}$ is reported to be unreactive with molecular oxygen.[46] When appreciable concentrations of Ru(IV) exist, the Ru(II) complex reacts with it to form *cis*-$[Ru(III)(dmp)_2(H_2O)(OH)]^{2+}$. For kinetic reasons, alkane oxidations require the electrophillic *cis*-$[Ru(VI)(dmp)_2(O)_2]^{2+}$

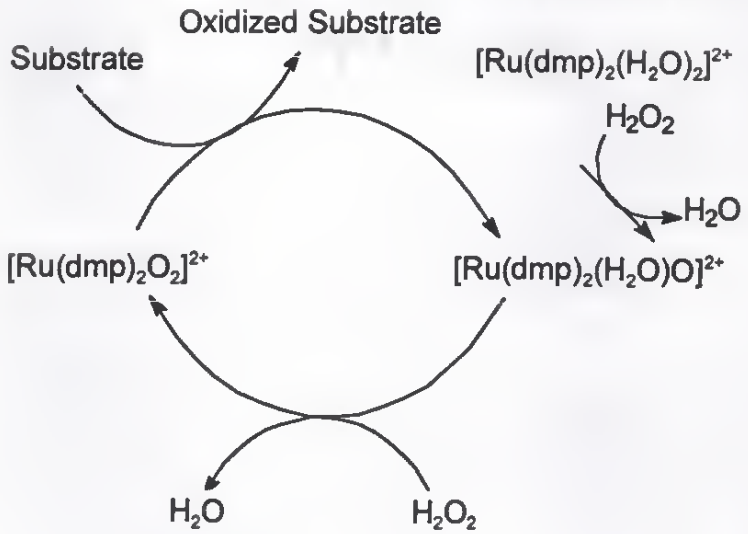

Figure 2-2: Proposed Catalytic Cycle for Alkane Oxidation via *cis*-$[Ru(dmp)_2(O)_2]^{2+}$

complex. The *cis*-$[Ru(IV)(dmp)_2(H_2O)(O)_2]^{2+}$ formed after oxygen atom transfer must be oxidized back to the Ru(VI) complex with hydrogen peroxide[40] to make the system catalytic in CH_3CN solvent. Figure 2-3 illustrates the catalytic cycle of the ruthenium analogue.

Methane was selected as the substrate for study because the oxidation of natural gas into a liquid product is of great industrial and economic importance.[47] Figure 2-4 depicts the worldwide distribution of natural gas resources. Currently, methanol is produced from methane by the steam reforming of methane into synthesis gas, followed by the catalytic conversion of the syn gas into methanol. In order to increase efficiency, the direct partial oxidation of methane to methanol is the desired pathway.[48] However, hydrogen atom abstraction, commonly involved in methane oxidation, occurs more rapidly with methanol than methane resulting in the over-oxidation of methanol to CO_2.

This research extends earlier reports of the use of *cis*-$[Ru(VI)(dmp)_2(O)_2]^{2+}$ as a catalyst for methane oxidation. Greatly improved conversions to oxygenates result by trapping methanol and slowing its over-oxidation. Also demonstrated is an improved catalyst precursor, evidence for oxidation of methane by O_2 with this catalyst, and demonstrate oxidation of methane by peracids.

Experimental

Materials and Methods

$RuCl_3 \cdot x\ H_2O$, 2,9-dimethyl-1,10-phenanthroline, LiCl, $NaPF_6$, 60% HPF_6, NH_4PF_6, $NaCF_3SO_3$, were all used as received from Aldrich. Ethylene glycol, acetonitrile, glacial acetic acid, acetic anhydride, 4Å molecular sieves and hydrogen

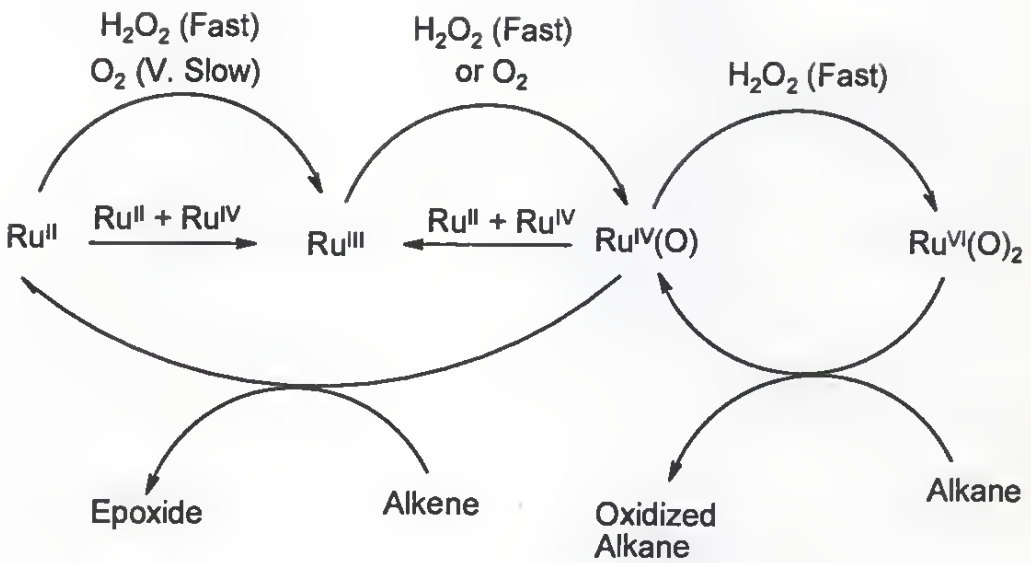

Figure 2-3: Detailed Catalytic Cycle for Ruthenium Analogue

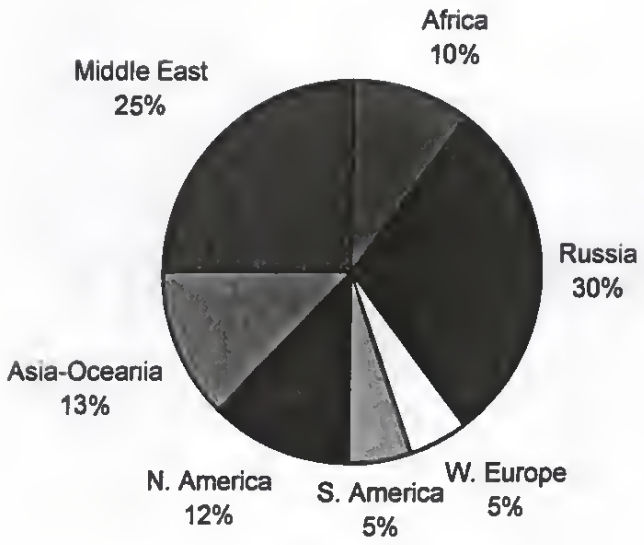

Figure 2-4: Distribution of Worldwide Natural Gas Resources

peroxide (30%) were all used as received from Fisher Scientific (ACS grade). Acetonitrile was distilled over P_2O_5 under dinitrogen and was stored over 4Å activated molecular sieves. Methane (99.99%) was purchased from Matheson and used as received.

Physical Measurements

UV-Vis measurements employed a Perkin Elmer lambda-6 spectrophotometer. The pH measurements were made with a Fisher Accumet model 630 pH meter. NMR spectra were recorded on a Varian VXR300 spectrometer. FAB mass spectral data were obtained by Dr. David Powell (U.F.) in a *m*-nitrobenzyl alcohol matrix. U.F. Analytical Services performed elemental analyses.

Synthesis of Compounds

***Cis*-Ruthenium(II) Bis(chloride)bis(2,9-dimethyl-1,10-phenanthroline) Monohydrate, $[Ru(dmp)_2Cl_2] \cdot H_2O$ (I).** *Cis*-$[Ru(dmp)_2Cl_2] \cdot H_2O$ was synthesized as reported.[40] Analysis: Calculated for $C_{28}H_{26}N_4OCl_2Ru$; C, 55.45; H, 4.29; N, 9.24. Found: C, 55.65; H, 4.35; N, 9.29.

***Cis*-Ruthenium(II) Bis(aquo)bis(2,9-dimethyl-1,10-phenanthroline) bis(hexafluorophosphate), *Cis*-$[Ru(dmp)_2(H_2O)_2](PF_6)_2$ (II).** A 1.0 g (1.7 mmol) portion of I was dissolved in 150 ml of deionized H_2O, under N_2 by heating 50°C for 30 minutes. After adding 50 ml of a saturated $NaPF_6$ (aq), the solution is cooled, placed in an ice bath for two hours, and filtered. The precipitate is redissolved in H_2O by heating to 50°C; a saturated $NaPF_6$ (aq) solution is added and reprecipitated as above. Re-crystallization and exchange of Cl^- for PF_6^- is repeated until the filtrate affords a negative

chloride test with $AgNO_3$. The product is dried in vacuum at 60°C overnight. Analysis: Calculated for $C_{28}H_{28}N_4O_2P_2F_{12}Ru$: C, 39.85; H, 3.32; N, 6.64. Found: C, 39.46; H 3.29; N, 6.72.

For comparison purposes *cis*-$[Ru(dmp)_2(H_2O)_2](PF_6)_2$ was also synthesized using the previously reported procedure.[40] Analysis: Calculated for $C_{28}H_{28}N_4O_2P_2F_{12}Ru$: C, 39.85; H, 3.32; N, 6.64. Found: C, 39.57; H 3.27; N, 6.63.

***Cis*-Ruthenium(II) Bis(aquo)bis(2,9-dimethyl-1,10-phenanthroline) bis(trifluoromethanesulfonate), *Cis*-$[Ru(dmp)_2(H_2O)_2](CF_3SO_3)_2$ (III).** A 1.0g (1.7 mmol) portion of I is slowly dissolved in H_2O as above. Following the addition of 50 ml of a saturated aqueous solution of $NaCF_3SO_3$, the resulting solution is cooled, and placed in an ice bath to complete precipitation. The product is collected, the filtrate tested for chloride, and recrystallized with $CF_3SO_3^-$ until the filtrate gives a negative chloride test. The resulting solid is dried under vacuum at 60°C overnight. Analysis: Calculated for $C_{30}H_{34}N_4O_8S_2F_6Ru$, C, 42.25; H, 3.31; N, 6.57. Found: C, 41.40, H, 3.26; N 6.39.

Oxidation Procedure

The pressurized oxidations were carried out as previously described[49], in glass, batch hydrogenation reactors. Figure 2-5 provides an illustration of such batch reactor. The reaction mixtures were varied as described in the table footnotes. Blank runs omitting certain reactants and solvent components are also described in the tables. Oxidations with oxygen use 30 psig of a 5% O_2 in helium mixture, to remain outside the explosion limits, and 20 psig methane. Reaction temperatures normally were maintained

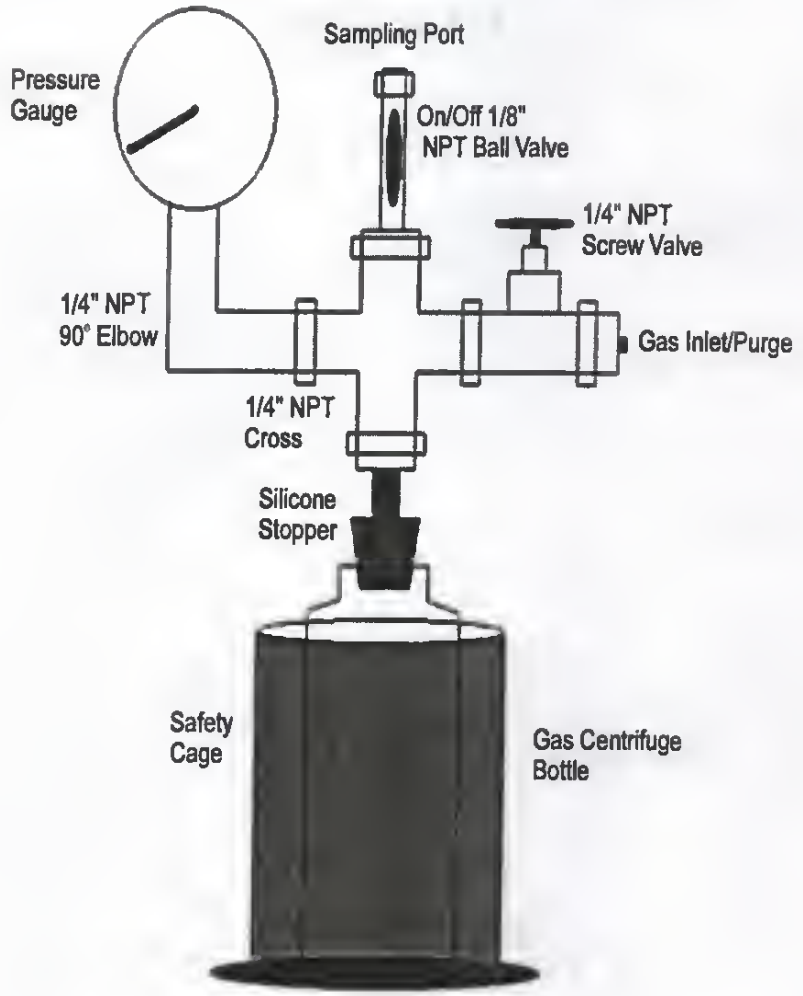

Figure 2-5: Diagram of Batch Type Hydrogenation Reactor

between 75 to 77°C. To remove air initially present, nitrogen gas is purged through the reactor, the apparatus is pressurized with the substrate, which is then released, and re-pressurized to the desired pressure.

The oxygenated products of the reaction were analyzed and quantified with a Hewlett-Packard 5890 Gas Chromatograph equipped with a FID detector and outfitted with a 30m Alltech RSL 160 column (5μm thickness). Helium was employed as the carrier gas. Carbon dioxide and carbon monoxide analyses were performed with a Varian 3700 Gas Chromatograph equipped with a TCD detector outfitted with a 15' Carboxen Column. Methane was quantified by gas chromatography (TCD) using N_2 as an internal standard. Three chromatograms were measured for each sample using injection volumes of 0.1ml for gas and 0.1μl for liquid samples.

The following definitions describe terms used in the presentation of the results. Selectivity to any product is the moles of a given product divided by the total moles of all products formed expressed in percent. The percent CO_2 produced is moles of CO_2 divided by the total moles of all products. The selectivity to oxygenates is the moles of H_2CO, CH_3OH and $CH_3C(O)OCH_3$ divided by the total moles of products in percent. Traces of $CH_2(OCH_3)_2$, $HCOOCH_3$ are formed, but not quantified. Percent peroxide efficiency is the moles of H_2O_2 needed to account for all oxidized products including CO_2 divided by the moles of H_2O_2 consumed. The percent conversion of CH_4 is the moles carbon in the oxidized products divided by the moles of CH_4 added to the reactor.

Safety Precautions, the combination of molecular oxygen with organic compounds and solvents at elevated temperatures and pressures are potentially explosive.

Extreme caution should be taken during the charging and disassembly of the experimental apparatus. Equipment which can generates sparks must be avoided, a safety shield and cooling of the batch reactor in an ice bath for 30 minutes prior to disassembly is recommended.

Results and Discussions

Anion Modification

Reproducibility for the oxidation of CH_4 *cis*-$[Ru(dmp)_2(H_2O)_2](PF_6)_2$ catalyst precursor[40] depends on the purity of the complex. Chloro complexes are inactive[41] and excess $AgPF_6$ used to remove the chloride from the dichloro precursor inhibits[38,39,40] the reaction. Using $NaPF_6$ instead of $AgPF_6$ requires a large amount of $NaPF_6$ and repeated recrystallizations. The hexafluorophosphate anion of the final product is hydrolytically unstable and extensive etching of the glass vial occurs during storage. With more than 20% fluorine, verification of the complex purity by elemental analysis is difficult. Complex degradation is evident as well as the inability to obtain an appropriate NMR spectrum for complex **II** as illustrated in Figure 2-6.

In an attempt to overcome these problems, the anion was changed to trifluoromethanesulfonate, a poorly coordinating anion. A shortened synthesis time, need for less anion in the synthesis, more reliable elemental analyses, and stability towards hydrolysis are immediate advantages of this new complex. The direct effects of altering the anion are exhibited in the lack of complex degradation and the ability to obtain an identifiable NMR spectrum. A NMR for this newly synthesis complex **III** is provided in Figure 2-7.

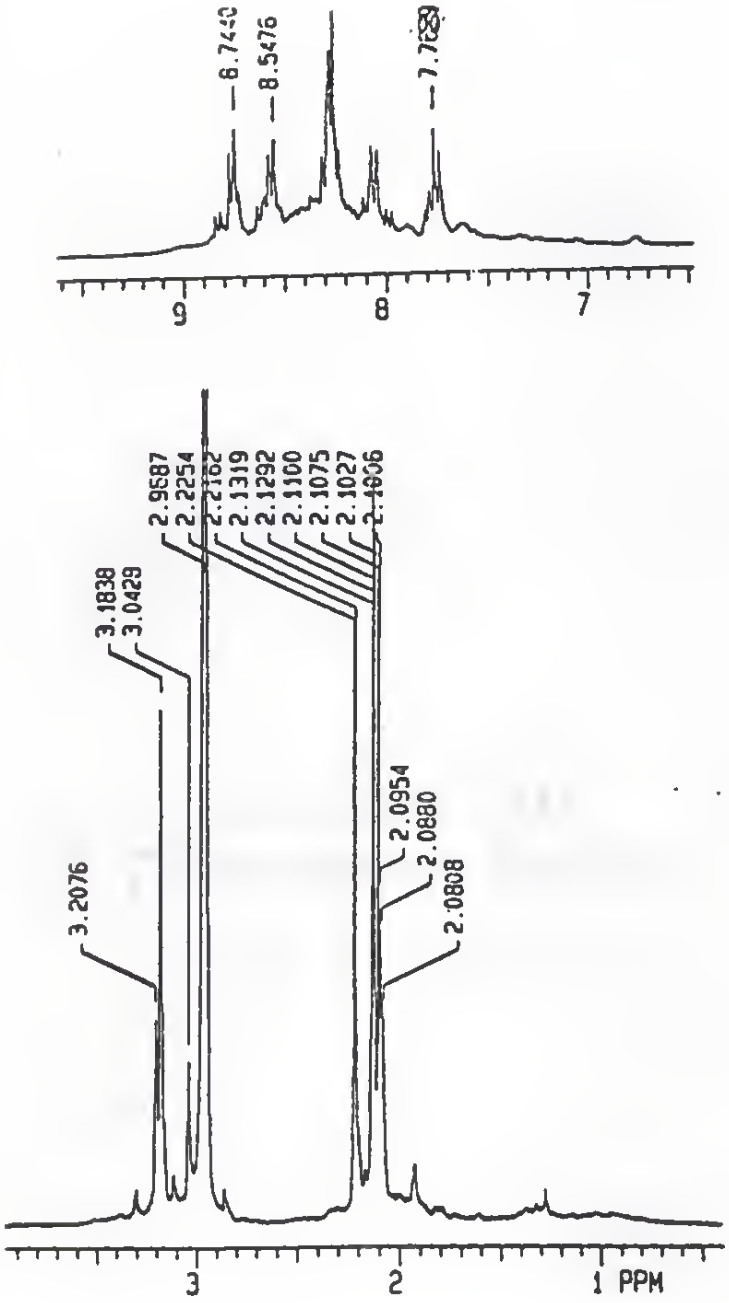

Figure 2-6: ^{1}H NMR Spectrum for *cis*-$[Ru(dmp)_2(H_2O)_2](PF_6)_2$

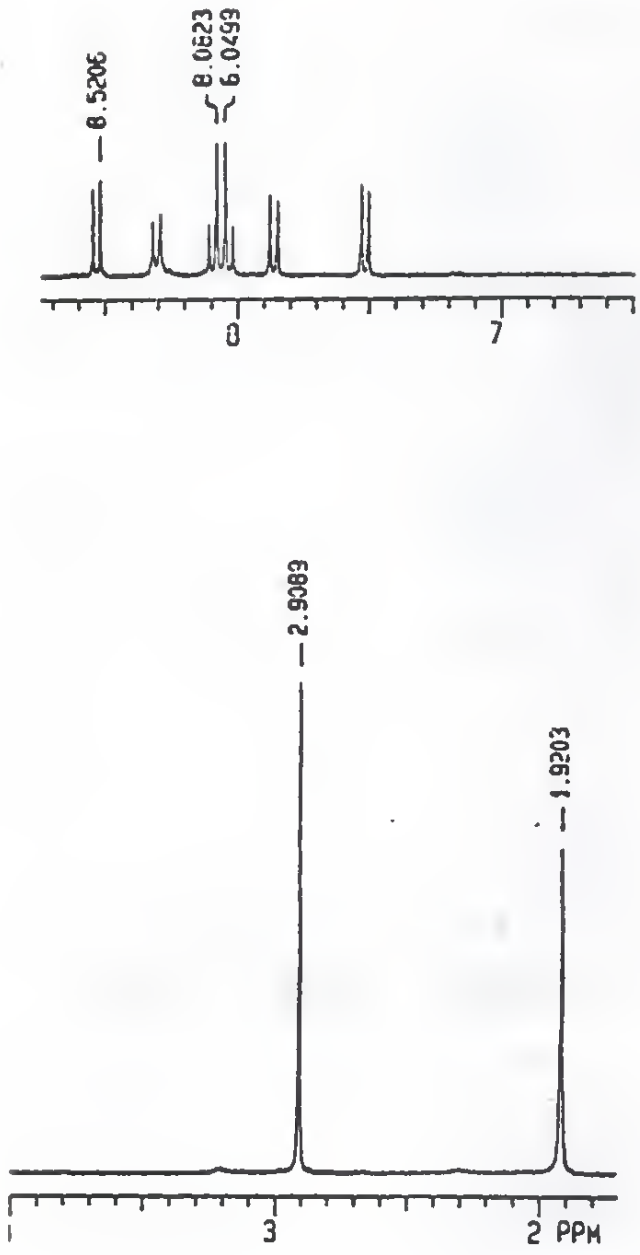

Figure 2-7: ^{1}H NMR Spectrum for *cis*-$[Ru(dmp)_2(H_2O)_2](CF_3SO_3)_2$

Ruthenium Catalyzed Oxidation of Methane with Hydrogen Peroxide

The trifluoromethanesulfonate derivative, complex **III**, is a potent catalyst for the oxidation of CH_4 by hydrogen peroxide in an acetonitrile solvent. Within 48 hours, at 75°C, CO_2, CO and traces of both methanol and formaldehyde appear which correspond to 60% of the initial concentration of methane. A more active catalyst, less methanol and more CO_2 result with **III** than with the PF_6^- derivative (**II**).

Previous reports suggest the di-oxo complex is necessary for the activation of the C-H bond in methane[40]. In water, the hydrogen peroxide potential[46] gives a negative free energy for the formation of the di-oxo species only when the solution pH is less than 5. However, at a pH of 2 in water, the oxidation of CH_4 by H_2O_2 with this catalyst is not observed at 75°C.[46] The relevant potentials are not known in acetonitrile but spectral studies indicate a high oxidation state complex is formed upon addition of H_2O_2.

The best condition reported for methane oxidation[40] with complex **II** in acetonitrile yield only 5 turnovers for methanol accompanied by extensive over-oxidation of methane to CO_2 occurs. This prompted an experiment to determine the activity of this catalyst for methanol oxidation to CO_2. Methanol, catalyst ($6.6x10^{-5}$ moles) and hydrogen peroxide ($5.0x10^{-2}$ moles) reacted in 4 hours at 75°C to convert 97% of the methanol to carbon dioxide and carbon monoxide. Thus, the main challenge to the use of these ruthenium catalysts for the selective oxidation of methane to methanol is to inhibit the over-oxidation. The successful oxidation of methane in H_2SO_4[50,51] and $CF_3C(O)OH$[52,53,54] to large quantities of available methanol can be attributed to trapping methanol as CH_3OSO_3H and $CF_3C(O)OCH_3$ respectively, and stabilizing it from over-

oxidation. This led to an attempt to trap methanol in our system as an ester by reaction with acetic acid and acetic anhydride. Acetic acid was used since it is an acidic solvent, and relatively difficult to oxidize. With aqueous H_2O_2 as the oxidant and water formed in the reaction, the anhydride can function to keep the water concentration low enhancing ester formation, as demonstrated in Equations 2-3, 2-4 and 2-5.

(Equation 2-3) $CH_3OH + CH_3C(O)OH \longrightarrow CH_3C(O)OCH_3 + H_2O$

(Equation 2-4) $H_2O + CH_3C(O)OC(O)CH_3 \longrightarrow 2\ CH_3C(O)OH$

(Equation 2-5) $CH_3C(O)OC(O)CH_3 + CH_3OH \longrightarrow CH_3C(O)OCH_3 + CH_3C(O)OH$

The anticipated product, methyl acetate, could be subsequently hydrolyzed to produce methanol and regenerate acetic acid.

The oxidative stability of methyl acetate to over-oxidation by our catalyst was shown with an experiment in which methyl acetate, catalyst ($6.6x10^{-5}$ moles) and hydrogen peroxide ($5.0x10^{-2}$ moles) dissolved in acetonitrile were reacted for 4 hours at 75°C. An 8% decrease in methyl acetate and formation of small amounts of carbon monoxide and carbon dioxide result, indicating that methyl acetate has the necessary stability to be an effective trap for methanol. The 8% oxidation observed could proceed through methanol formed from the equilibrium shown in Equation 2-3.

Using catalyst **III** and a solvent mixture composed of equal volumes of $CH_3CN/CH_3COOH/(CH_3CO)_2O$, 7.4 millimoles of oxygenates formed in 24 hours

representing a significant improvement over the previously reported 0.5 millimoles in acetonitrile.[38,39,40] Methyl acetate, methanol, formaldehyde, formic acid, methyl formate, carbon monoxide and carbon dioxide are all detected as products. As mentioned above, in the absence of acetic acid and acetic anhydride, only CO and CO_2 and trace amounts of formaldehyde are obtained with **III** as the catalyst.

Increasing the reaction time and hydrogen peroxide concentration in a series of experiments, gave increased amounts of CO_2, but led to an upper limit of $1.5x10^{-2}$ M methyl acetate in this solvent mixture. Apparently when methyl acetate approaches this concentration, the equilibrium concentration of CH_3OH reaches a level at which its rate of oxidation becomes equal to its rate of formation from methane. Decreasing the water in solution should produce a lower steady state concentrations of methanol (i.e. the position of the equilibrium in Equations 2-3 and 2-5 is shifted towards ester formation) and increase the trapping efficiency leading to decreased CO_2 and increased methyl acetate. To remove water, 4Å molecular sieves were added to the reaction mixture and shown to have a significant effect on the conversion of methane to methyl acetate. In comparable 24 hour runs, the conversion to oxygenates increased from 3 millimoles to 7 millimoles (Table 2-1, Experiment 1) with the addition of sieves even though some peroxide decomposition by the sieves occurs, vide infra. This result reinforces the proposal that efficient trapping is the main challenge for effective methanol synthesis.

Variation of the reaction time in Experiments 2 and 3 show that in four hours the maximum amount of methyl acetate and minimum amount of CO_2 form. The shorter time also led to an increase in the amount of formaldehyde. The methyl acetate formed corresponds to 61 turnover numbers (5 mmoles, $6.6x10^{-2}$ M) with a selectivity of 55%

Table 2-1: Oxidation Results for Methane @ 75°C with *cis*-$[Ru(dmp)_2(H_2O)_2](CF_3SO_3)_2$ Using H_2O_2[a]

Experiment Number	MeCOOMe mmol,(%)	CO_2 mmol,(%)	Total Oxygenates mmol,(%)	CH_4 Consumed (%)
1[a,c]	5,(44)	5,(44)	7,(62)	30
2[a,d]	4,(40)	3,(30)	7,(69)	26
3[a,e]	5,(57)	1,(11)	7,(80)	19
4[a,f]	10,(49)	9,(44)	10,(49)	62
5[b,g]	4,(70)	1,(17)	5,(87)	25
6[b,h]	9,(80)	3,(27)	8,(71)	49
7[b,i]	2,(100)	0	2,(100)	N/A
8[b,j]	3,(47)	0	4,(62)	28

a. Reactions 1-4 used 6.6×10^{-5} moles *cis*-$[Ru(dmp)_2(H_2O)_2](CF_3SO_3)_2$ catalyst, 5 ml 30% H_2O_2 (5.0×10^{-2} moles). The solvent mixture is 20 ml acetonitrile, 20 ml glacial acetic acid, 20 ml Acetic Anhydride, Initial methane pressure was 40 psig corresponding to 23 millimoles. 3.5g 4Å molecular sieves (MS) were used. The percent products are based on total products seen from all sources.

b. Reactions 5-8 used 2.4×10^{-5} moles *cis*-$[Ru(dmp)_2(H_2O)_2](CF_3SO_3)_2$ catalyst, 1 ml 35% H_2O_2 (1.1×10^{-2} moles). The solvent mixture is 3 ml σ-dichlorobenzene, 5 ml glacial acetic acid, 10 ml Acetic Anhydride, Initial methane pressure was 40 psig corresponding to 23 millimoles. 1.0g 4Å molecular sieves (MS) were used.

c. Reaction Time 24 hours. The percent products are based on total products from all sources.

d. Reaction Time 12 hours. The percent products are based on total products from all sources.

e. Reaction Time 4 hours. The percent products are based on total products from all sources.

f. Blank experiment, performed in the absence of catalyst, Reaction Time 1 hour.

g. Blank experiment, performed in the absence of catalyst and acetonitrile, Reaction Time 4 hours.

h. Reaction Time 4 hours.

i. Blank experiment, performed in the absence of catalyst and methane, Reaction Time 4 hours.

j. Blank experiment, performed in the absence of catalyst, Reaction time 4. Hours.

while formaldehyde corresponds to 24 turnover numbers (2 mmoles) with a selectivity of 28%. The CO and CO_2 produced correspond to 9 and 67 turnover numbers (0.2 mmoles and 5 mmoles) respectively. The total turnover numbers for all the products is 198, which if they all arose from methane would correspond to a methane conversion of 38%. The total moles of oxidant used are $1.3x10^{-2}$, so 21% of the peroxide has decomposed.

Peracid Formation and Reactivity

In view of the difficulty of oxidizing methane and its low concentration in solution, the importance of running control experiments to determine the source of products cannot be overemphasized. When the catalyst was eliminated from the reaction mixture, methyl acetate formed in significant amounts, Experiment 4 of Table 2-1. In earlier research from this laboratory it was shown that hydrogen peroxide is catalytically activated by forming peracids with organic acids[55]. To determine if peracetic acid forms, acetic acid, acetic anhydride, and 35% aqueous hydrogen peroxide were stirred at 25°C for thirty minutes in the absence of sieves. The difference in an iodometric titration of the products for total oxidant, and a cerium titration, for hydrogen peroxide, indicates by difference that 20% of the H_2O_2 was converted to peracid ($1.0x10^{-2}$ moles). At this point methane (40 psig) was introduced and the reaction vessel placed in an oil bath at 75°C. Experiment 4 (Table 2-1) shows that, in one hour of reaction time 10 mmoles of methyl acetate (49% selectivity), traces of formaldehyde, 0.4 mmoles of carbon monoxide and a large amount of carbon dioxide (9 mmoles or 44% of the products) were formed. This reaction led to about 19 mmoles of total products which, if they all arose from methane would correspond to 89% of the methane. The decrease observed in the amount of

methane by TCD is approximately 60% (Table 2-1) implying some of the oxygenates arise from peracid decomposition.

To limit over-oxidation by peracid, the reaction time was decreased to twenty minutes. The reaction produced $6.4x10^{-3}$ moles of methyl acetate (69% selectivity) ($1.1x10^{-1}$ M), $1.6x10^{-6}$ moles of formaldehyde (0.04% selectivity), $3.9x10^{-6}$ moles of carbon monoxide (0.06% selectivity) and $2.9x10^{-3}$ moles of carbon dioxide (31.1%). The peroxide utilization was 97% and $1.0x10^{-2}$ moles of products were observed. The decrease in reaction time leads to less products, but increased selectivity to methyl acetate.

Blank runs were performed with and without sieves to determine if hydrogen peroxide and acetonitrile form a peracid, $CH_3C(OOH)NH$, which oxidizes methane to produce methyl acetate. In these experiments, acetonitrile, hydrogen peroxide and methane were added together and allowed to react for 48 hours at 75°C. Iodometric titrations also confirmed the absence of peracid.

The next concern is the source of the products in the blank, as shown in Experiment 5. Oxidations of paraffins by 3,5-dinitroperbenzoic acid, perbenzoic acid and perfluoroperacetic acid result[56] in more than 50% conversion of the paraffin. A radical mechanism is suggested[57,58] for the formation of the hydroxylation products that is initiated by the decomposition of peracids as shown in Equations 2-6, 2-7, and 2-8.

(Equation 2-6) $R\text{-}CO_3H \longrightarrow RCO_2^{\bullet} + {}^{\bullet}OH$

$\longrightarrow R^{\bullet} + CO_2 + {}^{\bullet}OH$

(Equation 2-7) $R\text{-}H + R^{\bullet} \longrightarrow {}'R^{\bullet} + R\text{-}H$

(Equation 2-8) $'R^{\bullet} + R\text{-}CO_3H \longrightarrow {}'R\text{-}OH + R\text{-}CO_2^{\bullet}$

The $R\text{-}CO_2^{\bullet}$ radical decomposes to form CO_2 and the alkyl radical ($R^{\bullet}$) which abstracts a hydrogen atom from the paraffin R'H to form the '$R^{\bullet}$ alkyl radical which reacts with the peracid to form the alcohol generating R'OH and another $RCO_2^{\bullet}$. In our system, with CH_4 as the alkane and peracetic acid as the oxidant, decomposition of CH_3CO_3H would generate methyl radicals which may exchange with methane in Equation 2-7 and would have to react as shown in Equation 2-8 to produce CH_3OH. Methanol formation would in effect arise from peracid decomposition.

Alternatively, $RCO_2^{\bullet}$ can react with R'H to form $R'^{\bullet}$ which then reacts as shown in Equation 2-8. In this case CH_4 would be converted to methanol by $CH_3CO_2^{\bullet}$, formed in Equation 2-5, reacting with methane, as shown in Equation 2-6, to form methanol via Equation 2-8. Methane oxidation by peracid results, in contrast to the literature mechanism where the products would derive from the solvent. In view of the possible exchange of methyl radical with labeled methane, Equation 2-7, labeling experiments will not be definitive. One also notes that less methyl acetate is produced with the ruthenium complex present (Experiment 3, Table 2-1), than with it absent in Experiment 4, suggesting metal complex decomposition of H_2O_2. Crude estimates of the methane that disappeared in the experiments described above, indicate the metal complex is involved in Experiments 1-3 but more compelling evidence is required.

The question concerning the reactivity of methane with peracid raised above impacts not only on the metal catalyzed oxidations in acetic acid-acetic anhydride solvent but also on peracid oxidation of alkenes.[56] Blank runs at 75°C, with catalyst, hydrogen peroxide, acetic acid/acetic anhydride, acetonitrile and no methane, produced one millimole of methane and traces of methanol after four hours of reaction. A similar experiment in σ-dichlorobenzene, showed only traces of methane and methanol. The source of methane is thought to arise from solvent facilitated peracid decomposition in acetonitrile. This proposal was not investigated further, but the solvent was switched from acetonitrile to σ-dicholorbenzene and Experiment 5-8 were carried out. Since labeling experiments are uninformative, efforts were expended to accurately determine the methane disappearance to provide a material balance. To facilitate the metal catalyzed path, the catalyst and hydrogen peroxide concentrations were increased by 20%. Experiments 5 and 7 indicate that the beneficial effect of the sieves removing water is accompanied by the deleterious decomposition of hydrogen peroxide. In Experiment 6, methane oxidation is catalyzed by **III**, giving an amount of products equivalent to 49% conversion to oxygenates. Nine millimoles of methyl acetate, two millimoles of other oxygenates and 3 millimoles of CO_2 were formed. In Experiments 5 and 6 a good material balance for methane disappearance and product formation resulted.

When an identical blank experiment with no catalyst or methane was carried out, two millimoles of methyl acetate and no other products were formed from peracid decomposition, Experiment 7. When no catalyst was used and methane added, Experiment 8, three millimoles of methyl acetate and one millimole of other oxygenates

were formed. Experiment 7 indicates that methyl acetate can arise from the solvent via peracid decomposition. Since the amounts of oxygenates produced are doubled when methane is added, Experiment 8, methyl acetate is produced by the reaction of the peracid with methane. However, in Experiment 6 when the ruthenium catalyst is present, the almost three-fold increase in oxygenates compared to Experiment 7 establishes the metal catalyzed path.

All methane conversions given in Table 2-1 is based on the amount of methane consumed in the reaction. In the absence of a material balance for runs 1-4, an upper estimate results for conversions. Since peracid formation is not expected for oxidations with O_2, trapping with the acetic acid-acetic anhydride mixture was investigated next with this oxidant.

Oxidation of Methane with Molecular Oxygen

The direct conversion of methane to methanol using molecular oxygen is even a greater challenge than using hydrogen peroxide as the oxidant. Table 2-2 provides results for experiments using 30 psig of 5% O_2 in helium as the oxidant. The moles of oxidized products formed clearly exceed the moles hydrogen peroxide (2.5×10^{-5}) added to initiate the reaction by oxidizing **III**. After 48 hours (Experiment 9), methyl acetate (5 turnover numbers, 0.32 mmoles, 19% selectivity), and relatively large amounts of formaldehyde (20 turnover numbers, 0.65 mmoles, 38% selectivity) methanol and methyl formate were obtained. GC analysis (TCD) shows carbon monoxide (9 turnover numbers, 0.19 mmoles, 11% selectivity) and carbon dioxide (32 turnover numbers, 0.52 mmoles, 30% selectivity). At most a total of 0.4 turnovers (2.5×10^{-5} moles) for methyl

Table 2-2: Oxidation Results for Methane @ 75°C with *cis*-$[Ru(dmp)_2(H_2O)_2](CF_3SO_3)_2$ Using H_2O_2 and O_2

Experiment Number[a]	Sel. to MeAcetate (%)	CO_2 Formation (%)	Sel. To Oxygenates (%)	H_2O_2 Efficiency (%)	CH_4 Conversion (%)
9[b]	19.2	30.1	57.6	>100	16.8
10[c]	50.1	40.2	50.1	>100	6.3
11[d]	0.0	0.0	0.0	0.0	0.0
12[e]	0.0	0.0	0.0	0.0	0.0

a. 6.6×10^{-5} moles *cis*-$[Ru(dmp)_2(H_2O)_2](CF_3SO_3)_2$, 20 ml acetonitrile, 20 ml glacial acetic acid, 20 ml Acetic Anhydride, 20 psig CH_4 (1.0×10^{-2} moles), 3.5g Molecular Sieves (MS)., 75°C,

b. Reaction time 48 hours 2.5 µl 30% H_2O_2 (2.5×10^{-5} moles).

c. Reaction time 24 hours 2.0 µl 30% H_2O_2 (2.0×10^{-5} moles).

d. Blank Experiment, performed in the absence of H_2O_2 48 hours.

e. Blank Experiment, performed in the absence of catalyst 48 hours.

acetate could have resulted from the $2.5x10^{-5}$ moles of H_2O_2 assuming 100% peroxide efficiency. Clearly this catalytic system utilizes O_2 for the oxidation of methane at 75C. The total moles of products correspond to 1.7 mmoles, corresponding to a 17% percent conversion of methane. The formation of methyl acetate indicates the trapping of methanol is occurring.

The reaction of methane with O_2 was carried out for 24 hours (Experiment 10). Less CO_2 and less methane conversion results. The products are methyl acetate (5 turnover numbers, 0.30 mmoles, 50% selectivity), carbon monoxide (3 turnover numbers, 0.06 mmoles, 10% selectivity) and carbon dioxide (16 turnover numbers, 0.26 mmoles, 40% selectivity). A total of 0.63 mmoles are formed and the percent methane conversion was 6%. Since the same amount of methyl acetate forms in 24 or 48 hours, the extended time results in the oxidation of methanol that is in equilibrium with methyl acetate (Equation 2-2).

Experiment 11 was performed to determine if di-oxygen could catalyze the reaction without hydrogen peroxide to initiate formation of the ruthenium-oxo species. After 48 hours no oxidation products were observed. The $[Ru(dmp)_2(H_2O)_2]^{2+}$ catalyst precursor utilizes molecular oxygen in epoxidations[38,39] only after an initiation period in which an alkyl hydroperoxide is generate to oxidize the complex to the (IV) oxidation state. Upon oxygen atom transfer to the substrate from the (IV) oxidation state the (II) oxidation state forms, which reacts with the Ru (IV) to generate Ru (III). The (III) oxidation state reacts with molecular oxygen to regenerate the higher oxidation state metal-oxo species.[46] Since O_2 will not form methylhydroperoxide from methane, the inactivity of the ruthenium (II) complex with O_2 (Experiment 11), and the required

initiation by H_2O_2 suggests that a metal-oxo species generated from ruthenium (III) by O_2 is involved by either reacting with ruthenium (III) to form a metal-oxo species, catalyzing the reduction of O_2 to H_2O_2 by methane or inhibiting radical chain termination steps.

Conclusions

The use of the sterically hindered *cis*-$[Ru(dmp)_2(H_2O)_2]^{2+}$ complex to catalyze the oxidation of methane has been investigated. Using the poorly coordinating trifluoromethanesulfonate anion in place of hexafluorophosphate an improvement in reproducibility and catalytic activity of the complex has been demonstrated. This complex is a precursor to the proposed di-oxo catalyst that oxidizes methane to CO_2 with hydrogen peroxide at 75°C in acetonitrile. In order to stop the reaction at the methanol intermediate, an acetic acid/acetic anhydride mixture was chosen to trap methanol as methyl acetate. This ester, which is not as readily oxidized as the alcohol, increases the selectivity and inhibits the over-oxidation of methanol.

In oxidations with hydrogen peroxide, control experiments indicate the formation of peracetic acid from the solvent mixture of acetic acid/acetic anhydride. In the absence of methane, the peracid decomposes to produce methyl acetate. When the reaction is carried out in identical conditions under methane, a doubling of the methyl acetate, produced shows that methane is oxidized by peracid to form methyl acetate. A substantial increase in methyl acetate, for identical reaction conditions with metal complex added, clearly demonstrates that metal catalyzed oxidation occurs. The material balance shows that the predominant source of the methyl acetate is methane with at most a small contribution from peracid decomposition.

The *cis*-$[Ru(dmp)_2(H_2O)_2]^{2+}$ complex is a catalytic precursor for the oxidation of methane with dioxygen in acetonitrile at 75°C. It is necessary to initiate the reaction by oxidation of the complex with trace amounts of hydrogen peroxide. With molecular oxygen as the oxidant, a 6% conversion of methane and 50% selectivity to methyl acetate can be obtained after 24 hours of reaction.

CHAPTER 3
OXIDATION OF ALKANES WITH HYDROGEN PEROXIDE USING A RUTHENIUM METAL-OXO CATALYST

Introduction

The transformation of saturated hydrocarbons into their oxygentated derivatives (i.e. alcohols, aldehydes, ketones and carboxylic acids) has been the subject of intense investigation over the past two decades. Alkanes given their great abundance offer a cost effective and ideal feedstock for an industrial process.[59] However, the chemical inertness of saturated hydrocarbons make activation extremely difficult at mild conditions. The oxygenation products, vital intermediates in many industrial processes, are then converted into commercial products. In order for a process to be feasible on the industrial scale the catalyst must demonstrate two properties: selectivity towards the partial oxygenates and exhibit a specific regioselectivity. To achieve these requirements a commercial industrial application must maintain high temperatures and pressures.[60] Currently, research efforts are being directed towards the development of new efficient catalytic systems, which are able to oxygenate, saturated hydrocarbons under mild conditions using hydrogen peroxide and/or molecular oxygen.

Reagents with the capacity to oxidize paraffins and arylalkanes have been known for well over a century.[61,62] Two such compounds are chromyl chloride (CrO_2-Cl_2) and permanganate (MnO_4^-).[61,62] However, these oxidants are stoichiometric and a catalytic

one is desired. Numerous researchers[63,64,65] have reported organic radical mechanisms via homogeneous or heterogeneous oxidation. The essential properties that allow these oxidants to oxidize a relatively inert C-H bond are not fully understood.

A number of metal-oxo and metal-oxide surfaces perform as reagents or catalysts for the oxidation of hydrocarbons, on industrial and laboratory scales.[1,2,66,67,68] Metallo-enzyme sites also activate hydrocarbons, two well-documented examples being Cytochrome P-450[69] and methane monooxygenase[47] (MMO).

Current research in the area of hydrocarbon activation has utilized a variety of oxidants, catalysts and reaction conditions. Barton *et al.*[70,71] has developed the Gif system, as well as a number of variations (i.e. Barton-Gif). Gif uses a pyridine/acetic acid solution, substrate, Fe catalyst and an oxidant, usually *t*-BuOOH. The mechanism of oxidation has been reported as proceeding through the involvement of free radicals. Que[72] has been investigating the use of di-iron complexes, in this case a high valent $Fe_2(\mu\text{-}O)_2$ moiety. This complex has been proposed as the key oxidizing species for methane monooxygenase, as well as for other non-heme di-iron enzymes. Ribonucleotide reductase and fatty acid desaturase are mentioned.

This research demonstrates the *cis*-$[Ru(dmp)_2(H_2O)_2](CF_3SO_3)_2$ as a precursor for the catalytic oxidation of higher linear and branched alkanes with hydrogen peroxide in acetonitrile at 75°C. The complex generates a large fraction of products oxygenated at the primary carbon position. An increase in selectivity towards the alcohol product is observed upon addition of $CuCl_2$. The effect of temperature on reactions with this catalyst

is also investigated to determine the effect on overall hydrocarbon conversion, selectivity distribution of oxygenates.

Experimental

Materials and Methods

$RuCl_3 \cdot x\ H_2O$, 2,9-dimethyl-1,10-phenanthroline, LiCl, $NaCF_3SO_3$, hydrogen peroxide (35%) and pentane (99.9%) were all used as received from Aldrich. Ethylene glycol and acetonitrile were all used as received from Fisher Scientific (ACS grade). Acetonitrile was distilled over P_2O_5 under dinitrogen and was stored over 4Å activated molecular sieves. Ethane (99.9%), propane (99%), butane (99%) and *iso*-butane (99.5%) was purchased from Matheson and used as received.

Physical Measurements

UV-Vis measurements employed a Perkin Elmer lambda-6 spectrophotometer. The pH measurements were made with a Fisher Accumet model 630 pH meter. NMR spectra were recorded on a Varian VXR300 spectrometer. FAB mass spectral data were obtained by Dr. David Powell (U.F.) in a *m*-nitrobenzyl alcohol matrix. U.F. Analytical Services performed elemental analyses.

Synthesis of Compounds

***cis*-Ruthenium(II) Bis(chloride)bis(2,9-dimethyl-1,10-phenanthroline) Monohydrate, $[Ru(dmp)_2Cl_2] \cdot H_2O$ (I).** *Cis*-$[Ru(dmp)_2Cl_2] \cdot H_2O$ was synthesized as reported[40]. Analysis: Calculated for $C_{28}H_{26}N_4OCl_2Ru$; C, 55.45; H, 4.29; N, 9.24. Found: C, 55.65; H, 4.35; N, 9.29.

***cis*-Ruthenium(II) Bis(aquo)bis(2,9-dimethyl-1,10-phenanthroline) bis(trifluoromethanesulfonate), *Cis*-$[Ru(dmp)_2(H_2O)_2](CF_3SO_3)_2$ (II).** A 1.0g (1.7 mmol) portion of I is slowly dissolved in 150 ml of deionized H_2O under N_2 by heating at 50°C for 30 minutes. After adding 50 ml of a saturated $NaCF_3SO_3$ (aq), the solution cooled, placed in an ice bath for two hours and filtered. The precipitate is redissolved in H_2O by heating at 50°C, a saturated $NaCF_3SO_3$ (aq) (9g $NaCF_3SO_3$/ 25ml deionized H_2O) solution is added and reprecipitated as above. Recrystallization and exchange of Cl^- for $CF_3SO_3^-$ is repeated until the filtrate affords a negative chloride test with $AgNO_3$. The product is dried in vacuum at 60°C overnight. Analysis: Calculated for $C_{30}H_{34}N_4O_8S_2F_6Ru$, C, 42.25; H, 3.31; N, 6.57. Found: C, 41.40, H, 3.26; N 6.39.

Oxidation Procedure

The pressurized oxidations were carried out as previously described[49], in batch type hydrogenation reactors, Figure 2-5. The reaction mixtures were varied as described in table footnotes. Blank runs were performed omitting certain reactants and are also described in the text. Reaction temperatures were normally maintained at 75°C unless stated otherwise. To remove air initially present, nitrogen gas is purged through the reactor, the apparatus is pressurized with the substrate, which is then released, and re-pressurized to the desired pressure.

The oxygenated products of the reaction were analyzed and quantified with a Hewlett-Packard 5890 Series II gas chromatograph equipped with an FID detector and outfitted with a 30m HP 50+ (50% Ph Me Silicone Gum; 1 μm thickness). Helium was employed as the carrier gas. Carbon dioxide and carbon monoxide analysis were

performed with a Varian 3700 gas chromatograph equipped with a TCD detector outfitted with a 15' Carboxen Column, 1 μm thickness. Helium was utilized as the carrier gas. Concentrations of the substrate and oxidized products were quantified using acetonitrile as an internal standard. Three chromatograms were measured for each sample using injection volumes of 0.1 ml for gas and 0.1 μl for liquid samples.

A typical reaction mixture consisted of 60 ml of acetonitrile, 40 psig total pressure for gaseous reactants, $1.6x10^{-4}$ moles of catalyst and 5ml of 35% hydrogen peroxide ($5.0x10^{-2}$ moles). Experiments in the absence of oxidants were performed as blanks.

The following definitions describe terms used in the presentation of the results. Selectivity to any product is the moles of a given product divided by the total moles of all products formed expressed as a percent. The percent peroxide efficiency is the moles of H_2O_2 needed to account for all oxidized products divided by the moles of H_2O_2 consumed. The percent conversion of alkane is the moles carbon in the oxidized products divided by the moles of alkane added to the reactor.

Safety Precautions, the combination of molecular oxygen with organic compounds and solvents at elevated temperatures and pressures are potentially explosive. **Extreme caution** should be taken during the charging and disassembly of the experimental apparatus. Equipment which can generates sparks must be avoided, a safety shield and cooling of the batch reactor in an ice bath for 30 minutes prior to disassembly is recommended.

Results and Discussion

Alkane Oxidation

Attempts to oxidize alkanes with hydrogen peroxide in H_2O as the solvent at 75°C were unsuccessful after 48 hours with or without catalyst at solution pH values of 1 to 7. As suggested previously[46], the Ru(VI) oxidation state is necessary for the activation of the C-H bond of alkanes. The $[Ru(dmp)_2(H_2O)_2](CF_3SO_3)_2$ complex **II** has been shown to be a potent catalyst in an acetonitrile solvent.[73] Consequently alkane oxidations were performed in acetonitrile.

Each alkane (ethane, propane, butane, *iso*-butane and pentane) was reacted in acetonitrile (60ml) with hydrogen peroxide ($5.0x10^{-2}$ mole) and catalyst ($1.6x10^{-4}$ moles) for 15 hours at 75°C. The results are provided in Table 3-1 and Table 3-2. Propane, iso-butane and pentane allowed us to determine catalyst activity in terms of selectivity and regioselectivity.

After 15 hours, a 20.8% conversion of propane was observed corresponding to 3.4 mmoles of oxidized products. The selectivities of the oxidized products obtained are of interest. Oxidation at the primary carbon position accounts for 65.1% or 2.2 mmoles of the total oxidized products (1-propanol: 0.1 mmoles, 1.6% selectivity, and propionaldehyde: 2.1 mmoles, 63.6% selectivity). Trace amounts of propionoic acid were detected by gas chromatography analysis, however peak broadening and tailing make quantification difficult. Oxidation at the secondary carbon position was also observed, accounting for 34.9% or 1.2 mmoles of the total oxidized products (2-propanol:

Table 3-1: Oxidation Results for Ethane, Propane and Butane @ 75°C with *cis*-$[Ru(dmp)_2(H_2O)](CF_3SO_3)_2$ using H_2O_2

Substrate[a]	Oxidized Products mmoles (Selectivity)	Total mmoles Oxidant	Percent Peroxide Efficiency	Percent Conversion[b]
Ethane	Ethanol: 0.08 (2.3) Acetaldehyde: 2.50 (69.3) Acetic Acid: 1.00 (28.4)	8.10	16.2	20.1
Propane	1-Propanol: 0.05 (1.6) 2-Propanol: 0.07 (1.9) Propanal: 2.10 (63.6) Acetone: 1.20 (32.9) Propionoic Acid: Trace	6.80	13.5	20.8
Butane	1-Butanol: 0.08 (4.8) 2-Butanol: 0.94 (5.3) Butanal: 0.10 (5.5) 2-Butanone: 0.31 (18.1) Butanoic Acid: 1.20 (66.3)	5.40	10.7	26.2

a: 1.6×10^{-4} mole *cis*-$[Ru(dmp)_2(H_2O)](CF_3SO_3)_2$, 60ml acetonitrile, 5.0×10^{-2} moles 35% H_2O_2, 40psi substrate (1.9×10^{-2} moles), 15 hours at 75°C.

b: Percent conversion is based on the total of oxidized products divided by the initial amount of substrate.

Table 3-2: Oxidation Results for *Iso*-Butane and Pentane @ 75°C with *cis*-$[Ru(dmp)_2(H_2O)](CF_3SO_3)_2$ using H_2O_2

Substrate[a]	Oxidized Products mmoles (Selectivity)	Total mmoles Oxidant	Percent Peroxide Efficiency	Percent Conversion[c]
Iso-Butane	*Iso*-Butanol: 3.90 (99.0) *Iso*-Butyl-ol: 0.04 (0.9)	3.90	7.8	20.5
Pentane[b]	1-Pentanol: 0.58 (5.7) 2-Pentanol: 1.20 (11.5) 3-Pentanol: 1.20 (17.1) Pentanal: 2.20 (21.7) 2-Pentanone: 1.90 (18.4) 3-Pentanone: 2.60 (25.7) Pentanoic Acid: Trace	16.10	32.4	23.4

a: $1.6x10^{-4}$ mole *cis*-$[Ru(dmp)_2(H_2O)](CF_3SO_3)_2$, 60ml acetonitrile, $5.0x10^{-2}$ moles 35% H_2O_2, 40psi substrate ($1.9x10^{-2}$ moles), 15 hours at 75°C.

b: 2ml pentane ($2.0x10^{-2}$ moles) used.

c: Percent conversion is based on the total of oxidized products divided by the initial amount of substrate.

0.1 mmoles, 1.9% selectivity and acetone: 1.1 mmoles, 32.9% selectivity). Activation of propane by this catalyst produces a selectivity ratio of primary:secondary carbon oxidation of 2:1. A peroxide efficiency of 13.5% and 43 turnover numbers (TON's) was obtained for this reaction.

Ethane and butane were oxidized under identical conditions giving a 20.1% and 26.2% conversion respectively. The results are shown in Tables 3-1 and 3-2. Over-oxidation of the hydroxylated products to the corresponding aldehyde, ketone and carboxylic acid were also exhibited. As a result selectivity, overall conversion of the alkane, peroxide efficiency and catalyst lifetime are decreased by over-oxidation.

Iso-butane was investigated to demonstrate the ability of this catalyst to produce oxidation products at the tertiary and primary carbon position. After 15 hours of reaction, 3.9 mmoles of oxidized products were obtained. Oxidation at the tertiary carbon accounted for 99.0% (3.9 mmoles) of the oxidized products. Also detected were trace amounts (0.04 mmoles, 0.9% selectivity) of isobutyl alcohol (2-methyl-1-propanol), demonstrating some oxidation at the primary position.

Pentane can lead to oxidation at the C_1, C_2 and C_3 positions. This is also the first liquid alkane investigated. After 15 hours, a 23.4% conversion of pentane was observed accounting for 10 mmoles of oxidized products. Oxidation at the primary carbon position (C_1) afforded: 1-pentanol (0.6 mmoles, 5.7% selectivity), valeraldehyde (pentanal) (2.2 mmoles, 21.7% selectivity) and a trace amount of valeric acid (pentanoic acid), once again quantification was difficult due to peak broadening and tailing. Oxidation at the secondary carbon (C_2) position produced: 2-pentanol (1.2 mmoles, 11.5% sel.) and 2-pentanone (1.9 mmoles, 18.4% sel.). Activation at the C_3 position produces: 3-pentanol

(1.2 mmol, 17.1% sel.) and 3-pentanone (2.6 mmoles, 25.7% sel.). A total of 16 mmoles of oxidant was consumed in this reaction yielding a peroxide efficiency of 32.4% and 50 TON.

Mechanism of Oxidation

Two mechanisms, hydrogen abstraction or "rebound" and oxygen atom insertion, have been proposed for the oxidation of hydrocarbons with *cis*-$[Ru(dmp)_2(H_2O)_2]^{2+}$.[40,74] These mechanisms are illustrated in Figures 3-1 and 3-2 respectively.

The hydrogen abstraction or "rebound" mechanism produces an alkyl free radical. The free radical produced in the first step of the mechanism is the result of the *cis*-$\{Ru(O)_2\}^{2+}$ moiety abstracting a hydrogen atom from the alkane to produce a reduced ruthenium-hydroxide species. The active metal center, $Ru^{(VI)}$=O functions as a free radical[40] which is capable of abstracting a hydrogen atom from the hydrocarbon. The second step proceeds with the transfer of the hydroxo ligand to the formed radical to yield the hydroxylated product. The catalytic cycle involves regeneration of the high valent metal center by oxidation with O_2 or H_2O_2. Other ruthenium complexes have been proposed to proceed through this or a similar mechanism.[75,76,77]

The oxygen atom insertion mechanism has been proposed for the epoxidation of olefins.[40,78,79] It has also been reported that ruthenium-oxo complexes are able to epoxidize alkenes via a non-radical mechanism.[40] The first step in this mechanism for alkane oxidation is the insertion of the oxygen bound to ruthenium into the C-H bond of the substrate. This adduct forms a three coordinate oxygen and a five coordinate carbon

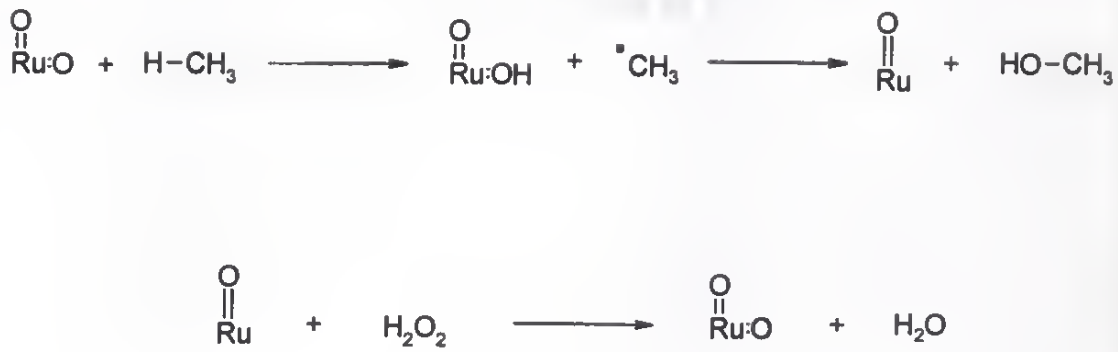

Figure 3-1: Proposed Hydrogen Atom Abstraction Mechanism for *cis*-$[Ru(dmp)_2(H_2O)_2]^{2+}$ Complex

similar to CH_5^+ obtained in an S_n2 mechanism. The next step is scission of the C-H bond forming a coordinated alcohol followed by displacement of the alcohol from the ruthenium complex. The final step is the regeneration of the high valent metal-oxo as previously described in the hydrogen abstraction mechanism.

Results from this laboratory[40,73] indicate that the activation of alkanes with *cis*-$[Ru(dmp)O_2]^{2+}$ is proceeding via the hydrogen abstraction mechanism.

Addition of $CuCl_2$

The majority of the oxidized products obtained are aldehydes, ketones and carboxylic acids. In order to obtain increased amounts of the partially oxidized products its direct over-oxidation must be prevented. Addition of a metal chloride could offer a solution. Addition of $NiCl_2$ to a methanol solution produces complexes with methanol bound to the nickel.[80] In this investigation formation of this metal-alcohol adduct was determined by IR analysis. Coordination of the alcohol produced in our oxidations to a metal could possibly retard over-oxidation and improve selectivity for the hydroxylated product.. To determine if an increase in selectivity towards the hydroxylated products can be obtained one mole equivalent of $CuCl_2$ ($1.6x10^{-4}$) was added to the previously described reaction with all other conditions held constant. The results are shown in Table 3-3 and Table 3-4.

After 15 hours at 75°C, an 18.2% conversion of propane was observed in the presence of $CuCl_2$. The addition of $CuCl_2$ led to a 2.4% decreased in conversion. However, an increase in alcohol selectivity to 6.1% for 1-propanol and a 18.5% for

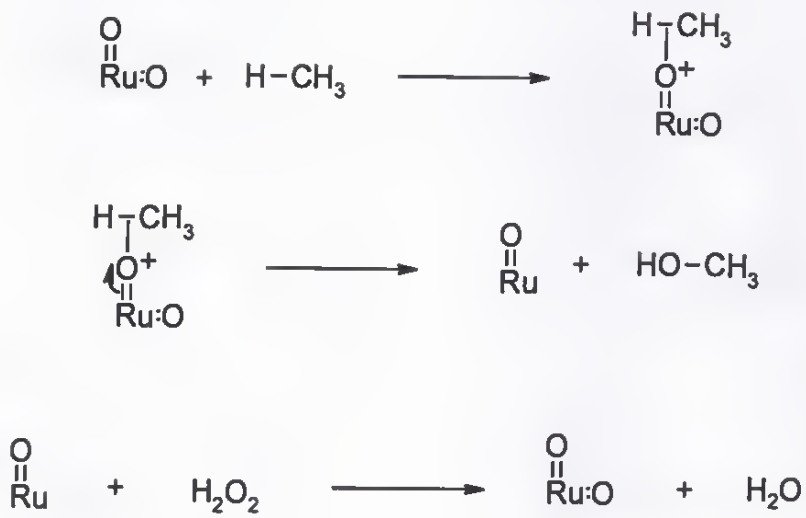

Figure 3-2: Proposed Oxygen Atom Insertion Mechanism for *cis*-$[Ru(dmp)_2(H_2O)_2]^{2+}$ Complex

2-propanol is observed, compared to selectivities of 1.6% and 1.9% when $CuCl_2$ is omitted. With the increase in alcohol selectivity a decrease in selectivity to the aldehyde and ketone results. A 61.0% selectivity to propionaldehyde and 14.4% selectivity for acetone is exhibited with the addition of $CuCl_2$. $CuCl_2$ addition leads to a decrease in the peroxide efficiency attributed to known peroxide decomposition by first row transition metal salts.[29] Increases in selectivity to the alcohol are also found for each of the alkanes studied. These results are presented in Table 3-3 and 3-4.

To determine the role of $CuCl_2$ a series of blank experiments were performed. When 60 ml of acetonitrile, $1.6x10^{-4}$ moles $CuCl_2$, $5.0x10^{-2}$ mole H_2O_2 and $1.9x10^{-2}$ moles of propane were reacted for 15 hours at 75°C no oxygenates were observed suggesting $CuCl_2$ is not participating in the oxidation of propane.

Experiments were performed to determine the stability of alcohol under reaction conditions. Ethanol (1ml, $1.9x10^{-2}$ mol), acetonitrile (60ml), $1.6x10^{-4}$ moles catalyst and $5.0x10^{-2}$ moles H_2O_2 were reacted for 15 hours at 75°C. A 77% decrease in ethanol and formation of acetaldehyde and acetic acid was observed. TCD gas chromatography analysis exhibited the trace amounts of carbon monoxide and carbon dioxide. The quantity of oxidized products corresponds to the decrease in moles of ethanol. Analysis of the resulting solution for peroxides with sodium metavanadate and iodometric titration showed none was present. An identical experiment was performed with the addition $CuCl_2$ ($1.6x10^{-4}$ mol) to the reaction solution. After 15 hours the amount of alcohol present in the final reaction solution corresponded to only a 43% decrease. Aldehyde and carboxylic acid also formed in decreased amounts according to mass balance calculations.

Table 3-3: Oxidation Results for Ethane, Propane and Butane @ 75°C with *cis*-$[Ru(dmp)_2(H_2O)](CF_3SO_3)_2$ and $CuCl_2$ using H_2O_2

Sub-strate[a]	Oxidized Products mmoles (Selectivity)	Total mmoles Oxidant	Percent Peroxide Efficiency	Percent Conversion[b]
Ethane	Ethanol: 0.18 (4.31) Acetaldehyde: 3.10 (74.7) Acetic Acid: 0.88 (21.0)	9.10	18.1	23.2
Propane	1-Propanol: 0.21 (6.1) 2-Propanol: 0.64 (18.5) Propanal: 2.10 (61.0) Acetone: 0.49 (14.4) Propionoic Acid: Trace	6.10	12.1	18.2
Butane	1-Butanol: 0.26 (12.5) 2-Butanol 0.15 (7.1) Butanal: 0.11 (5.3) 2-Butanone: 0.46 (21.8) Butanoic Acid: 1.10 (53.2)	4.90	9.7	30.9

a: 1.6×10^{-4} mole *cis*-$[Ru(dmp)_2(H_2O)](CF_3SO_3)_2$, 1.6×10^{-4} mole $CuCl_2 * 2\ H_2O$, 60ml acetonitrile, 5.0×10^{-2} moles 35% H_2O_2, 40psi substrate (1.9×10^{-2} moles), 15 hours at 75°C.

b: Percent conversion is based on the total of oxidized products divided by the initial amount of substrate.

Table 3-4: Oxidation Results for *Iso*-Butane and Pentane @ 75°C with $[Ru(dmp)_2(H_2O)](CF_3SO_3)_2$ and $CuCl_2$ using H_2O_2

Substrate[a]	Oxidized Products mmoles (Selectivity)	Total mmoles Oxidant	Percent Peroxide Efficiency	Percent Conversion[c]
Iso-Butane	*Iso*-Butanol: 3.50 (99.2) *Iso*-Butyl ol: 0.01 (0.8)	3.50	7.1	18.8
Pentane[b]	1-Pentanol: 0.94 (10.4) 2-Pentanol: 1.60 (17.5) 3-Pentanol: 2.70 (30.1) Pentanal: 1.30 (13.8) 2-Pentanone: 1.30 (13.7) 3-Pentanone: 1.30 (14.5) Pentanoic Acid: Trace	13.10	25.5	20.9

a: $1.6x10^{-4}$ mole *cis*-$[Ru(dmp)_2(H_2O)](CF_3SO_3)_2$, $1.6x10^{-4}$ mole $CuCl_2 * 2\ H_2O$, 60ml acetonitrile, $5.0x10^{-2}$ moles 35% H_2O_2, 40psi substrate ($1.9x10^{-2}$ moles), 15 hours at 75°C.

b: 2ml pentane ($2.0x10^{-2}$ moles) used.

c: Percent conversion is based on the total of oxidized products divided by the initial amount of substrate.

calculations. No peroxide was found in the resulting solution. These experiments confirm the role of $CuCl_2$ in producing more alcohol in the oxidation of alkanes.

In the absence of the catalyst and $CuCl_2$, a mixture of H_2O_2 ($5.0x10^{-2}$ moles) and ethanol ($1.9x10^{-2}$ moles) in acetonitrile (60 ml) leads to a 21% decrease of ethanol after 15 hours. Hydrogen peroxide an alcohol under these type of reactive conditions. When the reaction is carried out with $CuCl_2$ ($1.6x10^{-4}$ moles) added, the hydrogen peroxide ($5.0x10^{-2}$ moles) in acetonitrile (60 ml) oxidizes only 9% of the ethanol to acetaldehyde and acetic acid after 15 hours. This experiment demonstrates $CuCl_2$ either complexes the alcohol preventing oxidation or increases the rate of decomposition of the peroxide preventing oxidation of the products.

The effect of increased amounts of $CuCl_2$ on selectivity to the alcohol was investigated using the oxidation of propane at 75°C. The results of these experiments are given in Table 3-5 and illustrated in Figure 3-3.

Successive additions of $CuCl_2$ increased selectivity towards the alcohol with the accompanying decrease in selectivity to the aldehyde and ketone. With increased selectivity, a decrease in overall conversion is observed. This is most likely attributed to peroxide decomposition by the increased copper concentration present. Without $CuCl_2$ a 20.80% conversion is achieved. Addition of 1 mole equivalent decreases the conversion decreases to 18.12%. Additional $CuCl_2$ continues the trend reaching a 6.52% conversion with 5 mole equivalents added. This decrease in conversion is the result of increased peroxide decomposition, leading to a lower concentration of peroxide present to perform catalysts and over-oxidize the products.

Table 3-5: Oxidation Results for Propane @ 75°C with *cis*-$[Ru(dmp)_2(H_2O)](CF_3SO_3)_2$ and Varying Mole Equivalents of $CuCl_2$ using H_2O_2

Mole Equivalents $CuCl_2$[a]	mmoles Alcohol	mmoles Aldehyde	mmoles Ketone	Total mmoles Products	Percent Conversion[b]
0	0.12	2.14	1.18	3.44	20.80
1	0.59	1.45	0.34	2.38	18.24
2	0.84	0.14	0.33	1.30	7.19
3	0.84	0.13	0.32	1.29	7.14
4	0.90	0.11	0.22	1.22	6.73
5	0.91	0.10	0.18	1.18	6.52

a: $1.6x10^{-4}$ mole *cis*-$[Ru(dmp)_2(H_2O)](CF_3SO_3)_2$, $1.6x10^{-4}$ x mole eq. moles $CuCl_2$ * 2 H_2O, 60ml acetonitrile, $5.0x10^{-2}$ moles 35% H_2O_2, 40psi substrate ($1.9x10^{-2}$ moles), 15 hours at 75°C.

b: Percent conversion is based on the total of oxidized products divided by the initial amount of substrate.

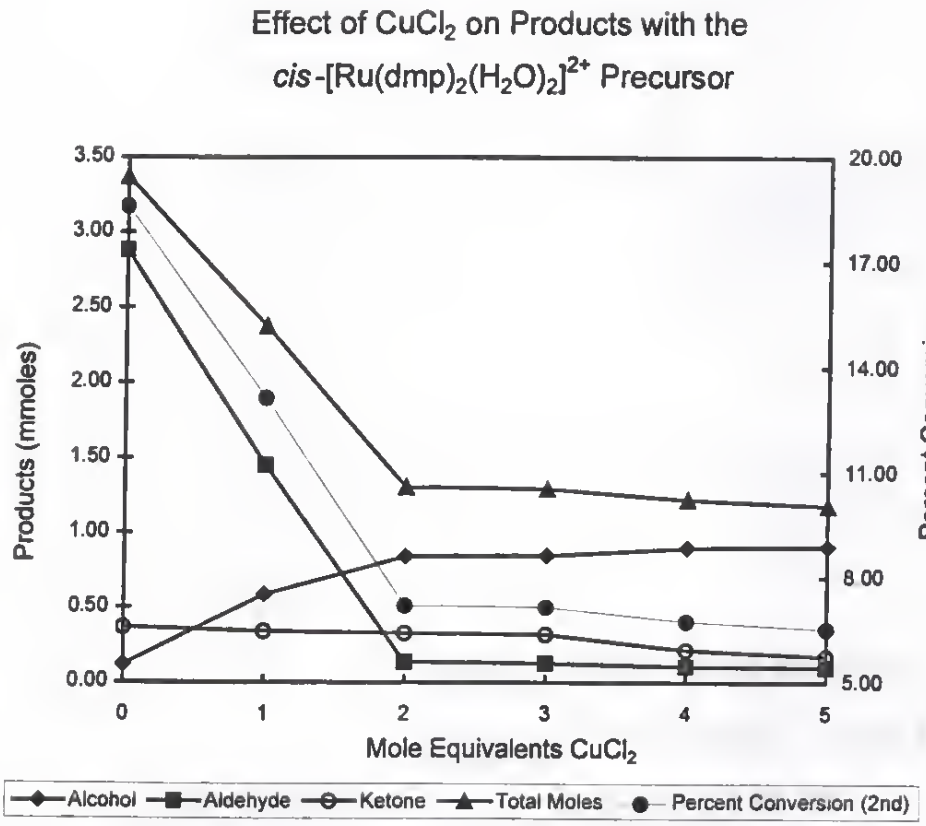

Figure 3-3: Oxidation of Propane with *cis*-$[Ru(dmp)_2(H_2O)](CF_3SO_3)_2$ and Varying Mole Equivalents of $CuCl_2$ using H_2O_2

Effect of Temperature

Increased temperature is expected to increase the rate on an oxidation reaction. Increase in substrate reactivity and solubility of the catalyst is also expected with an increase in reaction temperature. Disadvantages include an increased rate of peroxide decomposition. A series of experiments was performed at 25, 50, 75 and 100°C with and without $CuCl_2$ were performed to determine the effect of temperature on this oxidation reaction. The results provided in Tables 3-6 and 3-7, are illustrated in Figures 3-4 and 3-5.

Propane was again selected as the substrate for these experiments. A mixture of catalyst ($1.6x10^{-4}$ moles), acetonitrile (60 ml), H_2O_2 ($5.0x10^{-2}$ moles) and propane ($1.9x10^{-2}$) were allowed to react for 15 hours at each temperature. Even at 25°C the ruthenium produces oxygenates from propane with a 3.71% conversion. The moles of aldehyde and ketone produced are greater than the moles of alcohol generated. As the temperature increases, overall conversion increases along with an increase in the relative amounts of the aldehyde and ketone. The over-oxidation of alcohol present is also more rapid with the catalyst as the temperature is raised.

An identical series of experiments were performed with the addition of 1 mole equivalent of $CuCl_2$ ($1.6x10^{-4}$ mole). The result are given in Table 3-7 and graphically represented in Figure 3-5. The conversions obtained at high temperatures with $CuCl_2$ present are decreased when compared to those in the absence of $CuCl_2$. Again, a higher selectivity to the alcohol is obtained.

Table 3-6: Oxidation Results for Propane @ Varying Temperatures with *cis*-$[Ru(dmp)_2(H_2O)](CF_3SO_3)_2$ using H_2O_2

Temp. (°C)[a]	Mmoles Alcohol	mmoles Aldehyde	mmoles Ketone	Total mmoles Products	Percent Conversion[b]
25	0.14	0.28	0.26	0.67	3.71
50	0.13	0.55	0.40	1.08	5.52
75	0.12	1.58	0.49	2.19	12.09
100	0.10	2.04	0.89	3.03	16.72

a: 1.6×10^{-4} mole *cis*-$[Ru(dmp)_2(H_2O)](CF_3SO_3)_2$, 60ml acetonitrile, 5.0×10^{-2} moles 35% H_2O_2, 40psi substrate (1.9×10^{-2} moles), 15 hours.

b: Percent conversion is based on the total of oxidized products divided by the initial amount of substrate.

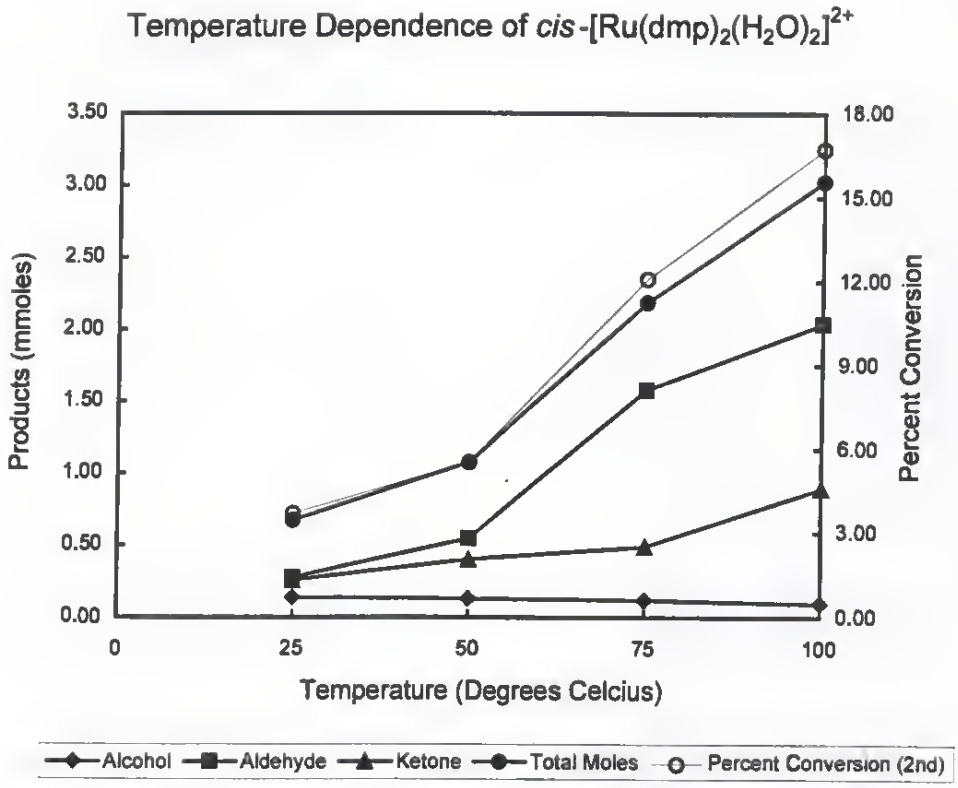

Figure 3-4: Oxidation of Propane @ Varying Temperatures with *cis*-$[Ru(dmp)_2(H_2O)](CF_3SO_3)_2$ using H_2O_2

Table 3-7: Oxidation Results for Propane @ Varying Temperatures with *cis*-$[Ru(dmp)_2(H_2O)](CF_3SO_3)_2$ and $CuCl_2$ using H_2O_2

Temp. (°C)[a]	Mmoles Alcohol	mmoles Aldehyde	mmoles Ketone	Total mmoles Products	Percent Conversion[b]
25	0.23	0.28	0.40	0.91	5.03
50	0.50	0.99	0.43	1.93	9.89
75	0.58	1.45	0.54	2.58	14.23
100	0.66	1.70	0.67	3.03	16.72

a: $1.6x10^{-4}$ mole *cis*-$[Ru(dmp)_2(H_2O)](CF_3SO_3)^2$, $1.6x10^{-4}$ mole $CuCl_2$ * 2 H_2O, 60ml acetonitrile, $5.0x10^{-2}$ moles 35% H_2O_2, 40psi substrate ($1.9x10^{-2}$ moles), 15 hours.

b: Percent conversion is based on the total of oxidized products divided by the initial amount of substrate.

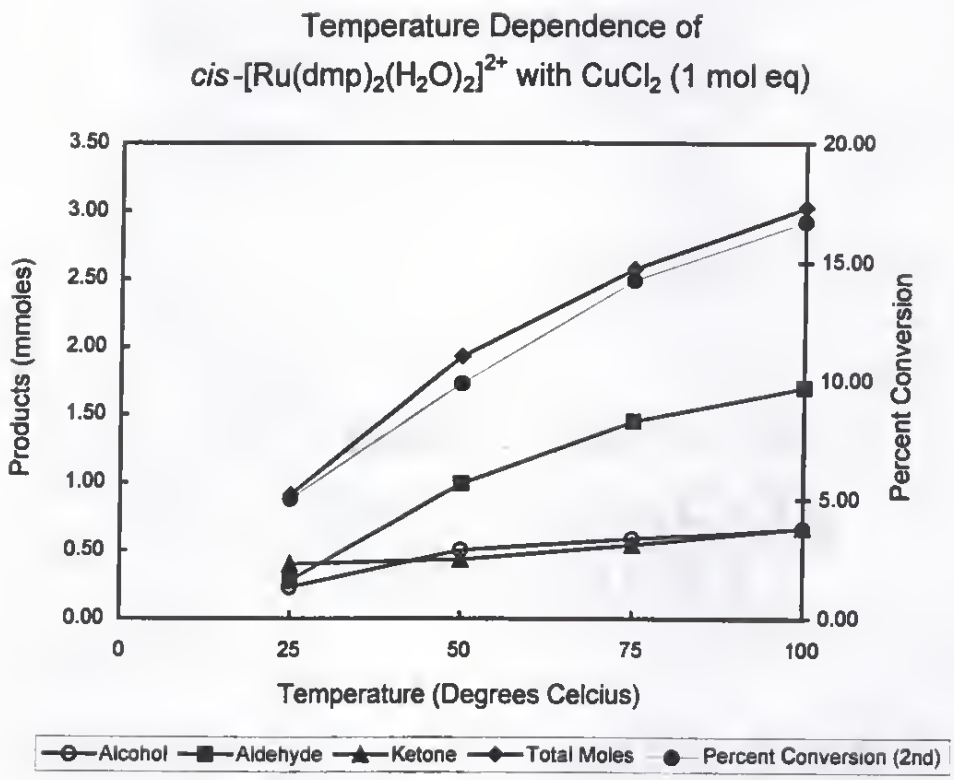

Figure 3-5: Oxidation of Propane @ Varying Temperatures with *cis*-$[Ru(dmp)_2(H_2O)](CF_3SO_3)_2$ and $CuCl_2$ using H_2O_2

Conclusions

The oxidizing ability of the *cis*-$[Ru(dmp)_2(H_2O)_2](CF_3SO_3)_2$ complex to activate linear and branched saturated hydrocarbons has been investigated. Using hydrogen peroxide as the oxidant, production of the respective alcohols and their over-oxidized products are seen after 15 hours at 75°C in an acetonitrile solution. An example of the oxidizing power of this system is shown by the 20.1% conversion of ethane to ethanol (2.3% selectivity, 0.08 mmoles), acetaldehyde (69.3% selectivity, 2.5 mmoles) and acetic acid (28.4% selectivity, 1.0 mmoles).

To deter production of the over-oxidized products and increase the selectivity of the hydroxylated products addition of one mole equivalent of $CuCl_2$ was performed. The addition of $CuCl_2$, illustrates a pronounced effect towards increasing the selectivity to the alcohols. Successive additions of $CuCl_2$ mole equivalents also exhibit a further increase in alcohol selectivity. Blank experiments performed also illustrate the ability of $CuCl_2$ to retard further oxidation of the alcohol. Additional blank experiments performed in the absence of catalyst, produce small quantities of oxidized products demonstrating the catalyst is responsible for the majority of the oxidation.

Temperature dependence studies were also performed with and without the addition of $CuCl_2$. The effect observed is the ability of this catalyst to produce oxygenates of propane at 25°C (3.2% conversion) to 100°C (16.7% conversion). The addition of $CuCl_2$ to the oxidations performed at variable temperatures also allowed for increased selectivity of the alcohol.

CHAPTER 4
SYNTHESIS AND CHARACTERIZATION OF IRON DIMETHYL PHENANTHROLINE COMPLEXES

Introduction

As previously discussed, a high valent metal-oxo complex is required for the activation of alkanes. The *cis*-$[Ru(dmp)_2(H_2O)_2]^{2+}$ precursor is converted to *cis*-$[Ru(O)_2)^{2+}$ to attain this high oxidation state moiety.[40,74] This oxidant effectively oxidizes alkanes with hydrogen peroxide, and methane with hydrogen peroxide and dioxygen.[73] The success with this complex prompted research directed towards the synthesis of analogous complexes in an attempt to prepare a more robust catalyst. This complex should be able to utilize dioxygen without the need of a co-oxidant and be less expensive. First row transition metals might produce a complex with these advantages, therefor the synthesis of an iron based catalyst was investigated.

Iron containing complexes including heme and non-heme enzymes are reported to effectively oxidize alkenes and alkanes.[81,82,83] The development of catalytic systems to mimic a variety of biological systems has been the subject of intense investigation. Cytochrome P-450, peroxidases, catalysases and high valent iron-oxo porphyrin complexes, all involve a 2-electron oxidation producing the reactive intermediate in hydrocarbon oxidation reactions.[69,84]

The use of iron porphyrins as model catalysts has allowed for further understanding of significant steps, which are involved in many enzymatic oxidation reaction mechanisms.[85] More recently, Watanabe and Morishima[82] have demonstrated the use of a (TMP)$Fe^{III}(RCO_2)$, where TMP is 5,10,15,20-tetramesityl porphyrin, complex for the epoxidation of norborylene and α-methylstyrene at -78°C with a variety of peracids. This research has suggested the $O=Fe^{IV}$(TMP) π-cation radical as being the active oxidant for this oxygenation reaction.

Catalysts based on iron complexes in the absence of porphyrins have also been investigated. Que[83] has demonstrated the reactivity of (μ-oxo) di-ferric complexes with *t*-BuOOH for the activation of cyclic hydrocarbons in acetonitrile. The μ-oxo di-ferric complex was synthesized as an effort to model the dinuclear sites found in non-heme iron-enzymes. This $[Fe(TPA)_2O(OAc)](ClO_3)_3$, where TPA is tris-(2-pyridyl)-methyl amine and OAc is acetate, complex is demonstrated to be a robust catalyst for the activation of cyclohexane at ambient temperature and pressure. The oxidation products produced from this reaction are cyclohexanol, cyclohexanone and (*t*-butylperoxy)-cyclohexane. Que has suggested the formation of the alcohol and ketone occur by catalyst initiated decomposition of *t*-BuOOH to afford a high valent metal-oxo complex via a heterolytic pathway. Additional research presented by Que[72] has been directed towards the further investigation of these non-heme iron centers. Furthermore, Que has proposed a high valent $Fe_2(\mu\text{-}O)_2$ diamond core structure, which is believed to be the key oxidizing species of methane monooxygenase (MMO).

Further research using iron coordinated ligand type complexes have also been reported. Sawyer[81] has reported a number of iron (II) complexes [$Fe^{II}L_x$); $Fe(DPAH)_2$, where $DPAH_2$ is 2,6-dicarboxylpyridine, $Fe^{II}(PA)_2$, where PA is picolinic acid, and $Fe^{II}(bpy)^{2+}$, where bpy is 2,2'-bipyridine. Each of these complexes with the addition of a reductant, [DH_2:PhNHNHPh] for example, are able to catalytically activate O_2 (1 atm) for the hydroxylation of phenol and substituted phenol. Results provided indicate the mechanism of oxidation is proceeding via a Fenton like intermediate.

The synthesis of an iron "analogue" based on the *cis*-$[Ru(dmp)_2(H_2O)_2](CF_3SO_3)_2$ complex is the focus of our research. By altering the metal center it is anticipated a more robust catalyst will result. The ligand was not altered due to its ability to impart a cis geometry[40], with respect to the two remaining coordination sites, when the metal is coordinated by two dmp ligands. This geometry, the result of steric hindrance created by the methyl groups α to the nitrogen atoms results in the cis isomer being a more powerful oxidant when compared to the trans counterpart.[74] The lesser oxidizing power of the trans isomer, measured to be on the order of 35 kcal mol^{-1}, [86] is attributed to the lower energy of the HOMO d_{xy}.[40] Additional benefits of this ligand include its ability to prevent the condensation of hydroxo or oxo bridged dinuclear species when two ligands are present on the metal center.

Based on accounts reported in literature and the success of the *cis*-$[Ru(dmp)_2(H_2O)_2]^{2+}$ complex, the synthesis of the iron analogues was attempted. Characterization of these newly formed complexes, as well as investigation for the

production of a high valent iron-oxo species, for the eventual use as an oxidation catalyst, was also performed.

Experimental

Materials and Methods

$FeCl_2 \bullet 4\ H_2O$, 2-9-dimethyl-1,10-phenanthroline, $NaCF_3SO_3$ and LiCl were all used as received from Aldrich. Acetonitrile, acetone and 30% hydrogen peroxide (aq) were all used as received from Fisher Scientific (ACS Grade). Acetonitrile was distilled over P_2O_5 and stored over 4Å molecular sieves.

Physical Measurements

UV-Vis measurements employed a Perkin Elmer lambda-6 spectrophotometer, all spectra were background corrected. Infrared Spectroscopy (IR) analysis were all collected either as Nujol mulls or KBr pellets on a Nicolet 5DXB spectrometer and were background corrected. Nuclear Magnetic Resonance (NMR) measurements were recorder on a multinuclear Varian VXR 300 MHz spectrometer or a multinuclear Gemini 300 MHz spectrometer. All samples analyzed by NMR were performed in deutrated solvents with 1% w/w TMS. Electrochemical studies were performed with a PAR model 175 Universal Programmer connected to a model 173 potentiostat/galvanostat. The electrodes used were a platinum working and auxiliary electrode, with an Ag/AgCl reference electrode. The pH measurements were made with a Fisher Accumet model 630 pH meter. FAB (+ and -) mass spectral data were obtained by Dr. David Powell (U.F.) in a *m*-nitrobenzyl alcohol matrix. Single crystal X-ray diffraction analysis were performed by Dr. Kalih Aboud using a Nicolet diffractometer equipped with a graphite-

monochromated Mo-Kα radiation source. The Nicolet Structure Determination Package was used for data collection, data recovery and structure elucidation. U.F. Analytical Services performed elemental analysis.

Synthesis of Compounds

Iron(II)bis(chloride)mono(2,9-dimethyl-1,10-phenanthroline), [Fe(dmp)Cl_2] (I). A 2.25 g (12 mmol) of 2,9-dimethyl-1,10-phenanthroline was dissolved in 100 ml of acetonitrile under nitrogen at 70°C. Next, 1.25 g (6 mmol) $FeCl_2 \cdot 4H_2O$ was added to the solution. Upon addition of the metal a precipitate is formed immediately. The resulting mixture is allowed to react for 30 minutes, the solution cooled and filtered. The product is then dried under vacuum at 60°C overnight. Analysis: Calculated for $C_{14}H_{12}N_2Cl_2Fe$: C, 50.29; H, 3.59; N, 8.38. Found: C, 50.12; H, 3.46; N, 8.23.

***Cis*-Iron(II)bis(aquo)bis(2,9-dimethyl-1,10-phenanthroline)bis(trifluoro-methanesulfonate), *cis*-[Fe(dmp)$_2$(H_2O)$_2$](CF_3SO_3)$_2$ (II).** This complex was synthesized using modification of a prior method.[86] A 4.5g (24 mmol) of 2,9-dimethyl-1,10-phenanthroline was added to 150 ml of deionized H_2O at 90°C and allowed to stir vigorously for 20 minutes under nitrogen. Upon complete dissolution of the ligand, 2.5g (12 mmol) of $FeCl_2 \cdot 4 H_2O$ was added, the resulting solution was then stirred for 2 hours. The solution is then filtered (hot) and the filtrate immediately added dropwise to a chilled saturated $NaCF_3SO_3$ (aq) solution (25ml H_2O / 9g $NaCF_3SO_3$). The resulting precipitate is allowed to stand in ice for 2 hours and filtered. The product is dried under vacuum at 60°C overnight. Analysis: Calculated for $C_{30}H_{28}N_4O_8F_6S_2Fe$: C, 44.66; H, 3.47; N, 6.94. Found: C, 44.87; H, 3.33; N, 7.01.

Results and Discussion

Characterization

A number of analytical techniques were utilized to characterize the complexes (**I** and **II**) synthesized in this chapter. The conditions employed for each spectroscopic technique are described within the experimental section of this chapter. Any variation in analysis will be described in the appropriate section. Elemental values obtained are provided at the end of each synthesis procedure.

Single Crystal X-ray Diffraction

Single crystal X-ray diffraction analysis was collected for the mono-2,9-dimethyl-1,10-phenanthroline (dmp) complex, $Fe(dmp)Cl_2$ (**I**) to provide structural information and confirm results obtained from elemental analysis. A brown-orange needle of **I** (0.26 x 0.19 x 0.16mm) was mounted on the end of a glass capillary tube and analysis performed. The crystal structure and crystal data obtained are provided in Figure 4-1 and Table 4-1. Additional information for this structure is given in Tables 4-2, 4-5 and 4-6.

In this structure iron has a four coordinate tetrahedral geometry with two coordination sites occupied by the nitrogen atoms of the dmp ligand and the remaining bound to the chlorine atoms leading to a 2^+ oxidation state. The coordination of only one dmp ligand leads to the possibility of μ-oxo dimer formation when this complex is oxidized in the presence of others.

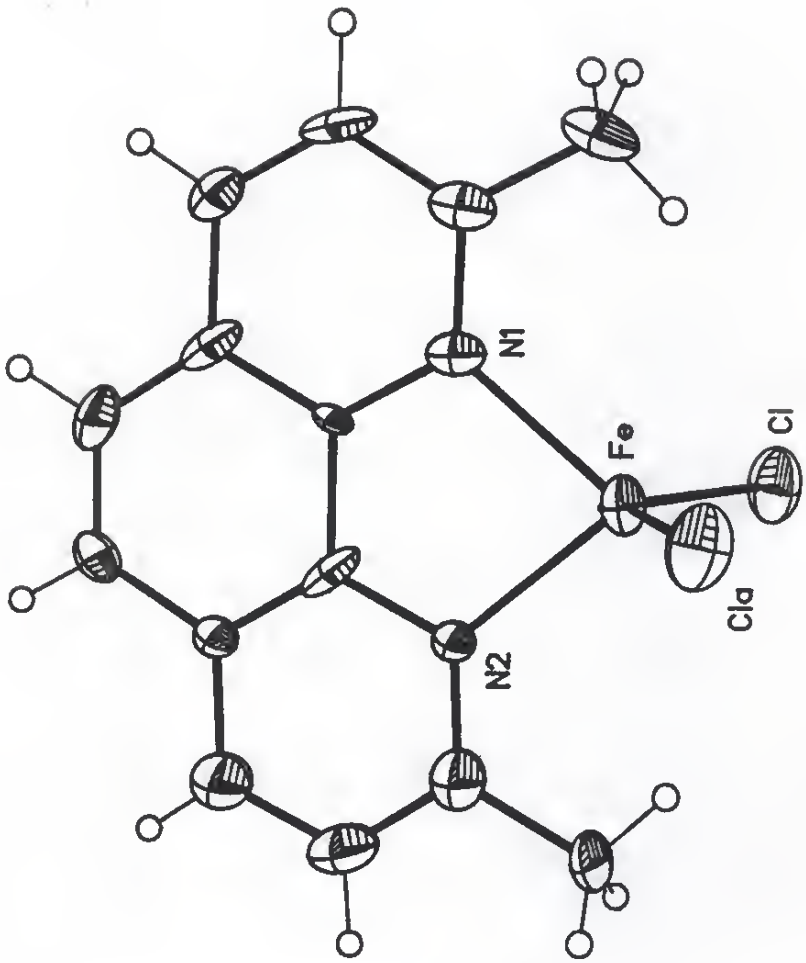

Figure 4-1: Crystal Structure for $Fe(dmp)Cl_2$.

Table 4-1: Crystal Data and Structure Refinement for $Fe(dmp)Cl_2$.

Empirical formula	$C_{14}H_{12}Cl_2FeN_2$
Formula weight	335.01
Temperature	173(2) K
Wavelength	0.71073 Å
Crystal system	Orthorhombic
Space group	Pnma
Unit cell dimensions	a = 11.2265(7) Å α = 90° B = 7.4630(5) Å β = 90° C = 17.788(1) Å γ = 90°
Volume, Z	1490.3(2) $Å^3$, 4
Density (calculated)	1.493 Mg/m^3
Absorption coefficient	1.356 mm^{-1}
F(000)	680
Crystal size	0.26 x 0.19 x 0.16 mm
Theta range for data collection	2.15 to 27.50 deg.
Limiting indices	-5<=h<=15, -4<=k<=10, -24<=l<=18
Reflections collected	5761
Independent reflections	1841 [R(int) = 0.0451]
Absorption correction	Semi-empirical from psi-scans
Max. and min. transmission	0.9660 and 0.7631

Table 4-1 (Cont'd)

Refinement method	Full-matrix least-squares on F^2
Data / restraints / parameters	1823 / 0 / 145
Goodness-of-fit on F^2	1.083
Final R indices [I>2sigma(I)]	R_1 = 0.0343, wR_2 = 0.0794
R indices (all data)	R_1 = 0.0475, wR_2 = 0.0912
Extinction coefficient	0.0070(7)
Largest diff. Peak and hole	0.346 and -0.323 $e.A^{-3}$

Table 4-2: Atomic Coordinates (x 10^4) and Equivalent Isotropic Displacement Parameters (A^2 x 10^3) for $Fe(dmp)Cl_2$.

	x	y	z	U(eq)
Fe	2624(1)	2500	3878(1)	27(1)
Cl	3133(1)	-114(1)	3367(1)	42(1)
N(1)	860(2)	2500	4289(1)	26(1)
N(2)	2936(2)	2500	5050(1)	26(1)
C(1)	-151(3)	2500	3890(2)	33(1)
C(2)	-1268(3)	2500	4257(2)	43(1)
C(3)	-1333(3)	2500	5019(2)	39(1)
C(4)	-277(3)	2500	5451(2)	28(1)
C(5)	799(3)	2500	5057(2)	24(1)
C(6)	1910(3)	2500	5461(2)	24(1)
C(7)	1892(3)	2500	6250(2)	29(1)
C(8)	3011(3)	2500	6613(2)	41(1)
C(9)	4032(3)	2500	6201(2)	43(1)
C(10)	3977(3)	2500	5411(2)	34(1)
C(11)	-263(3)	2500	6258(2)	35(1)
C(12)	775(3)	2500	6640(2)	35(1)
C(13)	-59(4)	2500	3051(2)	49(1)
C(14)	5085(3)	2500	4946(3)	46(1)

Note: U(eq) is defined as one third of the trace of the orthogonalized U_{ij} tensor.

The bond lengths and angles for complex **I** are provided in Tables 4-3 and 4-4 respectively. An important criterion for the determination of a crystal structure's accuracy is the amount of uncertainty in the bond lengths and angles. The small R-value of 4.8% obtained for this structure in the crystal data indicates a great deal of certainty. A bond length of 2.111(3)Å was obtained for the Fe-N(1) bond and 2.114(3)Å for the Fe-N(2) bond, for an average of 2.112Å. These bond lengths are slightly larger than those obtained for the *cis*-$[Ru(dmp)_2(H_2O)_2]^{2+}$ complex. In the ruthenium complex the four Ru-N bond lengths are reported as 2.085, 2.092, 2.063 and 2.094Å for an average length of 2.084Å.[87] Also of interest is the 79.3° N(1)-Fe-N(2) bite angle observed for the $Fe(dmp)Cl_2$ complex, which is almost identical to the 78.9° angle exhibited by the N(1)-Ru-N(2) and N(3)-Ru-N(4) in the *cis*-$[Ru(dmp)_2(H_2O)_2]^{2+}$ complex.

Attempts to obtain a crystal structure for the *cis*-$[Fe(dmp)_2(H_2O)_2](CF_3SO_3)_2$ complex (**II**) were unsuccessful. Crystal growth was attempted in water (acidic and basic conditions), acetonitrile, ethanol, methanol, dimethylforamide (DMF), tetrahyrdofuran (THF), methylene chloride and propylene carbonate, however a suitable crystal could not be obtained. Crystal growth attempted in acetone led to the formation of small orange-brown crystals, which were submitted for single crystal X-ray diffraction. The structure collected illustrated the presence of two protonated dmp ligands, which were not coordinated to iron. The $FeCl_2$ and H_2O molecules were present in the crystal lattice, indicating the instability of this complex. To allow for confirmation of this complex (**II**) an alternative spectroscopic method was needed.

Table 4-3: Bond Lengths [Å] for $Fe(dmp)Cl_2$.

Fe-N(1)	2.111(3)
Fe-N(2)	2.114(3)
Fe-Cl#1	2.2273(6)
Fe-Cl	2.2273(6)
N(1)-C(1)	1.338(4)
N(1)-C(5)	1.368(4)
N(2)-C(10)	1.334(4)
N(2)-C(6)	1.364(4)
C(1)-C(2)	1.414(5)
C(1)-C(13)	1.497(5)
C(2)-C(3)	1.357(6)
C(2)-H(2)	0.86(5)
C(3)-C(4)	1.412(5)
C(3)-H(3)	0.96(4)
C(4)-C(5)	1.396(4)
C(4)-C(11)	1.437(5)
C(5)-C(6)	1.440(4)
C(6)-C(7)	1.403(4)
C(7)-C(8)	1.412(5)
C(7)-C(12)	1.434(5)
C(8)-C(9)	1.361(5)
C(8)-H(8)	0.99(4)
C(9)-C(10)	1.407(5)
C(9)-H(9)	0.95(5)
C(10)-C(14)	1.493(5)
C(11)-C(12)	1.348(5)
C(11)-H(11)	0.94(4)
C(12)-H(12)	0.97(4)
C(13)-H(13A)	0.86(6)
C(13)-H(13B)	0.98(4)
C(14)-H(14A)	0.84(8)
C(14)-H(14B)	0.89(5)

Note: Symmetry transformations used to generate equivalent atoms:
#1 x,-y+1/2,z

Table 4-4: Bond Angles [°] for $Fe(dmp)Cl_2$.

N(1)-Fe-N(2)	79.28(9)
N(1)-Fe-Cl#1	112.48(3)
N(2)-Fe-Cl#1	111.10(3)
N(1)-Fe-Cl	112.48(3)
N(2)-Fe-Cl	111.10(3)
Cl#1-Fe-Cl	122.33(4)
C(1)-N(1)-C(5)	119.1(3)
C(1)-N(1)-Fe	127.7(2)
C(5)-N(1)-Fe	113.1(2)
C(10)-N(2)-C(6)	118.9(3)
C(10)-N(2)-Fe	128.3(2)
C(6)-N(2)-Fe	112.9(2)
N(1)-C(1)-C(2)	120.5(3)
N(1)-C(1)-C(13)	118.1(3)
C(2)-C(1)-C(13)	121.4(3)
C(3)-C(2)-C(1)	120.6(3)
C(3)-C(2)-H(2)	124(3)
C(1)-C(2)-H(2)	116(3)
C(2)-C(3)-C(4)	119.8(3)
C(2)-C(3)-H(3)	124(2)
C(4)-C(3)-H(3)	117(2)
C(5)-C(4)-C(3)	117.0(3)
C(5)-C(4)-C(11)	119.5(3)
C(3)-C(4)-C(11)	123.5(3)
N(1)-C(5)-C(4)	123.0(3)
N(1)-C(5)-C(6)	117.1(3)
C(4)-C(5)-C(6)	119.9(3)
N(2)-C(6)-C(7)	123.2(3)
N(2)-C(6)-C(5)	117.6(3)
C(7)-C(6)-C(5)	119.1(3)
C(6)-C(7)-C(8)	116.4(3)
C(6)-C(7)-C(12)	119.8(3)
C(8)-C(7)-C(12)	123.8(3)
C(9)-C(8)-C(7)	120.2(3)

Table 4-4 (Cont'd)

C(9)-C(8)-H(8)	124(2)
C(7)-C(8)-H(8)	116(2)
C(8)-C(9)-C(10)	120.1(3)
C(8)-C(9)-H(9)	124(3)
C(10)-C(9)-H(9)	116(3)
N(2)-C(10)-C(9)	121.2(3)
N(2)-C(10)-C(14)	117.7(3)
C(9)-C(10)-C(14)	121.1(3)
C(12)-C(11)-C(4)	120.9(3)
C(12)-C(11)-H(11)	124(2)
C(4)-C(11)-H(11)	115(2)
C(11)-C(12)-C(7)	120.8(3)
C(11)-C(12)-H(12)	122(2)
C(7)-C(12)-H(12)	117(2)
C(1)-C(13)-H(13A)	113(4)
C(1)-C(13)-H(13B)	112(2)
H(13A)-C(13)-H(13B)	113(3)
C(10)-C(14)-H(14A)	112(5)
C(10)-C(14)-H(14B)	119(3)
H(14A)-C(14)-H(14B)	105(4)

Note: Symmetry transformations used to generate equivalent atoms:
#1 x,-y+1/2,z

Table 4-5: Anisotropic Displacement Parameters ($A^2 \times 10^3$) for $Fe(dmp)Cl_2$.

	U11	U22	U33	U23	U13	U12
Fe	30(1)	26(1)	24(1)	0	4(1)	0
Cl	47(1)	30(1)	48(1)	-8(1)	14(1)	0(1)
N(1)	26(1)	26(1)	26(1)	0	-3(1)	0
N(2)	21(1)	29(1)	27(1)	0	-1(1)	0
C(1)	34(2)	29(2)	35(2)	0	-13(1)	0
C(2)	27(2)	51(2)	49(2)	0	-16(2)	0
C(3)	20(2)	44(2)	51(2)	0	-2(2)	0
C(4)	21(1)	29(2)	34(2)	0	0(1)	0
C(5)	23(1)	23(1)	26(1)	0	-3(1)	0
C(6)	20(1)	25(2)	27(1)	0	0(1)	0
C(7)	28(2)	34(2)	26(2)	0	-2(1)	0
C(8)	36(2)	61(3)	25(2)	0	-7(1)	0
C(9)	27(2)	63(3)	38(2)	0	-9(1)	0
C(10)	20(2)	43(2)	37(2)	0	-3(1)	0
C(11)	29(2)	44(2)	31(2)	0	9(1)	0
C(12)	39(2)	45(2)	20(2)	0	5(1)	0
C(13)	51(2)	60(3)	36(2)	0	-19(2)	0
C(14)	22(2)	62(3)	53(2)	0	6(2)	0

Note: The anisotropic displacement factor exponent takes the form:

$$-2\pi^2 [h^2 a^2 * U11 + ... + 2 h k a^* b^* U12]$$

Table 4-6: Hydrogen Coordinates (x 10^4) and Isotropic Displacement Parameters (A^2 x 10^3) for $Fe(dmp)Cl_2$.

	x	y	z	U(eq)
H(2)	-1880(41)	2500	3965(24)	52(13)
H(3)	-2070(34)	2500	5293(21)	35(10)
H(8)	2993(31)	2500	7167(21)	32(9)
H(9)	4811(41)	2500	6416(24)	54(12)
H(11)	-1016(35)	2500	6489(21)	40(11)
H(12)	803(33)	2500	7186(22)	39(10)
H(13A)	-747(55)	2500	2833(32)	94(20)
H(13B)	461(35)	1536(50)	2870(21)	92(13)
H(14A)	5698(69)	2500	5213(41)	129(28)
H(14B)	5197(41)	1613(64)	4623(24)	124(19)

FAB Analysis

The analytical method chosen for further characterization of complex **II** was fast atom bombardment (FAB) (positive (+) and negative (-)). FAB mass spectroscopy spectral analysis permits the determination of a complex's atomic weight, including the identification of cations (FAB^+) or anions (FAB^-) specifically. The results obtained from FAB mass spectrometry of complex **II** are illustrated in Figure 4-2.

The FAB^+ spectrum contains a number of peaks each of which were correlated to predicted fragments from the *cis*-$[Fe(dmp)_2(H_2O)_2]$ $(CF_3SO_3)_2$ complex. A peak at 638.3 amu was found to correspond to the *cis*-$[Fe(dmp)_2(H_2O)_2](CF_3SO_3)^+$ fragment. Further fragmentation of the title complex yielded peaks at 507.2 amu (*cis*-$[Fe(dmp)_2(H_2O)_2]^{2+}$), 299.0 amu ($[Fe(dmp)(H_2O)_2]^{2+}$) and 209.1 amu (dmp^+). The inability to identify the complete complex is due to its overall neutral charge. To further characterize complex **II**, FAB^- spectroscopy was performed. In this spectrum a peak at 155 amu which corresponds to the CF_3SO_3 anion was found.

IR Analysis

Although there is limited variability for the coordination of the two dmp ligands, IR spectroscopy was employed to further investigate coordination of the ligands in complex **II**. The IR spectra obtained are illustrated in Figure 4-3. Sauvage and Collin[88] have reported the infrared spectral bands for the *cis*-$[Ru(dmp)_2(H_2O)_2]^{2+}$ complex. Since the only difference between this complex and our *cis*-$[Fe(dmp)_2(H_2O)_2](CF_3SO_3)_2$ is the

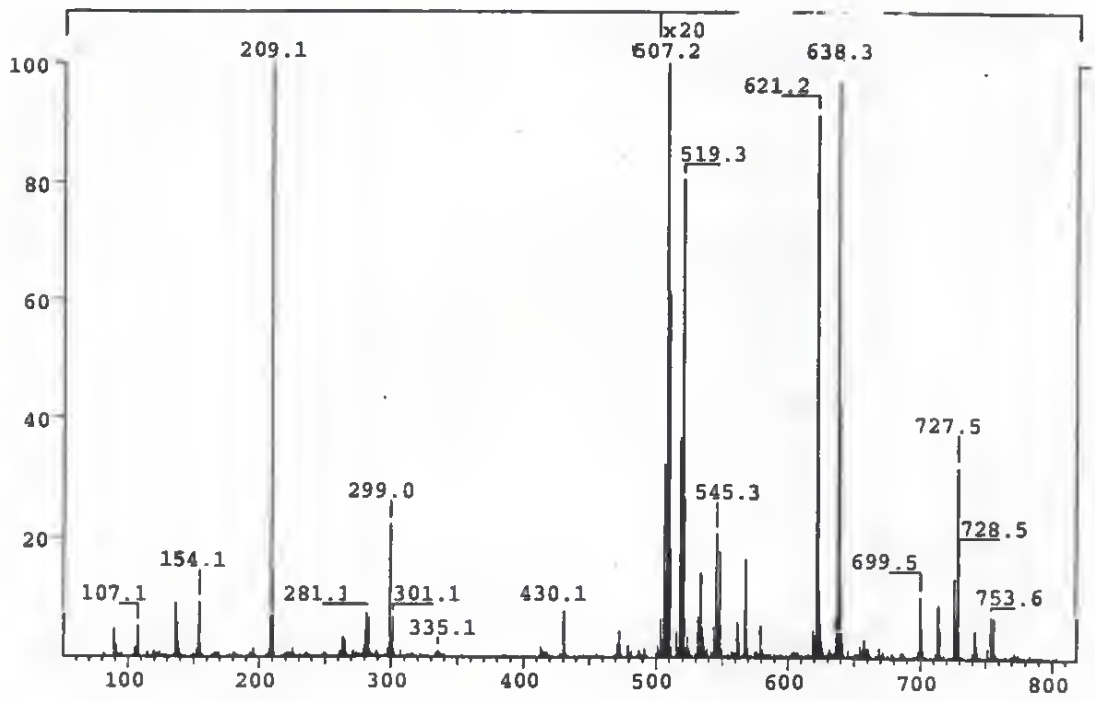

Figure 4-2: FAB$^+$ Spectral Results for *cis*-$[Fe(dmp)_2(H_2O)_2](CF_3SO_3)_2$.

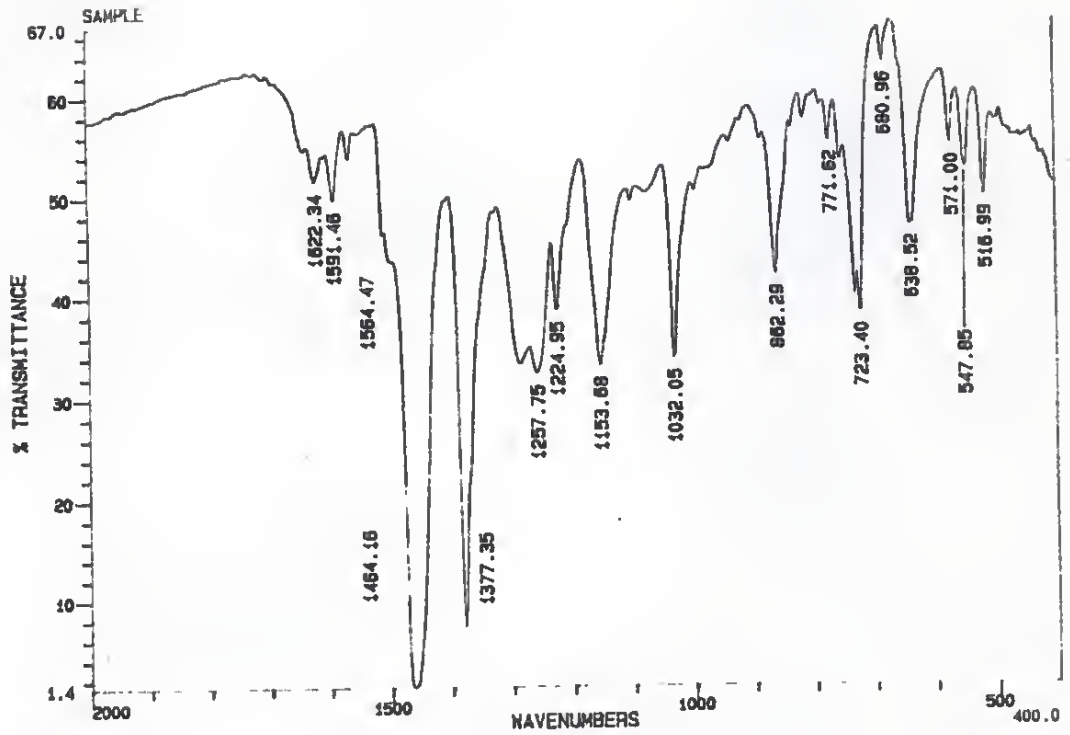

Figure 4-3: Infrared Spectrum for *cis*-$[Fe(dmp)_2(H_2O)_2](CF_3SO_3)_2$.

metal center, the spectra obtained should be similar with only a small shift in the bands for the iron complex. The following bands were reported for the ruthenium complex: 1630, 1580, 1500, 1280, 1220, 1050, 860, 730, 560, 530 and 500 cm^{-1}. IR analysis performed on complex **II** exhibited the following bands: 1622, 1564, 1464, 1257, 1153, 1032, 862, 771, 571, 543 and 518 cm-1. Upon comparison of the two sets observed, a small shift is exhibited, suggesting the iron complex synthesized is analogous in coordination to the ruthenium complex.

NMR Analysis

A number of NMR experiments were performed to further characterize the newly synthesized $Fe(dmp)Cl_2$ and *cis*-$[Fe(dmp)_2(H_2O)_2](CF_3SO_3)_2$ complexes. The ^1H NMR spectrum of complex **I**, $Fe(dmp)Cl_2$, in deutrated acetonitrile is provided in Figure 4-4. In this spectrum, a single methyl resonance at 2.0 ppm is expected since both ancillary methyl groups on the phenanthroline ligand are chemically equivalent. In the aromatic region, 7 to 9 ppm, the presence of two doublets (7.6 and 8.3 ppm) and one singlet (7.8 ppm) are found from the coordination of only one dmp ligand.

Obtaining an NMR spectrum for the *cis*-$[Fe(dmp)_2(H_2O)_2](CF_3SO_3)_2$ complex was difficult. The use of ^1H NMR spectroscopy would allow for further determination of the dmp ligand geometry about the metal center. Spectra could not be obtained in deutrated water, acetonitrile and methylene chloride due to the slight solubility of the complex. Greater solubility of this complex (**II**) occurs in acetone. The resulting solution in deutrated acetone was passed through a syringe filter, to remove any undissolved

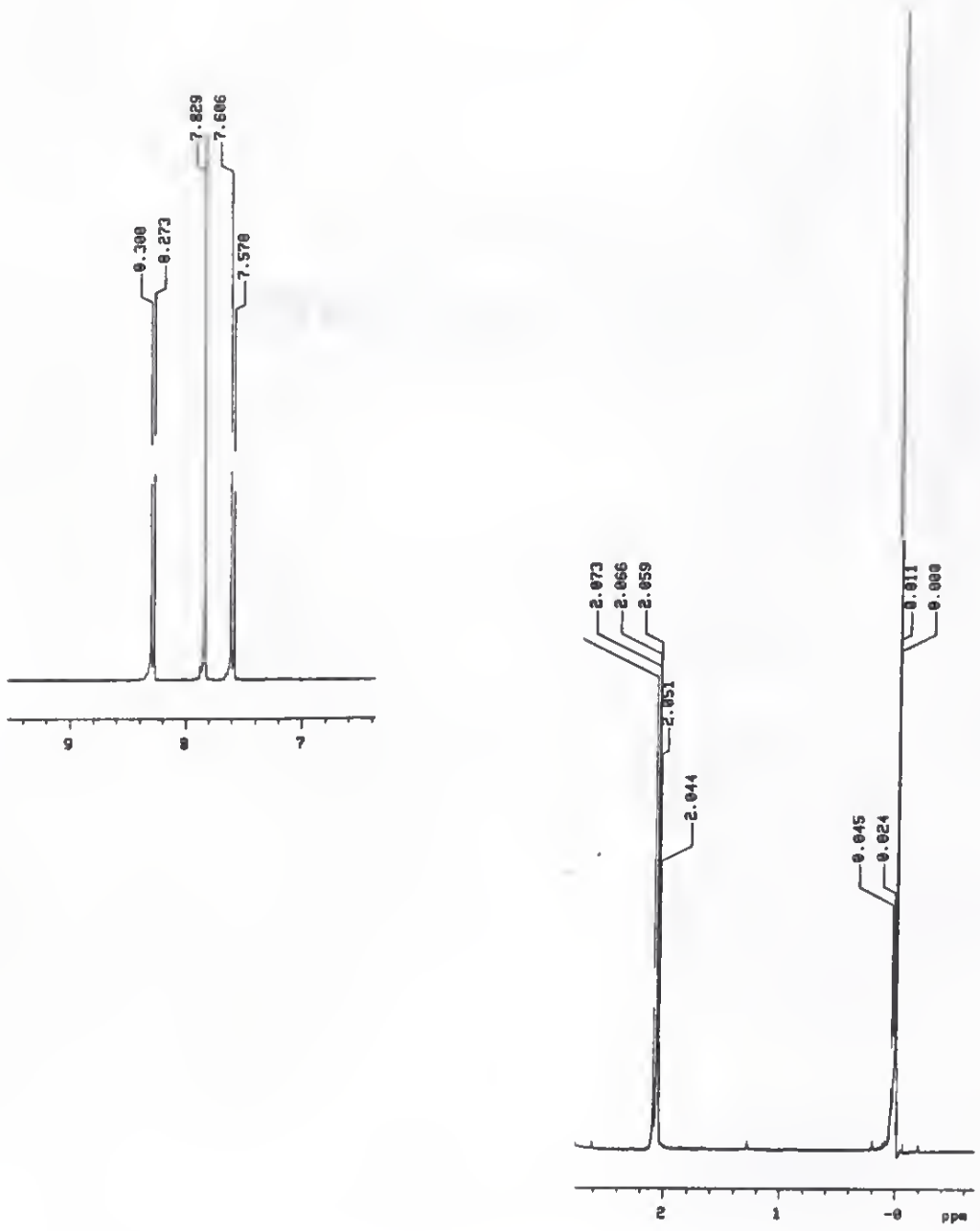

Figure 4-4: ^{1}H NMR Spectrum for $Fe(dmp)Cl_2$.

particulates, and added to the NMR sample tube. This NMR spectrum is shown in Figure 4-5. Two non-equivalent methyl peaks, the result of each methyl being chemically non-equivalent, at 2.0 and 3.1 ppm indicate the expected *cis* geometry. However, a detailed spectrum in the aromatic region was not obtained. The expected 3 sets of AB systems (3.4; 5,6; 7,8) characteristic of a di-substituted phenanthroline are not observed because of broadening of the peaks in the aromatic region. This broadening is attributed to iron (III) impurities in the complex. Several ^{1}H NMR spectra on different batches of purified complexes, each produced the same result.

Upon review of the literature the synthesis and crystal structure for the $Fe(dmp)_2(NCS)_2 \cdot ¼ H_2O$ complex was found, which proceeds through a membrane[89]. In one compartment $FeCl_2 \cdot 4 H_2O$ (1 mmol) and dmp (1.9 mmol) are mixed into a 30% H_2O / 70% ethanol solution. The other compartment contains an aqueous solution of 15 ml NaSCN (2.4 mmol). Crystal formation occurs at the interface after several days. Single crystal analysis confirmed the synthesis of this compound and is provided in Figure 4-6.[89]

In this structure the octahedral iron center is bound to the four nitrogen atoms of the two dmp ligands and the two nitrogen atoms from the thiocynate ligands in a *cis* orientation with respect to the two thiocynate ligands. The dmp ligands also impart a distortion on the octahedral metal center which is greater than the 76.1° angle observed for the $Fe(phen)_2(NCS)_2$ complex, where phen is 1,10-phenanthroline.[89] The phen-anthroline complex gives a trans orientation producing a much larger N-Fe-N angle. The smaller N-Fe-N angles, the result of the ligands trying to remain on different planes,

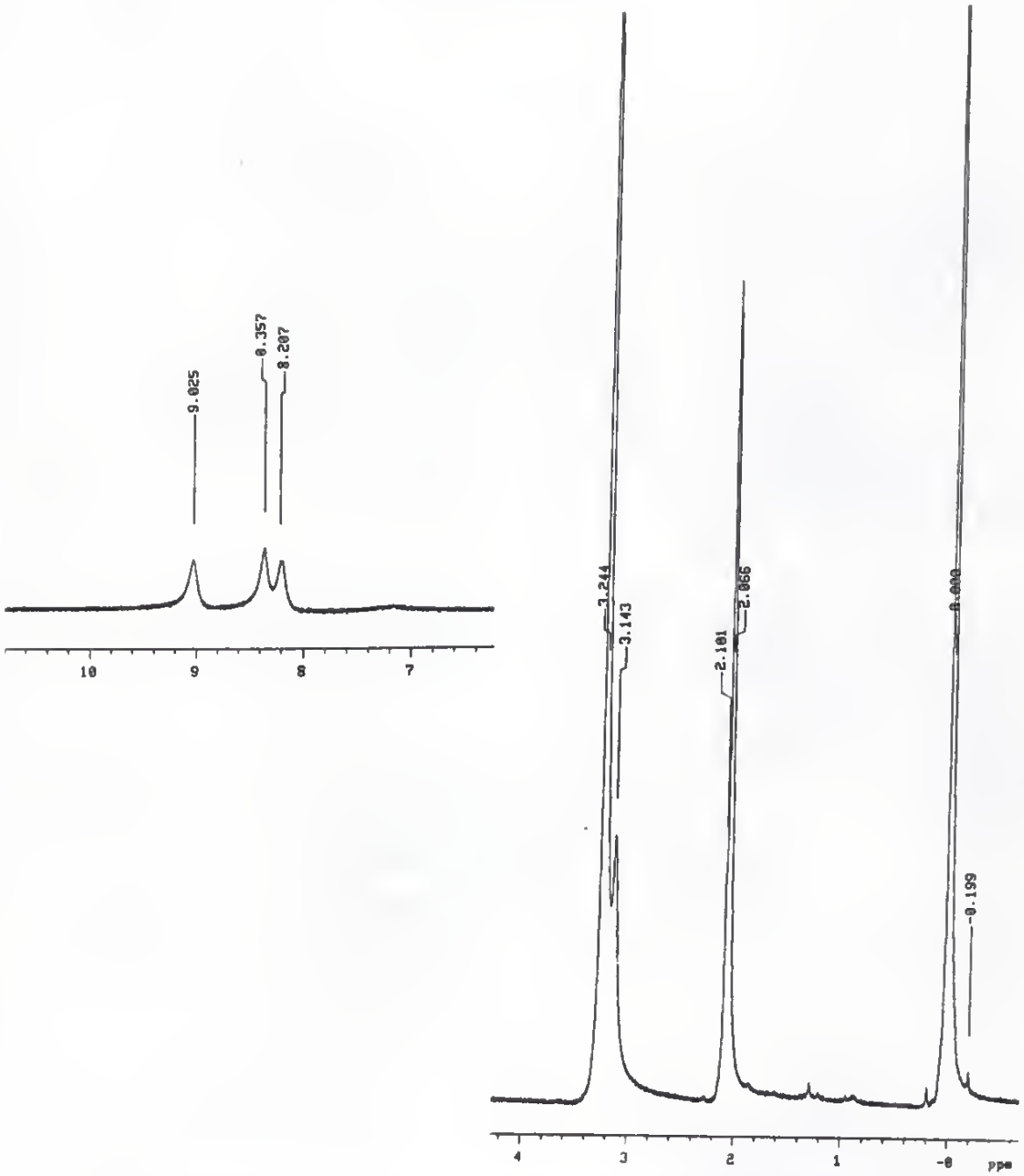

Figure 4-5: ^{1}H NMR Spectrum for *cis*-$[Fe(dmp)_2(H_2O)_2](CF_3SO_3)_2$.

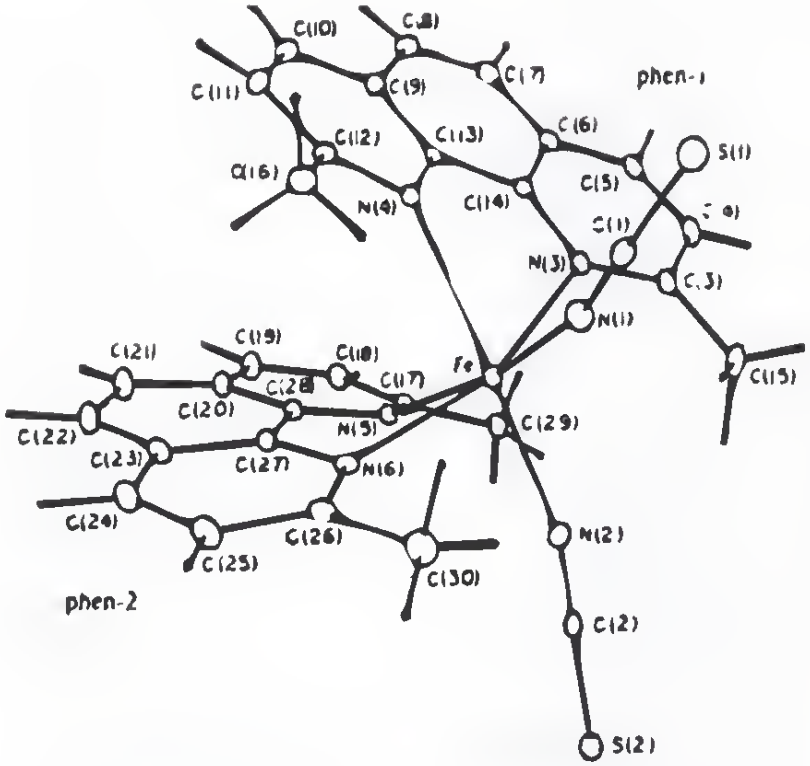

Figure 4-6: Crystal Structure for *cis*-$Fe(dmp)_2(NCS)_2$.[89]

exhibited by the *cis*-$Fe(dmp)_2(NCS)_2$ complex are attributed to the methyl groups on this ligand,. Thus inhibiting formation of the trans isomer. The average bite angle (N-Fe-N) for the dmp complex is 73.0°; identical to that obtained for the $Fe(dmp)Cl_2$ complex (**I**). This angle is also smaller than those observed for iron complexes with other non-substituted ligands. Such examples are $Fe(phen)_2(NCS)_2$ (76.1°)[89], $Fe(bpy)_2(NCS)_2$ (75.1°)[90] and $Fe(bt)_2(NCS)_2$ (73.8°).[91] The substituted ligand forces a distortion about the metal center. The effect of distortion is the result of the inability of the two ligands to reside on the same plane. As the ligands are forced to opposite planes the N-Metal-N bite angle becomes smaller.

Heber related the Fe-N bond distances to crystal field arguments. The two $Fe\text{-}N_{CS}$ distances observed in this complex average out to 2.067Å and the four $Fe\text{-}N_{DMP}$ bond distances average out to 2.27 Å. The $Fe\text{-}N_{DMP}$ bond distance average is reported to be the longest average reported in literature for an iron (II) complex with a bi-dentate nitrogen donor ligand.[90,91,92,93] This elongated iron-nitrogen bond explains the difficulty we encountered in crystal growth. Heber attributes the abnormally elongated Fe-N to steric crowding from each dmp ligand. Each dmp ligand is bending away from the other causing elongation of the bond. In addition a large dihedral angle (153.5°) is observed between each dmp ligand, much larger than the 86.9° angle observed in the $Fe(phen)_2(NCS)_2$ complex. The deviation of Fe from the dmp plane suggests the π-back donation from the ligand to the iron metal center should be significantly reduced when compared to the unsubstituted $Fe(phen)_2(NCS)_2$ complex.

IR, NMR and FAB^+ spectral analysis confirms the synthesis of the *cis*-$[Fe(dmp)_2(H_2O)_2](CF_3SO_3)_2$ complex.

High Valent Iron-Oxo Formation Studies

The generation of a high valent iron-oxo species must occur in order for these complexes to be efficient catalysts for the activation of alkanes. The characterization of a such species, in this case *cis*-$[Fe(dmp)_2(O)(H_2O)]^{2+}$ or *cis*-$[Fe(dmp)_2(O)_2)]^{2+}$ was attempted with Ultraviolet-Visible spectroscopy.

The formation of a high valent iron (V)-oxo complex with a porphorin ligand by oxidation of an iron (III) complex with hydrogen peroxide has been reported by Larpent[92]. Equation 4-1 illustrates this reaction. The newly formed $Fe^{(V)}=O$ species is then able to hydroxylate the alkane producing an alcohol and the reduced Fe(III) complex. Upon addition of hydrogen peroxide the $Fe^{(V)}=O$ complex is regenerated closing the catalytic cycle.

(Equation 4-1):

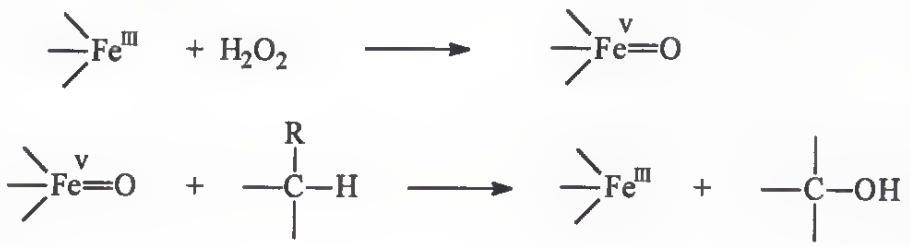

As with other attempts to characterize the *cis*-$[Fe(dmp)_2(H_2O)_2](CF_3SO_3)_2$ complex, problems were encountered. An UV-VIS spectrum was taken with $1.6x10^{-4}$ moles of complex (II) dissolved in 60 ml of acetonitrile. Next, hydrogen peroxide was

added in $4.0x10^{-5}$ mol aliquots until a total of $3.2x10^{-4}$ moles had been added, with a UV-VIS spectrum taken after addition of each aliquot. The full range of spectra acquired is illustrated in Figure 4-7.

It was anticipated upon addition of each hydrogen peroxide aliquot a spectral change would be observed, resulting in formation higher oxidation state species. These new species would allow for identification in change of the oxidation state of the complex. Analysis of these spectra illustrates minimal formation of other species. Analysis of the initial spectra (faint yellow solution) resulted in a peak at 276nm and a small shoulder at 295nm. Upon addition of each aliquot of hydrogen peroxide the solution became orange brown (dark) in color resulting in an a small shift and increase in absorbance for each peak. After complete addition of the hydrogen peroxide, the peak at 276nm has become split into two smaller peaks. Analysis of each peak was unable to provide any additional information.

Although this UV-VIS experiments performed resulted in the inconclusive evidence for the formation of a high valent iron-oxo. Results published by Larpent[92] have demonstrated the formation of such iron-oxo compound with the addition of hydrogen peroxide. Que[83] has also reported the generation of an iron-oxo species upon addition of *t*-BuOOH. In our situation the resulting spectra for the newly formed iron-oxo species could be similar to that for the *cis*-$[Ru(dmp)_2(H_2O)_2](CF_3SO_3)_2$ complex. To investigate the ability of the *cis*-$[Fe(dmp)_2(H_2O)_2](CF_3SO_3)_2$ complex to react with hydrogen peroxide the following experiment was performed. To 60 ml of acetonitrile $1.6x10^{-4}$ moles this complex was added, followed by addition of $3.2x10^{-4}$ moles of

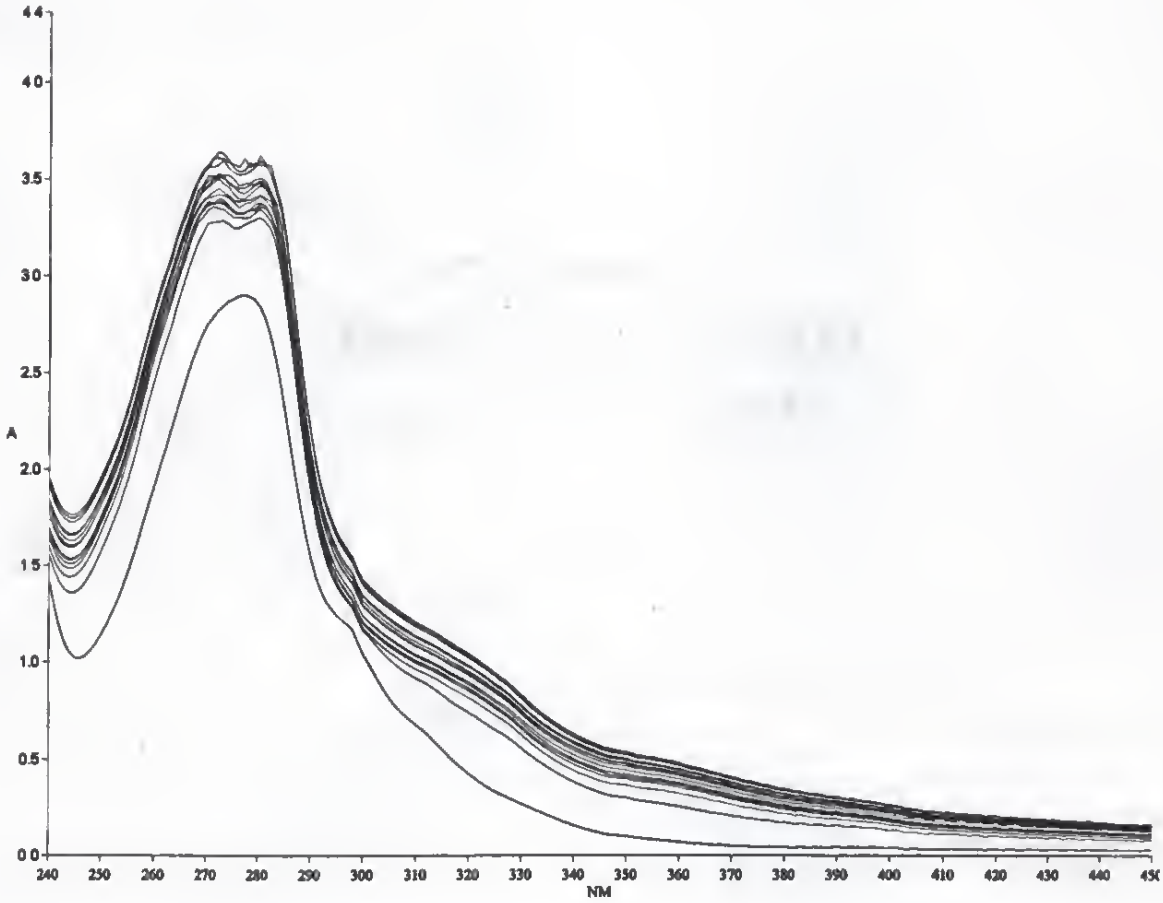

Figure 4-7: UV-VIS Spectra for the Addition of H_2O_2 to *cis*-$[Fe(dmp)_2(H_2O)_2](CF_3SO_3)$.

hydrogen peroxide. Upon addition of the hydrogen peroxide effervescence was exhibited, the result of hydrogen peroxide decomposition which may led to formation of the desired high valent iron-oxo species. The solution was allowed to stir for 10 hours at room temperature, at this point an iodometric titration of the solution was taken. The results obtained indicated an 88% decrease in the peroxide concentration due to decomposition. This result suggests the ability of our complex to be oxidized by H_2O_2, however the inability to identify this newly formed species still exist.

An identical set of UV-VIS experiments were also performed for the $Fe(dmp)Cl_2$ complex. The experiment for the stepwise addition of hydrogen peroxide produced the spectra, which is illustrated in Figure 4-7. In these spectra formation of the high valent iron-oxo species did not occur. What did result was the formation of a new peak (392nm) after addition of one hydrogen peroxide aliquot as well as a shift of the original peak (333 to 369nm). Upon additional aliquots a small shift of the new peak is observed. This peak could possibly be a mono-oxo iron species, $[Fe(dmp)H_2O(O)]^{2+}$. However exact confirmation of this could not be obtained. The experiment for the generation of a high valent iron-oxo also suggested formation of such species. Iodometric titration results exhibited a 95% decrease of hydrogen peroxide after ten hours at room temperature. A difficulty in quantification of any iron-oxo species generated is attributed to the uncertainty of the amount of peroxide lost to decomposition.

Conclusions

The synthesis and characterization of two additional "analogues" $Fe(dmp)Cl_2$ (**I**) and *cis*-$[Fe(dmp)_2(H_2O)_2]$ $(CF_3SO_3)_2$ (**II**) have been performed. Characterization of

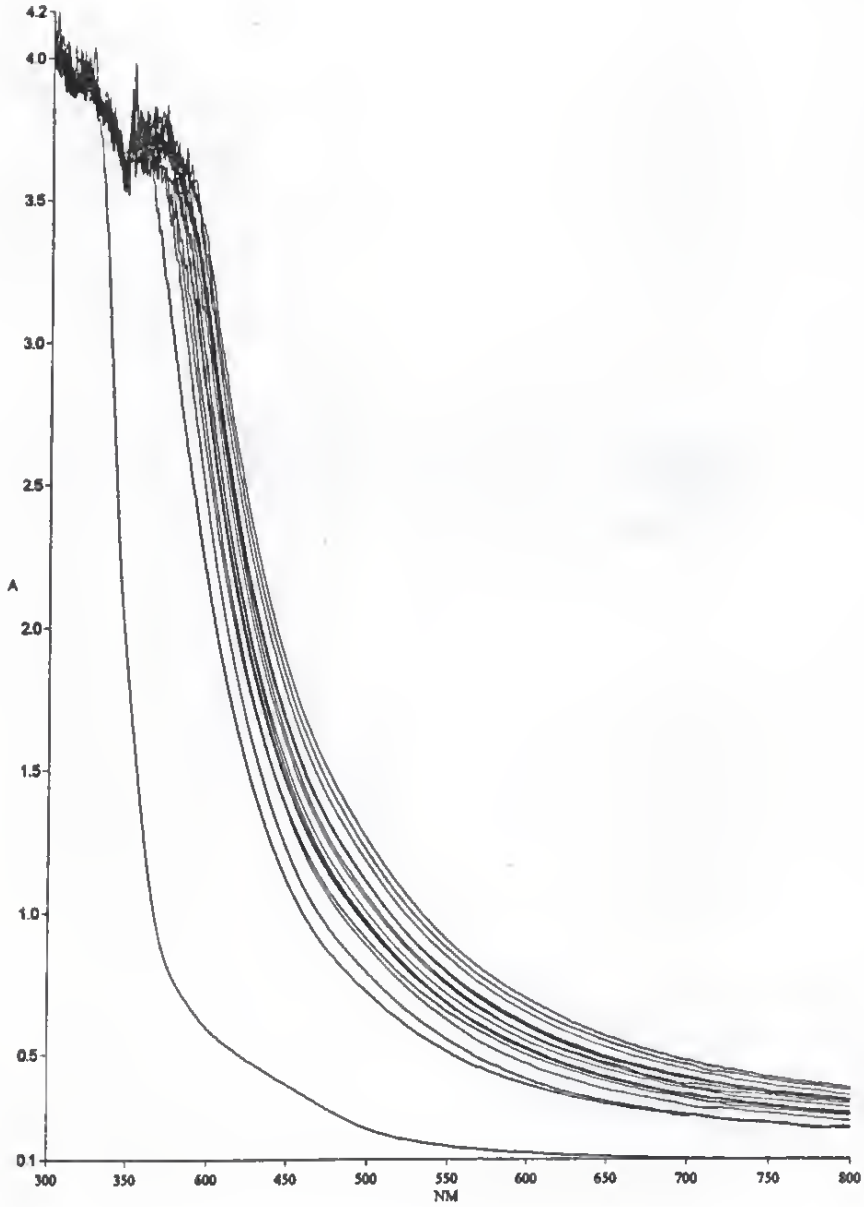

Figure 4-8: UV-VIS Spectra for the Addition of H_2O_2 to Fe(dmp)Cl_2.

complex **I** by X-ray crystallography analysis exhibits iron in a tetrahedral geometry, complexed by only one dmp ligand. Further analysis of this complex by IR, FAB^+, FAB^-, and NMR were also performed. Although a crystal structure for complex **II** was not obtained, characterization was determined using FAB^+, FAB^-, IR and NMR spectroscopy. Complex (**II**) has iron in an octahedral geometry, complexed by two dmp ligands, which enforce the desired cis geometry.

Attempts to generate and characterize high valent iron-oxo species for the two newly synthesized complexes were also attempted, however data obtained does not allow for conclusive evidence to be drawn at this time.

CHAPTER 5
OXIDATION OF ALKANES WITH HYDROGEN PEROXIDE USING AN IRON METAL-OXO CATALYST

Introduction

A substantial amount of interest for use of non-heme complexes as catalysts for the activation of alkanes has occurred in recent years. These complexes, similar to methane monooxygenase or P-450, serve as models to the reactivity of non-heme iron centers in enzymes.[70,94,95,96,97,98] Of these complexes, those described as being the most active normally employ nitrogen based pyridine ligands. These ligands are preferred due to the enhance electrophillicity they provide to the metal center. Some examples of complexes which utilize the pyridine based ligands include Bartons's[70] "Gif" catalyst, Fontecave's[95] $[Fe_2O(byp)_4]^{4+}$/*t*-BuOOH complex and Que's[97] Fe(TPA)/*t*-BuOOH system where TPA is tris(2-pyridylmethyl)amine. The newly synthesized iron complexes: $[Fe(dmp)Cl_2]$ (**I**) and *cis*-$[Fe(dmp)_2(H_2O)_2](CF_3SO_3)_2$ (**II**) also fall within this category, however hydrogen peroxide is the oxidant used in our catalytic system.

All of the above mentioned catalytic systems have precursors metal complexes which have the ability to generate a metal-peroxide intermediate or a high valent iron-oxo species. Either of these species is necessary for the successful functionalization of an alkane as shown in Equation 5-1.

(Equation 5-1)

$$RH + LFe^{III}\text{-}OOR \text{ or } LFe^{V}=O \longrightarrow R^{\cdot} + Fe^{IV}\text{-}OH$$

$$\longrightarrow R\text{-}OH + LFe^{III}$$

We have investigated the use of the *cis*-$[Fe(dmp)_2(H_2O)_2](CF_3SO_3)_2$ (**II**) complex for the activation of methane at 75°C in an acetic acid/acetic anhydride solvent mixture. To further demonstrate the ability of this complex to activate methane, oxidation experiments using molecular oxygen were also performed at ambient and high pressures. Furthermore, complex (**II**) and the $[Fe(dmp)Cl_2]$ (**I**) precursor were also investigated for the activation of C_2-C_5 linear and branched alkanes with hydrogen peroxide at 75°C in acetonitrile. Although significant selectivity profiles to products were achieved, attempts to further increase selectivity to the hydroxylated product with addition of a mole equivalent of a metal chloride was also performed. The effects of additional mole equivalents and temperature dependence on the catalyst's activity as well as mechanistic considerations were also investigated.

Experimental

Materials and Methods

$FeCl_2 \cdot 4\ H_2O$, 2-9-dimethyl-1,10-phenanthroline, $NaCF_3SO_3$ and LiCl were all used as received from Aldrich. Acetonitrile, acetone and 30% hydrogen peroxide (aq)

were all used as received from Fisher Scientific (ACS Grade). Acetonitrile was distilled over P_2O_5 and stored over 4Å molecular sieves.

Physical Measurements

The pH measurements were made with a Fisher Accumet model 630 pH meter. U.F. Analytical Services performed elemental analysis.

Synthesis of Compounds

Iron(II)bis(chloride)mono(2,9-dimethyl-1,10-phenanthroline), [Fe(dmp)Cl_2] (I). A 2.25 g (12 mmol) of 2,9-dimethyl-1,10-phenanthroline was dissolved in 100 ml of acetonitrile under nitrogen at 70°C. Next, 1.25 g (6 mmol) $FeCl_2 \cdot 4H_2O$ was added to the solution. Upon addition of the metal a precipitate is formed immediately. The resulting mixture is allowed to react for 30 minutes, the solution cooled and filtered. The product is then dried under vacuum at 60°C overnight. Analysis: Calculated for $C_{14}H_{12}N_2Cl_2Fe$: C, 50.29; H, 3.59; N, 8.38. Found: C, 50.12; H, 3.46; N, 8.23.

***Cis*-Iron(II)his(aquo)bis(2,9-dimethyl-1,10-phenanthroline)bis(trifluoro-methanesulfonate), *cis*-[Fe(dmp)$_2$(H_2O)$_2$](CF_3SO_3)$_2$ (II).** This complex was synthesized using modification of a prior method.[86] A 4.5g (24 mmol) of 2,9-dimethyl-1,10-phenanthroline was added to 150 ml of deionized H_2O at 90°C and allowed to stir vigorously for 20 minutes under nitrogen. Upon complete dissolution of the ligand, 2.5g (12 mmol) of $FeCl_2 \cdot 4 H_2O$ was added, the resulting solution was then stirred for 2 hours. The solution is then filtered (hot) and the filtrate immediately added dropwise to a chilled saturated $NaCF_3SO_3$ (aq) solution (25ml H_2O / 9g $NaCF_3SO_3$). The resulting precipitate is allowed to stand in ice for 2 hours and filtered. The product is dried under vacuum at

60°C overnight. Analysis: Calculated for $C_{30}H_{28}N_4O_8F_6S_2Fe$: C, 44.66; H, 3.47; N, 6.94. Found: C, 44.87; H, 3.33; N, 7.01.

Oxidation Procedure

The pressurized oxidations were carried out as previously described[49], in glass, batch hydrogenation reactors. Figure 2-5 provides an illustration of such batch reactor. The reaction mixtures were varied as described in the table footnotes. Blank runs omitting certain reactants and solvent components are also described in the tables. Oxidations with oxygen use 30 psig of a 5% O_2 in helium mixture, to remain outside the explosion limits, and 20 psig alkane. Reaction temperatures normally were maintained between 75 to 77°C. To remove air initially present, nitrogen gas is purged through the reactor, the apparatus is pressurized with the substrate, which is then released, and re-pressurized to the desired pressure.

Oxidation of Methane

The oxygenated products of the reaction were analyzed and quantified with a Hewlett-Packard 5890 gas chromatograph equipped with a F ID detector and outfitted with a 30m Alltech RSL 160 column (5μm thickness). Helium was employed as the carrier gas. Carbon dioxide and carbon monoxide analyses were performed with a Varian 3700 gas chromatograph equipped with a TCD detector outfitted with a 15' Carboxen Column. Methane was quantified by gas chromatography (TCD) using N_2 as an internal standard. Three chromatograms were measured for each sample using injection volumes of 0.1ml for gas and 0.1μl for liquid samples.

The following definitions describe terms used in the presentation of the results. Selectivity to any product is the moles of a given product divided by the total moles of all products formed expressed in percent. The percent CO_2 produced is moles of CO_2 divided by the moles of all products. The selectivity to oxygenates is the moles of H_2CO, CH_3OH and $CH_3C(O)OCH_3$ divided by the total moles of products in percent. Traces of $CH_2(OCH_3)_2$, $HCOOCH_3$ are formed, but not quantified. Percent peroxide efficiency is the moles of H_2O_2 needed to account for all oxidized products including CO_2 divided by the moles of H_2O_2 consumed. The percent conversion of CH_4 is the moles carbon in the oxidized products divided by the moles of CH_4 added to the reactor.

Oxidation of Higher Alkanes

The oxygenated products of the reaction were analyzed and quantified with a Hewlett-Packard 5890 Series II gas chromatograph equipped with an FID detector and outfitted with a 30m HP 50+ (50% Ph Me Silicone Gum; 1 μm thickness). Helium was employed as the carrier gas. Carbon dioxide and carbon monoxide analysis were performed with a Varian 3700 gas chromatograph equipped with a TCD detector outfitted with a 15' Carboxen Column, 1 μm thickness. Helium was utilized as the carrier gas. Concentrations of the substrate and oxidized products were quantified using acetonitrile as an internal standard. Three chromatograms were measured for each sample using injection volumes of 0.1 ml for gas and 0.1 μl for liquid samples.

A typical reaction mixture consisted of 60 ml of acetonitrile, 40 psig total pressure for gaseous reactants, $1.6x10^{-4}$ moles of catalyst and 5ml of 35% hydrogen peroxide ($5.0x10^{-2}$ moles). Experiments in the absence of oxidants were performed as blanks.

The following definitions describe terms used in the presentation of the results. Selectivity to any product is the moles of a given product divided by the total moles of all products formed expressed as a percent. The percent peroxide efficiency is the moles of H_2O_2 needed to account for all oxidized products divided by the moles of H_2O_2 consumed. The percent conversion of alkane is the moles carbon in the oxidized products divided by the moles of alkane added to the reactor.

Safety Precautions, the combination of molecular oxygen with organic compounds and solvents at elevated temperatures and pressures are potentially explosive. **Extreme caution** should be taken during the charging and disassembly of the experimental apparatus. Equipment which can generates sparks must be avoided, a safety shield and cooling of the batch reactor in an ice bath for 30 minutes prior to disassembly is recommended.

Results and Discussion

Oxidation of Methane with H_2O_2

Although two iron analogues have been synthesized, the *cis*-$[Fe(dmp)_2(H_2O)_2](CF_3SO_3)_2$ (**II**) complex was chosen for activation of methane studies. This was done to allow for a direct comparison to the results obtained for the *cis*-$[Ru(dmp)_2(H_2O)_2](CF_3SO_3)_2$ catalyzed oxidation of methane under similar conditions. The results obtained from this oxidation study are provided in Table 5-1.

Experiment 1 proceeded for 24 hours, after which 12 mmol of methyl acetate (69% selectivity) was produced, the largest quantity obtained to date. Carbon dioxide (4 mmol, 24% selectivity) and the corresponding intermediate oxygenates (i.e.

Table 5-1: Oxidation Results for Methane @ 75°C with *cis*-$[Fe(dmp)_2(H_2O)_2](CF_3SO_3)_2$ Using H_2O_2

Experiment Number[a]	MeCOOMe mmol,(%)	CO_2 mmol,(%)	Total Oxygenates mmol,(%)	CH_4 Consumed (%)
1[a,b]	12,(69)	4,(24)	13,(76)	72
2[a,b,c]	6,(50)	4,(31)	9,(69)	60
3[a,b,d]	0,(0)	5,(99)	Trace,(1)	20
4[a,e]	11,(71)	3,(20)	13,(80)	70
5[a,f]	10,(73)	2,(16)	12,(84)	67
6[a,f,g]	5,(54)	3,(32)	6,(67)	42

a. 6.6×10^{-5} moles *cis*-$[Fe(dmp)_2(H_2O)_2](CF_3SO_3)_2$ catalyst, 5 ml 30% H_2O_2 (5.0×10^{-2} moles). The solvent mixture is 20 ml glacial acetic acid, 40 ml acetic anhydride, initial methane pressure was 40 psig corresponding to 23 millimoles. 3.5g 4Å molecular sieves (MS) were used. The percent products are based on total products seen from all sources.
b. Reaction time 24 hours. The percent products are based on total products from all sources.
c. 0.1ml concentrated H_2SO_4 added.
d. Solvent mixture 60ml acetic acid.
e. Reaction Time 12 hours. The percent products are based on total products from all sources.
f. Reaction Time 4 hours. The percent products are based on total products from all sources.
g. Molecular sieves omitted.

formaldehyde, formic acid and carbon dioxide) in a quantity corresponding to 1 mmol (7% selectivity) were also produced. Furthermore, a 72% conversion of methane was obtained, exhibiting the robust oxidizing power of this iron analogue (II) when compared to the ruthenium catalyst. The continued ability of the solvent system to trap methanol as methyl acetate with this iron-dmp analogue is also demonstrated.

In an effort to enhance the esterification reaction, 0.1 ml of concentrated H_2SO_4 was introduced. In addition to a larger quantity of ester produced, the acidic environment may influence the redox potentials of this catalyst. The results provided in Experiment 2 of Table 5-1 exhibit the decreased activity of the catalyst when exposed to acidic conditions. Overall a 60% conversion was obtained, a decrease when compared to 72% obtained in the absence of acid. The increased acidity also exhibits a detrimental effect on the trapping reaction, as evidenced by the decrease in selectivity to the methyl ester (50% selectivity). A subsequent increase in selectivity towards carbon dioxide (31% selectivity) also results. However, the quantity of carbon dioxide obtained in both Experiments 1 and 2 remains at 4 mmol. The decrease in the selectivities obtained provides evidence for the decreased efficiency of the trapping reaction. A decrease in the quantity of methyl acetate obtained (6 mmol) is also exhibited, a result of decreased catalytic activity.

Experiment 3 performed in the absences of trapping agents was allowed to react in 60 ml of glacial acetic acid for 24 hours. This resulted in the mineralization of methane to carbon dioxide and an overall conversion of 20%. A selectivity profile of 99% for CO_2 and 1% for the intermediate oxygenates was exhibited, demonstrating the need for trapping the alcohol as an ester.

To increase the selectivity of methyl acetate the reaction time was decreased to 12 hours. The result, Experiment 4, is an increase in methyl acetate selectivity from 69% in Experiment 1 to 72%. However, a decrease in the quantity of methyl acetate obtained (from 12 to 11 mmol) results, the function of a decrease in reaction time. When comparing the 24 and 12 hour runs, the quantity (4 and 3 mmol) and selectivity (24 and 20%) of CO_2 obtained exhibits the ability to alter reaction conditions to produce a selectivity towards a desired product. An increase in production of the intermediate oxygenates from 1 mmol for Experiment 1 to 2 mmol for Experiment 4 was also demonstrated. The shorter reaction time had a minimal effect on the overall conversion, only resulting in a decrease of 2% (from 72 to 70%).

To further investigate the effect of decreased reaction time, Experiment 5 was allowed to proceed for four hours. As a result, the anticipated increase in selectivity towards methyl acetate (73%) when compared to the 71% obtained for the 12 hour run (Experiment 4) was achieved. The lesser reaction time also increases the quantity of intermediate oxygenates produced from 2 to 3 mmol. The quantity (2 mmol) and selectivity (20%) of carbon dioxide obtained was also favorable, as well as a the minimal decrease in the overall conversion of methane to 67% which was observed.

Experiment 6 was performed in the absence of 4Å molecular sieves with a reaction time of four hours. The results obtained indicate a need for a dehydrating environment, which facilitates the esterification reaction. Although methyl acetate (5 mmol, 54% selectivity) is produced, the quantity is decreased from the 10 mmol and 73% selectivity obtained with the sieves present. The over-oxidation of methanol to carbon

dioxide (3 mmol, 32% selectivity) is also observed. Also affected by the absence of the molecular sieves is a decrease in overall conversion to 42%.

Mechanism for Oxidation of Methane

Preliminary mechanistic data suggests the activation of methane with the *cis*-$[Fe(dmp)_2(H_2O)_2](CF_3SO_3)_2$ complex is parallel to the mechanism suggested for the *cis*-$[Ru(dmp)_2(H_2O)_2](CF_3SO_3)_2$ analogue. This analogy is suggested due to the similar reaction conditions present in both systems, as well as the established literature which suggests ruthenium and iron as proceeding through identical reaction mechanism when each are performed under analogous conditions.

The formation of a peracid in the ruthenium system was demonstrated and explained in Chapter 2, as well as its ability to oxidize methane in the absence of the catalyst precursor. Therefore, the role of the metal complex must be explained. As with the ruthenium catalyst a decrease in overall conversion is exhibited when the iron complex is added to the reaction system. This related decrease could be attributed to the metal complex facilitating decomposition of the peracid, which is generated *in situ*, along with decomposition of the hydrogen peroxide oxidant. However, further investigation is warranted.

Oxidation of Methane with O_2

The favorable results obtained with the *cis*-$[Fe(dmp)_2(H_2O)_2](CF_3SO_3)_2$ (**II**) catalyst with hydrogen peroxide, initiated the investigation of this catalyst's ability to activate methane with molecular oxygen. A series of experiment provided in Table 5-2, were performed in an identical manner as those for the *cis*-$[Ru(dmp)_2(H_2O)_2](CF_3SO_3)_2$

Table 5-2: Oxidation Results for Methane @ 75°C with *cis*-$[Fe(dmp)_2(H_2O)_2](CF_3SO_3)_2$ Using H_2O_2 and O_2

Experiment Number	Sel. To MeAcetate (%)	CO_2 Formation (%)	Sel. To Oxygenates (%)	H_2O_2 Efficiency (%)	CH_4 Conversion (%)
7[a,b]	36.2	62.8	37.2	>100	5.9
8[a,c]	47.4	52.4	47.6	>100	4.5
9[d,e]	78.1	18.1	79.9	>100	9.5
10[a,e]	0.0	0.0	0.0	0.0	0.0
11[a,f]	0.0	0.0	0.0	0.0	0.0

a. 6.6×10^{-5} moles *cis*-$[Fe(dmp)_2(H_2O)_2](CF_3SO_3)_2$, 20 ml glacial acetic acid, 40 ml acetic anhydride, 20 psig CH_4 (1.0×10^{-2} moles), 30 psig HeOx (1.0×10^{-2} moles), 3.5g molecular sieves (MS), 75°C.

b. Reaction time 24 hours 2.0 µl 30% H_2O_2 (2.0×10^{-5} moles).

c. Reaction time 12 hours 2.0 µl 30% H_2O_2 (2.0×10^{-5} moles).

d. Parr bomb reactor used. 250psi CH_4 (6.6×10^{-2} moles), 250psi O_0 (6.6×10^{-2} moles), 500 psi He (1.8×10^{-1} moles), 1.3×10^{-4} moles *cis*-$[Fe(dmp)_2(H_2O)_2](CF_3SO_3)_2$, 20 ml glacial acetic acid, 40 ml acetic anhydride, 3.5g molecular sieves (MS), 100°C.

e. Performed in the absence of H_2O_2 24 hours.

f. Blank experiment, performed in the absence of catalyst 24 hours.

system investigated in Chapter 2. Once again reaction parameters (reaction time, solvent and gas mixtures) were held constant, allowing for direct comparison of results obtained.

Table 5-2 illustrates the results for the direct conversion of methane to methanol using molecular oxygen (5% O_2 in He) as the oxidant. As with the ruthenium analogue, the quantities of products obtained exceed the amount of oxidant ($2.0x10^{-5}$) provided to initiate the iron complex (II), which suggests oxygen is contributing to the production of oxygenates. After 24 hours (Experiment 7), a 5.9% conversion of methane is obtained producing a 36.2% selectivity to methyl acetate. The presence of deep oxygenates (carbon dioxide), 62.8% selectivity, was also detected. A total of $6.0x10^{-4}$ moles of oxidized products were obtained, an amount which exceeds the $2.0x10^{-5}$ moles of oxidant supplied by hydrogen peroxide. Clearly demonstrating the ability of this complex to utilize molecular oxygen in the oxidation process.

Experiment 8 was performed as an attempt to further increase selectivity of methyl acetate. After 12 hours a 4.5% conversion of methane to oxygenates was observed. A selectivity profile of 47.4% for methyl acetate and 47.6 for carbon dioxide was achieved, exhibiting the ability to allow for control of reaction condition to alter product selectivity.

It was apparent one of limiting factors is the solubility of each gas in this solvent matrix. To allow for an improved solubility, oxidation experiments were performed in a high-pressure environment. To do this a Parr® High-Pressure apparatus was employed. This configuration allows for the use of high pressures of oxygen and methane, as well as being able to operate at higher temperatures. Helium was also introduced to serve as a dilutant, allowing ourselves to remain within the safety limits for a hydrocarbon-oxygen

mixture. The reactor body, head and stirrer were constructed out of titanium for corrosive resistivity. To allow for a further increase in gas solubility, a novel stirrer was used. The stirrer referred to as the gasperator, is designed to allow for use of the convective flow which exists over the liquid in the head gas space. This stirrer is equipped with vertical slits in a bored out shaft and holes in the stirrer blades which are connected to the hollow shaft. The vertical slits in the shaft, which are above the liquid level, draw the gas from the headspace into the shaft, where it is then passed through the blades. The gas is then released from the blades as bubbles and then disperses through the solvent, thus improving solubility of the gas. In order for this stirrer to function properly a revolution rate of 500 rpm must be attained. An additional benefit of the increased stirring rate is a more favorable interaction between the catalyst and gaseous substrate.

Experiment 9, performed in the Parr® Bomb used 250 psi of methane ($6.6x10^{-2}$ moles), 250 psi O_2 ($6.6x10^{-2}$ moles), 500 psi helium ($1.8x10^{-1}$ moles), $1.3x10^{-4}$ moles *cis*-$[Fe(dmp)_2(H_2O)_2](CF_3SO_3)_2$ (II), 20 ml of glacial acetic acid and 40 ml of acetic anhydride. After 1 hour of reaction time, a 9.5% conversion of methane to oxygenates was observed. This oxidation allowed for a high selectivity to methyl acetate to be achieved (78.1%), while limiting the amount of carbon dioxide (18.1% selectivity) to be produced. With the oxidant being molecular oxygen a lower concentration of hydrogen peroxide is present within the system, therefore subsequent oxidation of the methanol to carbon dioxide does not occur as readily allowing for a higher selectivity of methyl acetate to be observed. This result is extremely encouraging from the standpoint of the minimal reaction time and low temperature necessary to achieve a large product selectivity and relatively high overall conversion with molecular oxygen as the oxidant.

Experiments 10 and 11 detail blank experiments performed. A detailed explanation of each experiment is provided in Chapter 2.

Alkane Oxidations with *cis*-$[Fe(dmp)_2(H_2O)_2](CF_3SO_3)_2$

Attempts to oxidize C_2-C_5 saturated hydrocarbons with hydrogen peroxide in deionized water at 75°C were unsuccessful after 48 hours with and without catalyst at pH solution values of 1 to 7. The inability to activate the Fe(II) center to a higher oxidation state, which is necessary for C-H bond activation, can be explained in a manner similar to that for the *cis*-$[Ru(dmp)_2(H_2O)_2](CF_3SO_3)_2$ precursor described in Chapter 2. As a result, alkane oxidation experiments were performed in acetonitrile.

Each alkane (ethane, propane, butane, *iso*-butane and pentane) was reacted in acetonitrile (60ml) with hydrogen peroxide ($5.0x10^{-2}$ mole) and catalyst ($1.6x10^{-4}$ mole) for 15 hours at 75°C. The results obtained are provided in Tables 5-3 and 5-4. Again propane, *iso*-butane and pentane allow ourselves to determine the catalyst's activity in terms of selectivity and regioselectivity.

After 15 hours, a 33.2% conversion of propane was obtained corresponding to 6.3 mmoles of oxidized products. Of note is the selectivity profile of the products produced. Oxidation at the primary carbon position accounts for 45.4% or 2.9 mmoles of the total oxidized products: 1-propanol (0.1 mmoles, 1.8% selectivity) and propionaldehyde (2.8 mmoles, 43.6% selectivity). Trace amounts of propionoic acid were detected, however peak broadening and tailing made quantification difficult. Oxidation at the secondary carbon was also observed, totaling to 54.6% selectivity or 3.4 mmoles of the oxidized products: 2-propanol (0.8 mmoles, 13.1% selectivity) and acetone (2.6 mmoles, 41.5

Table 5-3: Oxidation Results for Ethane, Propane and Butane @ 75°C with *cis*-$[Fe(dmp)_2(H_2O)](CF_3SO_3)_2$ using H_2O_2

Substrate[a]	Oxidized Products mmoles (Selectivity)	Total mmoles Oxidant	Percent Peroxide Efficiency	Percent Conversion[b]
Ethane	Ethanol: 0.15 (2.20) Acetaldehyde: 2.47 (36.0) Acetic Acid: 4.25 (61.8)	17.8	35.7	36.2
Propane	1-Propanol: 0.11 (1.80) 2-Propanol: 0.83 (13.1) Propanal: 2.77 (43.6) Acetone: 2.59 (41.5) Propionoic Acid: Trace	11.7	23.3	33.2
Butane[c]	1-Butanol: 0.15 (6.30) 2-Butanol: 0.33 (14.3) Butanal: 0.35 (15.4) 2-Butanone: 0.85 (36.9) Butanoic Acid: 0.62 (27.1)	4.74	9.48	24.2

a: 1.6×10^{-4} mole $[Fe(dmp)_2(H_2O)](CF_3SO_3)_2$, 60ml acetonitrile, 5.0×10^{-2} moles 35% H_2O_2, 40psi substrate (1.9×10^{-2} moles), 15 hours at 75°C.

b: Percent conversion is based on the total of oxidized products divided by the initial amount of substrate.

c: 20psi (9.5×10^{-3} moles) butane used.

Table 5-4: Oxidation Results for *Iso*-Butane and Pentane @ 75°C with *cis*-$[Fe(dmp)_2(H_2O)](CF_3SO_3)_2$ using H_2O_2

Substrate[a]	Oxidized Products mmoles (Selectivity)	Total mmoles Oxidant	Percent Peroxide Efficiency	Percent Conversion[b]
Iso-Butane	*Iso*-Butanol: 3.0 (97.1) *Iso*-Butyl ol: 0.09 (2.90)	3.09	6.18	19.5
Pentane[c]	1-Pentanol: 0.36 (3.90) 2-Pentanol: 0.94 (10.0) 3-Pentanol: 1.19 (12.7) Pentanal: 1.63 (17.5) 2-Pentanone: 2.58 (27.6) 3-Pentanone: 2.64 (28.3) Pentanoic Acid: Trace	16.2	32.4	47.8

a: $1.6x10^{-4}$ mole $[Fe(dmp)_2(H_2O)](CF_3SO_3)_2$, 60ml acetonitrile, $5.0x10^{-2}$ moles 35% H_2O_2, 40psi substrate ($1.9x10^{-2}$ moles), 15 hours at 75°C.

b: Percent conversion is based on the total of oxidized products divided by the initial amount of substrate.

c: 2ml ($2.0x10^{-2}$ moles) pentane used

mmoles). A selectivity ratio of primary:secondary carbon oxidation of 1:1 was achieved by this catalyst. A peroxide efficiency of 23.3% and 48 turnover numbers (TON's) was obtained for this reaction.

Ethane and butane were also oxidized under the previously described conditions accounting for a 36.2% and 24.2% overall conversion respectively. These results are also provided in Table 5-3. As with the other catalytic system, over-oxidation of the products to the corresponding aldehyde, ketone and carboxylic acid is also exhibited. The deep oxidation of the desired alcohol results in a decrease in alcohol selectivity, overall conversion, peroxide efficiency and catalyst lifetime.

Oxidation of *iso*-butane with this catalyst resulted in the production of oxidation products at the primary and tertiary position. After 15 hours of reaction, 3.1 mmoles of oxidized products were obtained, corresponding to a 19.5% conversion. Oxidation at the tertiary carbon accounts for 97.1% (3.0 mmoles) of the total products. Trace amounts (0.09 mmoles, 2.9% selectivity) of 2-methyl-1-propanol was also detected, demonstrating the ability of this catalyst to activate the primary carbon position.

Pentane, the first liquid alkane investigated, was activated by this catalyst to lead to oxidation products at the C_1, C_2 and C_3 carbon position. After 15 hours, a 47.8% conversion was obtained, accounting for 9.3 mmoles of oxidized products. Primary carbon oxidation (C_1) led to production of: 1-pentanol (0.3 mmoles, 3.9% selectivity), valeraldehyde (pentanal) (1.6 mmoles, 17.5% selectivity) and trace quantities of valeric acid (pentanoic acid), which was not quantified due to peak broadening and tailing. Oxidation at the secondary carbon position (C_2) position afforded: 2-pentanol (0.9 mmoles, 10.1% selectivity) and 2-pentanone (2.6 mmoles, 27.6% selectivity). C_3 carbon

activation produced 3-pentanol (1.2 mmoles, 12.7% selectivity) and 3-pentanone (2.6 mmoles, 28.3% selectivity). A total of 16 mmoles of oxidant was consumed, yielding a peroxide efficiency of 32.4% and accounting to 51 TON's.

Alkane Oxidation with $[Fe(dmp)Cl_2]$

As with the *cis*-$[Fe(dmp)_2(H_2O)_2](CF_3SO_3)_2$ complex an attempt to activate saturated hydrocarbons (C_2-C_5) in deionized H_2O were also unsuccessful under a number of conditions. This resulted in oxidation reactions to proceed in an acetonitrile solvent matrix. Reaction conditions are identical to those described in the previous section. Results obtained for alkane oxidation with the $[Fe(dmp)Cl_2]$ catalyst precursor are detailed in Tables 5-5 and 5-6.

Ethane and butane oxidation resulted in a 36.7% and 22.3% conversion respectively. In this reaction mixture, subsequent over-oxidation of the hydroxylated product was also observed. Results detailing the effect of over-oxidation for these substrates are provided in Table 5-5.

After 15 hours, a 18.8 % conversion of propane was observed, corresponding to 3.6 mmoles of oxidized products. Products resulting from oxidation at the primary carbon position accounted for 1.7 mmoles or a 48.2% selectivity: 1-propanol (0.01 mmoles, 2.5% selectivity) and propionaldehyde: (1,7 mmoles, 45.7% selectivity). Trace amounts of propionoic acid were also observed, but not quantified. Secondary carbon oxidation products were also observed totaling 1.9 mmoles and 51.8% selectivity: 2-propanol (0.7 mmoles, 18.9% selectivity) and acetone (1.2 mmoles, 32.9% selectivity). A selectivity ratio of primary:secondary carbon oxidized products of 1:1 was also

Table 5-5: Oxidation Results for Ethane, Propane and Butane @ 75°C with $Fe(dmp)Cl_2$ using H_2O_2

Substrate[a]	Oxidized Products mmoles (Selectivity)	Total mmoles Oxidant	Percent Peroxide Efficiency	Percent Conversion[b]
Ethane	Ethanol: 0.13 (1.80) Acetaldehyde: 3.85 (55.3) Acetic Acid: 2.99 (42.9)	16.8	33.6	36.7
Propane	1-Propanol: 0.01 (2.50) 2-Propanol: 0.68 (18.9) Propanal: 1.68 (45.7) Acetone: 1.21 (32.9) Propionoic Acid: Trace	6.47	12.9	18.8
Butane[c]	1-Butanol: 0.09 (10.7) 2-Butanol: 0.10 (12.1) Butanal: 0.19 (22.5) 2-Butanone: 0.31 (37.5) Butanoic Acid: 1.43 (17.2)	5.48	11.0	22.3

a: 1.6×10^{-4} mole $Fe(dmp)_2Cl_2$, 60ml acetonitrile, 5.0×10^{-2} moles 35% H_2O_2, 40psi substrate (1.9×10^{-2} moles), 15 hours at 75°C.

b: Percent conversion is based on the total of oxidized products divided by the initial amount of substrate.

c: 20psi (9.5×10^{-3} moles) butane used.

Table 5-6: Oxidation Results for *Iso*-Butane and Pentane @ 75°C with $Fe(dmp)Cl_2$ using H_2O_2

Substrate[a]	Oxidized Products mmoles (Selectivity)	Total mmoles Oxidant	Percent Peroxide Efficiency	Percent Conversion[b]
Iso-Butane	*Iso*-Butanol: 2.91 (99.1) *Iso*-Butyl ol: 0.03 (0.90)	2.94	5.86	15.4
Pentane[c]	1-Pentanol: 0.15 (2.20) 2-Pentanol: 0.56 (8.00) 3-Pentanol: 1.47 (20.9) Pentanal: 1.61 (22.9) 2-Pentanone: 1.97 (28.2) 3-Pentanone: 1.25 (17.8) Pentanoic Acid: Trace	11.8	23.7	36.9

a: 1.6×10^{-4} mole $Fe(dmp)_2Cl_2$, 60ml acetonitrile, 5.0×10^{-2} moles 35% H_2O_2, 40psi substrate (1.9×10^{-2} moles), 15 hours at 75°C.

b: Percent conversion is based on the total of oxidized products divided by the initial amount of substrate.

c: 2ml (2.0×10^{-2} moles) pentane used.

observed for this iron analogue. A peroxide efficiency of 12.9% and 39 TON's was also obtained for this oxidation.

Iso-butane oxidation by this catalyst also resulted in the production of oxidized products at the primary and tertiary carbon positions. At the end of 15 hours, a 15.4% conversion was obtained accounting for 2.9 mmoles of oxidized products. Oxidation at the tertiary carbon accounts for the majority of products, identical to that observed for the *cis*-$[Fe(dmp)_2(H_2O)_2](CF_3SO_3)_2$ catalyst, 2.9 mmoles of *iso*-butyl alcohol (99.1% selectivity. Limited quantities of 2-methyl-1-propanol were also detected, accounting for 0.03 mmoles of the total products (0.09% selectivity).

Pentane oxidation with the $[Fe(dmp)Cl_2]$ catalyst precursor also occurred. After 15 hours of reaction, a 36.9% conversion was demonstrated totaling 7.01 mmoles of oxidized products. Primary carbon (C_1) oxidation (1.8 mmoles, 25.1% selectivity) led to the production of: 1-pentanol (0.2 mmoles, 2.2% selectivity), valeraldehyde (pentanal) (1.6 mmoles, 22.9% selectivity) and trace amounts of valeric acid (pentanoic acid) (not quantified). Oxidation at the secondary carbon (C_2) position (2.5 mmoles, 36.2% selectivity) was also observed: 2-pentanol (0.6 mmoles, 8.0% selectivity) and 2-pentanone (2.0 mmoles, 28.2% selectivity). Products arising from oxidation at the C_3 position (2.8 mmoles, 38.7% selectivity) were 3-pentanol (1.5 mmoles, 20.9% selectivity) and 3-pentanone (1.3 mmoles, 17.8% selectivity). A total of 11.8 mmoles of oxidant was consumed as well as the catalyst providing 35 TON's for this reaction.

Upon comparison of the results obtained for the activation of alkanes with the two iron derivatives (Complexes **I** and **II**) and the ruthenium analogue, the mono dmp complex, $[Fe(dmp)Cl_2]$ (**I**), is the least active. Nearly identical results in terms of

activity, selectivity, regioselectivity and overall conversion were obtained for the two complexes that exhibited cis geometry. The decreased activity of the [Fe(dmp)Cl_2] precursor may be attributed dimerization, thus leading to the lack of available sites need for oxidation. Additional factors include the metal center being less electrophillic, due to the presence of one ligand and also the instability of this complex, which may lead to an increase in complex degradation.

Mechanism for Higher Alkane Oxidation

The "rebound" mechanism has been proposed for the activation of higher alkanes for both iron derivatives. This free radical pathway is constant with reports published in literature for substrate activation with iron complexes under similar conditions. In the hydrogen abstract mechanism "Rebound", an alkyl free radical is produced. The alkyl free radial is the result of a high valent iron-oxo species abstracting a hydrogen from the substrate molecule. This results in formation of an iron-hydroxide, Fe^{IV}-OH, species. The hydroxyl ligand is then donated to the radical alkyl species to product the hydroxylated species. The catalytic cycle is then completed with the regeneration of the Fe^{III} species to Fe^{V}=O with molecular oxygen or hydrogen peroxide. Collins[99], Que[98] and Groves[85] have suggested similar mechanisms.

Other supporting evidence for this proposed mechanism is obtained upon analysis of final reaction mixture when radical initiators and inhibitors have been added. Upon addition of AIBN, 15 mole equivalents, (a free radical initiator, azo-bis-(iso-butyronitrile)) to the reaction mixture, no change in catalyst activity was observed. With addition of 15 mole equivalents of BQ (benzoquinone, a free radical inhibitor), no

oxidation products were observed within the first 3 hours. After this time period, which allows for consumption of the radical inhibitor, product formation is then observed. Based on these results, additional evidence is provided to further suggest radical formation is involved in the induction steps necessary for alkane activation with these iron catalysts.

An additional mechanism, which cannot be ignored, is the Fenton Mechanism. In this mechanism hydrogen peroxide can be decomposed by an iron complex into a hydroxyl radical and hydroxyl anion as well as the oxidized species of the iron complex. The hydroxyl species generated, which is extremely reactive only second to elemental fluorine, may be able to partake in the oxidation reaction. Resulting in the production of oxygenated products. The effect of this mechanism in our system was not studied extensively, so additional experimentation is needed.

Addition of $CuCl_2$

As exhibited in Chapter 2, the addition of $CuCl_2$ to the reaction mixture demonstrated a pronounced effect on the ability to retain the alcohol and retard further oxidation of the desired product. To determine if this increase in alcohol selectivity could also be obtained with the two iron derivatives, one mole equivalent ($1.6x10^{-4}$) of $CuCl_2$ was added to each of the previously described reactions. All other conditions were held constant, allowing for a direct comparison. Tables 5-7 and 5-8 provide the results obtained with the *cis*-$[Fe(dmp)_2(H_2O)_2](CF_3SO_3)_2$ precursor, while Tables 5-9 and 5-10 exhibit the results obtained with the $[Fe(dmp)Cl_2]$ complex.

Table 5-7: Oxidation Results for Ethane, Propane and Butane @ 75°C with *cis*-$[Fe(dmp)_2(H_2O)](CF_3SO_3)_2$ and $CuCl_2$ using H_2O_2

Substrate[a]	Oxidized Products mmoles (Selectivity)	Total mmoles Oxidant	Percent Peroxide Efficiency	Percent Conversion[b]
Ethane	Ethanol: 0.17 (2.20) Acetaldehyde: 6.45 (78.9) Acetic Acid: 1.55 (18.9)	17.7	35.4	43.1
Propane	1-Propanol: 0.67 (14.9) 2-Propanol: 1.71 (38.4) Propanal: 2.26 (25.4) Acetone: 1.90 (21.3) Propionoic Acid: Trace	10.7	21.4	34.4
Butane[c]	1-Butanol: 0.15 (6.30) 2-Butanol: 0.33 (14.3) Butanal: 0.35 (15.4) 2-Butanone: 0.85 (36.9) Butanoic Acid: 0.62 (27.1)	4.74	9.48	24.2

a: 1.6×10^{-4} mole $[Fe(dmp)_2(H_2O)](CF_3SO_3)_2$, 1.6×10^{-4} mole $CuCl_2$, 60ml acetonitrile, 5.0×10^{-2} moles 35% H_2O_2, 40psi substrate (1.9×10^{-2} moles), 15 hours at 75°C.

b: Percent conversion is based on the total of oxidized products divided by the initial amount of substrate.

c: 20psi (9.5×10^{-3} moles) butane used.

Table 5-8: Oxidation Results for *Iso*-Butane and Pentane @ 75°C with *cis*-$[Fe(dmp)_2(H_2O)](CF_3SO_3)_2$ and $CuCl_2$ using H_2O_2

Substrate[a]	Oxidized Products mmoles (Selectivity)	Total mmoles Oxidant	Percent Peroxide Efficiency	Percent Conversion[b]
Iso-Butane	*Iso*-Butanol: 3.6 (99.0) *Iso*-Butyl ol: 0.04 (1.00)	3.64	7.28	19.2
Pentane[c]	1-Pentanol: 0.36 (4.60) 2-Pentanol: 1.67 (21.4) 3-Pentanol: 1.99 (25.6) Pentanal: 0.96 (12.3) 2-Pentanone: 1.45 (18.6) 3-Pentanone: 1.36 (17.5) Pentanoic Acid: Trace	11.6	23.1	41.0

a: $1.6x10^{-4}$ mole $[Fe(dmp)_2(H_2O)](CF_3SO_3)_2$, $1.6x10^{-4}$ mole $CuCl_2$, 60ml acetonitrile, $5.0x10^{-2}$ moles 35% H_2O_2, 40psi substrate ($1.9x10^{-2}$ moles), 15 hours at 75°C.

b: Percent conversion is based on the total of oxidized products divided by the initial amount of substrate.

c: 2ml ($2.0x10^{-2}$ moles) pentane used.

Oxidation experiments with propane, *cis*-$[Fe(dmp)_2(H_2O)_2](CF_3SO_3)_2$ and $CuCl_2$ resulted in a 34.3% overall conversion after 15 hours. An increase in overall conversion of 1.2% was obtained when compared to an oxidation performed in the absence of $CuCl_2$. Also exhibited was the desired increase in alcohol selectivity to 14.1% for 1-propanol and 38.4% for 2-propanol, both increased from the 1.8% and 13.1% selectivities achieved when $CuCl_2$ is omitted. The accompanying decrease in selectivity to the aldehyde and ketone also results. Similar results were obtained for the remaining alkanes, as shown in Tables 5-7 and 5-8.

Oxidation of propane experiments performed with the $[Fe(dmp)Cl_2]$ complex and $CuCl_2$ resulted in a 20.1% overall conversion of the alkane after 15 hours. Once again a minimal increase in conversion (1.2%) is achieved when compared to the results obtained in the absence of $CuCl_2$. Alcohol selectivity increases once again from 2.5 to 3.8% for1-propanol and from 18.9 to 34.9% for 2-propanol. Aldehyde and ketone selectivities were also decreased to 29.9% for propanal and 31.4% for acetone. Tables 5-9 and 5-10 further demonstrate the desired increases in alcohol selectivities for the remaining alkanes.

The role of $CuCl_2$ in this reaction mixture has been investigated through blank analysis and control experiments. An explanation and discussion of the results are provided in Chapter 2.

The effect of increased mole equivalents of $CuCl_2$ on the selectivity of the alcohol were also investigated using both precursors, *cis*-$[Fe(dmp)_2(H_2O)_2](CF_3SO_3)_2$ and $[Fe(dmp)Cl_2]$ at 75°C. The results for the oxidation of propane with the *cis*-$[Fe(dmp)_2(H_2O)_2](CF_3SO_3)_2$ complex are provided in Table 5-11 and illustrated in Figure

Table 5-9: Oxidation Results for Ethane, Propane and Butane @ 75°C with $Fe(dmp)Cl_2$ and $CuCl_2$ using H_2O_2

Substrate[a]	Oxidized Products mmoles (Selectivity)	Total mmoles Oxidant	Percent Peroxide Efficiency	Percent Conversion[b]
Ethane	Ethanol: 0.51 (6.50) Acetaldehyde: 5.76 (74.3) Acetic Acid: 1.48 (19.2)	16.5	32.9	40.8
Propane	1-Propanol: 0.14 (3.80) 2-Propanol: 1.31 (34.9) Propanal: 1.12 (29.9) Acetone: 1.17 (31.4) Propionoic Acid: Trace	6.03	12.1	20.1
Butane[c]	1-Butanol: 0.09 (5.60) 2-Butanol: 0.07 (4.20) Butanal: 0.17 (10.2) 2-Butanone: 0.25 (15.2) Butanoic Acid: 1.07 (64.8)	4.21	8.42	17.4

a: $1.6x10^{-4}$ mole $Fe(dmp)_2Cl_2$, $1.6x10^{-4}$ mole $CuCl_2$, 60ml acetonitrile, $5.0x10^{-2}$ moles 35% H_2O_2, 40psi substrate ($1.9x10^{-2}$ moles), 15 hours at 75°C.

b: Percent conversion is based on the total of oxidized products divided by the initial amount of substrate.

c: 20psi ($9.5x10^{-3}$ moles) butane used.

Table 5-10: Oxidation Results for *Iso*-Butane and Pentane @ 75°C with $Fe(dmp)Cl_2$ and $CuCl_2$ using H_2O_2

Substrate[a]	**Oxidized Products moles (Selectivity)**	**Total mmoles Oxidant**	**Percent Peroxide Efficiency**	**Percent Conversion[b]**
Iso-Butane	*Iso*-Butanol: 3.5 (98.3) *Iso*-Butyl ol: 0.06 (1.7)	3.56	7.12	18.7
Pentane[c]	1-Pentanol: 0.15 (2.50) 2-Pentanol: 0.77 (13.1) 3-Pentanol: 1.37 (23.3) Pentanal: 1.61 (27.3) 2-Pentanone: 1.23 (20.8) 3-Pentanone: 0.77 (13.0) Pentanoic Acid: Trace	9.51	19.1	31.1

a: $1.6x10^{-4}$ mole $Fe(dmp)_2Cl_2$, $1.6x10^{-4}$ mole $CuCl_2$, 60ml acetonitrile, $5.0x10^{-2}$ moles 35% H_2O_2, 40psi substrate ($1.9x10^{-2}$ moles), 15 hours at 75°C.

b: Percent conversion is based on the total of oxidized products divided by the initial amount of substrate.

c: 2ml ($2.0x10^{-2}$ moles) pentane used.

Table 5-11: Oxidation Results for Propane @ 75°C with *cis*-$[Fe(dmp)_2(H_2O)](CF_3SO_3)_2$ and Varying Mole Equivalents of $CuCl_2$ using H_2O_2

Mole Equivalents $CuCl_2$[a]	mmoles Alcohol (% Sel.)	mmoles Aldehyde (% Sel.)	mmoles Ketone (% Sel.)	Total mmoles Products	Percent Conversion[b]
0	0.94 (14.9)	2.77 (43.6)	2.59 (41.5)	6.30	33.2
1	2.38 (53.3)	2.26 (25.4)	1.90 (21.3)	6.54	34.4
2	1.08 (35.0)	1.49 (48.3)	0.52 (16.7)	3.08	17.10
3	1.86 (54.2)	1.09 (32.1)	0.46 (13.7)	3.41	18.40
4	2.35 (65.6)	0.69 (19.2)	0.54 (15.2)	3.58	19.79
5	2.75 (70.6)	0.60 (15.4)	0.55 (14.0)	3.90	21.50

a: 1.6×10^{-4} mole *cis*-$[Fe(dmp)_2(H_2O)](CF_3SO_3)_2$, 1.6×10^{-4} x mole eq. moles $CuCl_2$, 60ml acetonitrile, 5.0×10^{-2} moles 35% H_2O_2, 40psi substrate (1.9×10^{-2} moles), 15 hours at 75°C.

b: Percent conversion is based on the total of oxidized products divided by the initial amount of substrate.

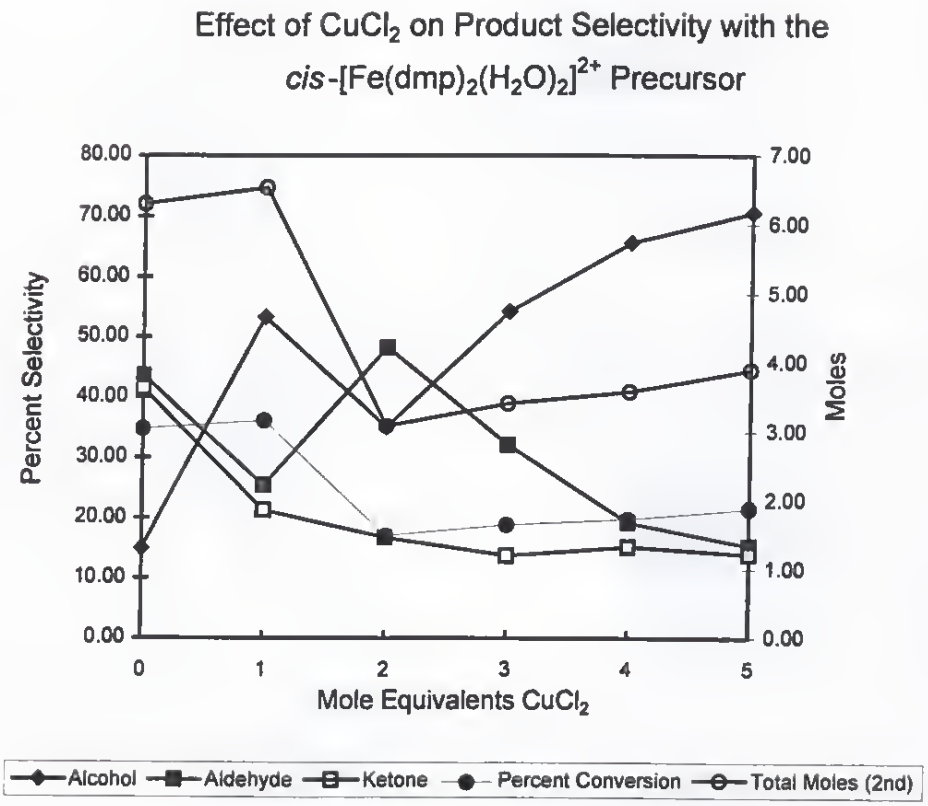

Figure 5-1: Oxidation of Propane with *cis*-$[Fe(dmp)_2(H_2O)](CF_3SO_3)_2$ and Varying Mole Equivalents of $CuCl_2$ using H_2O_2

Table 5-12: Oxidation Results for Propane @ 75°C with $Fe(dmp)Cl_2$ and Varying Mole Equivalents of $CuCl_2$ using H_2O_2

Mole Equivalents $CuCl_2$[a]	mmoles Alcohol (% Sel.)	mmoles Aldehyde (% Sel.)	mmoles Ketone (% Sel.)	Total mmoles Products	Percent Conversion[b]
0	0.69 (21.4)	1.68 (45.7)	1.21 (32.9)	3.58	18.8
1	1.45 (38.7)	1.12 (29.9)	1.17 (31.4)	3.74	19.7
2	1.27 (55.6)	0.50 (21.9)	0.52 (22.5)	2.29	12.66
3	1.83 (68.8)	0.48 (17.9)	0.35 (13.3)	2.66	14.70
4	2.30 (70.9)	0.54 (16.5)	0.41 (12.6)	3.25	17.95
5	2.93 (76.0)	0.54 (14.0)	0.59 (10.0)	4.05	21.28

a: 1.6×10^{-4} mole *cis*-$[Fe(dmp)_2(H_2O)](CF_3SO_3)_2$, 1.6×10^{-4} x mole eq. moles $CuCl_2$, 60ml acetonitrile, 5.0×10^{-2} moles 35% H_2O_2, 40psi substrate (1.9×10^{-2} moles), 15 hours at 75°C.

b: Percent conversion is based on the total of oxidized products divided by the initial amount of substrate.

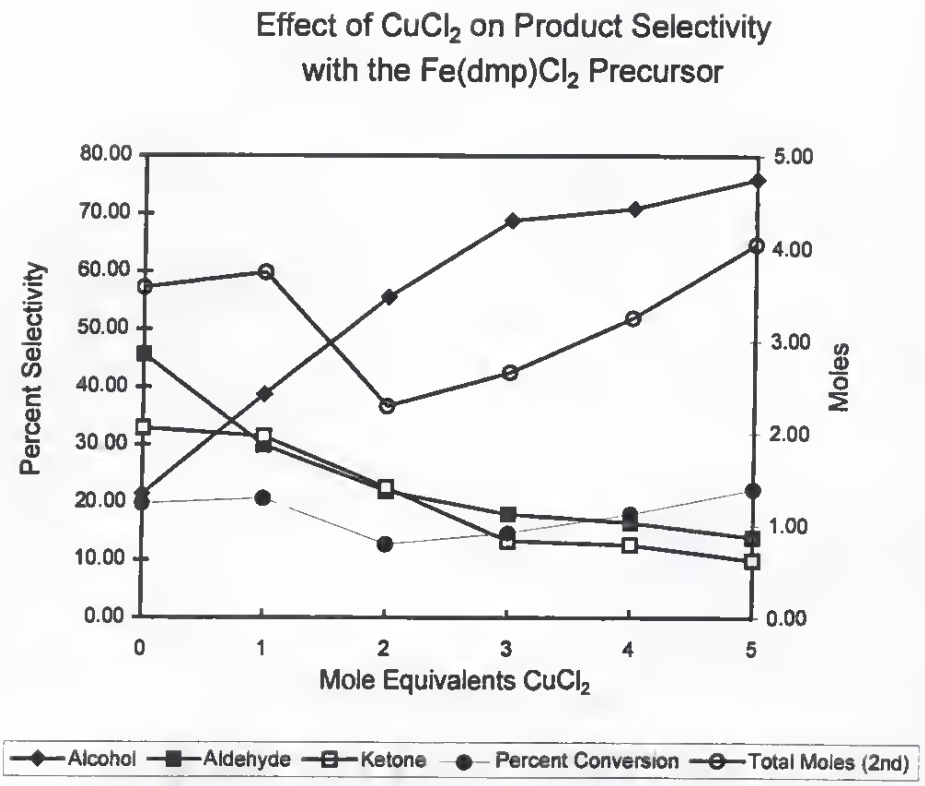

Figure 5-2: Oxidation of Propane with $Fe(dmp)Cl_2$ and Varying Mole Equivalents of $CuCl_2$ using H_2O_2

5-1. The results for the [Fe(dmp)Cl_2] complex are given in Table 5-12 and graphically represented in Figure 5-2.

As with the *cis*-[Ru(dmp)$_2$(H_2O)$_2$](CF_3SO_3)$_2$ analogue, successive addition of $CuCl_2$ mole equivalents to both iron derivatives resulted in an increase in selectivity to the alcohol, along with the decreased selectivity to the aldehyde and ketone. Although the trend exhibited by the iron complexes are not as smooth as that observed for the ruthenium analogue, the effect of the added copper is exhibited. Variations in results for the iron complexes can be attributed to the presence of two first row transition metals (Cu and Fe) which lead to an increased rate of peroxide decomposition, thus the varied results. Peroxide decomposition observed in the ruthenium system is not as rapid, when compared to the iron analogue. The decrease in overall conversion exhibited can be attributed to a lower concentration of peroxide present due to decomposition.

Effect of Temperature

A series of experiments were performed on both iron analogues with and without one mole equivalent of $CuCl_2$ at 25, 50, 75 and 100°C to determine the effect of temperature on each complex. The increase in temperature is expected to allow for increased substrate reactivity, solubility of the catalyst and rate of oxidation. The results for the oxidation of propane at each temperature for both catalysts are provided in Tables 5-13, 5-14, 5-15 and 5-16.

A mixture of catalyst ($1.6x10^{-4}$ moles), acetonitrile (60ml), hydrogen peroxide ($5.0x10^{-2}$ moles) and propane ($1.9x10^{-2}$ moles) were allowed to reaction for 15 hours at each temperature. Oxidations with the *cis*-[Fe(dmp)$_2$(H_2O)$_2$](CF_3SO_3)$_2$ precursor

Table 5-13: Oxidation Results for Propane @ Varying Temperatures with *cis*-$[Fe(dmp)_2(H_2O)](CF_3SO_3)_2$ using H_2O_2

Temp. (°C)[a]	mmoles Alcohol (% Sel.)	mmoles Aldehyde (% Sel.)	mmoles Ketone (% Sel.)	Total mmoles Products	Percent Conversion[b]
25	0.16 (12.7)	0.55 (44.4)	0.54 (42.9)	1.25	5.90
50	0.64 (14.0)	1.96 (43.0)	1.97 (43.10)	4.56	23.1
75	0.94 (14.9)	2.77 (44.0)	2.59 (41.1)	6.30	34.9
100	1.15 (23.1)	1.57 (31.5)	2.26 (45.8)	4.98	29.5

a: 1.6×10^{-4} mole *cis*-$[Fe(dmp)_2(H_2O)](CF_3SO_3)_2$, 60ml acetonitrile, 5.0×10^{-2} moles 35% H_2O_2, 40 psi substrate (1.9×10^{-2} moles), 15 hours.

b: Percent conversion is based on the total of oxidized products divided by the initial amount of substrate.

Table 5-14: Oxidation Results for Propane @ Varying Temperatures with *cis*-$[Fe(dmp)_2(H_2O)](CF_3SO_3)_2$ and $CuCl_2$ using H_2O_2

Temp. (°C)[a]	mmoles Alcohol (% Sel.)	mmoles Aldehyde (% Sel.)	mmoles Ketone (% Sel.)	Total mmoles Products	Percent Conversion[b]
25	0.86 (46.2)	0.50 (26.9)	0.50 (26.9)	1.86	8.82
50	0.69 (12.1)	4.06 (71.1)	0.96 (16.8)	5.71	29.3
75	2.38 (53.3)	2.26 (25.4)	1.90 (21.3)	4.46	24.9
100	1.67 (42.4)	1.36 (34.5)	0.91 (23.1)	3.94	23.3

a: 1.6×10^{-4} mole *cis*-$[Fe(dmp)_2(H_2O)](CF_3SO_3)_2$, 1.6×10^{-4} mole $CuCl_2$, 60ml acetonitrile, 5.0×10^{-2} moles 35% H_2O_2, 40psi substrate (1.9×10^{-2} moles), 15 hours.

b: Percent conversion is based on the total of oxidized products divided by the initial amount of substrate.

Table 5-15: Oxidation Results for Propane @ Varying Temperatures with $Fe(dmp)Cl_2$ using H_2O_2

Temp. (°C)[a]	mmoles Alcohol (% Sel.)	mmoles Aldehyde (% Sel.)	mmoles Ketone (% Sel.)	Total mmoles Products	Percent Conversion[b]
25	0.17 (13.9)	0.70 (57.9)	0.34 (28.3)	1.21	5.72
50	0.98 (18.1)	2.07 (38.2)	2.37 (43.8)	5.43	27.85
75	0.79 (21.5)	1.68 (45.7)	1.21 (32.9)	3.68	20.5
100	2.15 (46.2)	1.57 (22.9)	1.44 (30.9)	4.66	27.6

a: 1.6×10^{-4} mole $Fe(dmp)Cl_2$, 60ml acetonitrile, 5.0×10^{-2} moles 35% H_2O_2, 40psi substrate (1.9×10^{-2} moles), 15 hours.

b: Percent conversion is based on the total of oxidized products divided by the initial amount of substrate.

Table 5-16: Oxidation Results for Propane @ Varying Temperatures with $Fe(dmp)Cl_2$ and $CuCl_2$ using H_2O_2

Temp. (°C)[a]	mmoles Alcohol (% Sel.)	mmoles Aldehyde (% Sel.)	mmoles Ketone (% Sel.)	Total mmoles Products	Percent Conversion[b]
25	0.59 (49.4)	0.29 (24.2)	0.32 (26.5)	1.20	5.70
50	1.97 (35.3)	1.66 (33.6)	1.29 (26.1)	4.94	25.4
75	1.45 (38.8)	1.12 (29.9)	1.17 (31.4)	3.74	20.9
100	3.38 (56.4)	1.63 (27.1)	0.99 (16.6)	6.00	35.6

a: 1.6×10^{-4} mole $Fe(dmp)Cl_2$, 1.6×10^{-4} mole $CuCl_2$, 60ml acetonitrile, 5.0×10^{-2} moles 35% H_2O_2, 40psi substrate (1.9×10^{-2} moles), 15 hours.

b: Percent conversion is based on the total of oxidized products divided by the initial amount of substrate.

proceeded at a temperature as low as 25°C (5.9% overall conversion) and as high as 100°C (29.5% overall conversion). Addition of one mole equivalent of $CuCl_2$ resulted in the anticipated increase in alcohol selectivity.

Experiments at each temperature using the [Fe(dmp)Cl_2] complex also followed a similar trend when compared to *cis*-[Fe(dmp)$_2$(H_2O)$_2$](CF_3SO_3)$_2$ complex. However, upon addition of $CuCl_2$ no increase in overall conversion was obtained, but an increase in selectivity to the alcohol was achieved.

Conclusions

The investigation of the iron derivatives: *cis*-[Fe(dmp)$_2$(H_2O)$_2$](CF_3SO_3)$_2$ (**II**) and [Fe(dmp)Cl_2] (**I**) for the activation of linear and branched alkanes has been performed. Oxidation of methane experiments conducted with the sterically hindered *cis*-[Fe(dmp)$_2$(H_2O)$_2$](CF_3SO_3)$_2$ (**II**) precursor and hydrogen peroxide exhibited the production of methyl acetate in an acetic acid/acetic anhydride solvent mixture in four hours at 75°C. Methyl acetate, produced from the hydrolysis of methanol and acetic acid, is generated as prevention to the over-oxidation of methanol. As a result, selectivity to the alcohol increases. To further demonstrate the activity of this complex, methane activation experiments were conducted with molecular oxygen. This resulted in the production of methyl acetate in reaction times as low as one hour at 100°C.

Functionalization of C_2-C_5 alkanes were also investigated using each complex and hydrogen peroxide in an acetonitrile at 75°C. In an effort to increase selectivity to the hydroxylated product, $CuCl_2$ (one mole equivalent) was added to the reaction mixture. This resulted in a selectivity increase to the alcohol without a significant decrease in the

catalytic activity of the precursor. Also exhibited was the associated decrease in selectivity to the aldehyde and ketone.

The effect of subsequent additions of $CuCl_2$ mole equivalents was also investigated, resulting in a further increase in alcohol selectivity, however catalyst activity and lifetime were decreased.

Temperature dependence studies performed demonstrated the ability of each catalyst precursor to activate propane at temperatures as low as 25°C with comparable selectivities to those obtained at 75°C.

CHAPTER 6
CONCLUSIONS

A series of homogeneous catalysts able to activate saturated hydrocarbons under mild and ambient conditions have been developed, synthesized, characterized and oxidation catalysis performed. The ability to design a such catalyst has been the subject of ongoing research throughout the industrial sector. This family of catalyst is offered as a substitute to processes, which operate under stringent conditions, as well as a catalyst able to utilize alternative feedstocks for the production of viable synthetic compounds.

The use of the *cis*-$[Ru(dmp)_2(H_2O)_2](CF_3SO_3)_2$ complex for methane activation, via a peracid assisted mechanism, provides a direct pathway to the production of methanol. The reaction conditions (75°C, four hours of reaction and a mild oxidant, H_2O_2) offers an attractive reaction from an industrial standpoint. Attempts to introduce aerobic conditions to this oxidation were also successful, allowing for a more detailed investigation. An additional novel feature of this oxidation system is the trapping of the methanol product as methyl acetate. The ester formed is resistant to further oxidation, thereby allowing for higher selectivities to be attained. Hydrolysis of the ester allows for recovery of methanol and regeneration of the trapping agent.

This ruthenium complex also functionalized linear and branched alkanes at 75°C using hydrogen peroxide. The peroxide allows for generation of the high valent ruthenium-oxo species, necessary for alkane functionalization. This reaction proceeds via

a free radical mechanism and offers the selective partial oxidation of each alkane investigated while maintaining a relatively high overall conversion. Further modification of alcohol selectivity can be obtained upon addition of $CuCl_2$.

Attempts to synthesize additional "analogues" based on the *cis*-$[Ru(dmp)_2(H_2O)_2](CF_3SO_3)_2$ architecture but with greater oxidizing potential were performed. As a result, the synthesis of two additional catalyst precursors *cis*-$[Fe(dmp)_2(H_2O)_2](CF_3SO_3)_2$ and $[Fe(dmp)Cl_2]$, was attained. These complexes were characterized by IR, NMR, and FAB and X-ray crystallography providing insight into this family of homogeneous catalysts.

Investigation into the catalytic activity for *cis*-$[Fe(dmp)_2(H_2O)_2](CF_3SO_3)_2$ complex for hydroxylation of methane with hydrogen peroxide and molecular oxygen at 75°C was also performed. The iron complex offers a higher catalytic activity when compared to the ruthenium analogue, yet initial mechanistic studies suggest it proceeds via a peracid mechanism identical to that of the ruthenium system.

The mono-dmp complex, $[Fe(dmp)Cl_2]$, and the sterically hindered *cis*-$[Fe(dmp)_2(H_2O)_2](CF_3SO_3)_2$ were both studied for their ability to activate the higher alkanes. Again, each offered a more robust activity when compared to the ruthenium analogue and their selectivities could be modified upon addition of $CuCl_2$. Preliminary mechanistic studies suggest oxygenates are formed via a free radical hydrogen abstraction mechanism.

GLOSSARY

AIBN	A radical chain initiator. Azo-bis-(*iso*-Butyrolnitrile).
BQ	A radical chain inhibitor. Benzoquinone.
Catalyst	A complex which allows for increase in rate for a chemical process.
Conversion	Amount of reaction consumed in a chemical process, usually expressed as a percentage.
Coordination	The addition of ancillary ligands which are directly bonded to the metal center.
DMP	2,9-dimethyl-1,10-phenanthroline, also known as neocouprine.
Heterolysis	Fragmentation of a neutral compound into an anion and cation species.
Homolysis	Fragmentation of a neutral compound into two identically electronically charge species.
Inhibitor	A compound which prevents the propagation of a radical or catalytic cycle.
Initiator	A compound which begins propigation of a radical or catalytic cycle.
Oxidation	Electron removal from a chemical species.
Selectivity	The relative rates of two or more simultaneous processes occurring on the same substrate. Usually expressed as a percentage.
Yield	The amount of a particular product formed divided by the amount of reactant provided. Usually expressed as a percentage.

REFERENCES

1. Shilov, A.E., "Historical Evolution of Homogeneous Alkane Activation Systems," in Activation and Functionalization of Alkanes; Hill, C., Ed., John Wiley and Sons, New York, **1989**, 2.

2. Shilov, A.E., Activation of Saturated Hydrocarbons by Transition Metal Complexes; Reidel Publishing Co., Dordrecht, **1984**.

3. Crabtree, R.H., *Chem. Rev.*, **1985**, *85*, 245.

4. Bergman, R.G., *Science*, **1984**, *223*, 902.

5. Goldstein, A.S., Ph.D. Dissertation, University of Florida, **1991**.

6. Lyons, J.E., "Transition Metal Complexes as Catalysts for the Addition of Oxygen to Reactive Organic Substrates," in Aspects of Homogeneous Catalysis, Volume 3; Ugo, R., Ed., Reidel Publishing Co., Dordrecht, **1977**, 10.

7. Shilov, A.E., Activation of Saturated Hydrocarbons by Transition Metal Complexes; Reidel Publishing Co., Dordrecht, **1984**, 15-20.

8. Shilov, A.E., Activation of Saturated Hydrocarbons by Transition Metal Complexes; Reidel Publishing Co., Dordrecht, **1984**, 163-182.

9. Shilov, A.E., "Historical Evolution of Homogeneous Alkane Activation Systems" in Activation and Functionalization of Alkanes; Hill.C., Ed., John Wiley and Sons, New York; **1989**, 3-11.

10. Heck, R.F., *Adv. Organomet. Chem.*, **1966**, *4*, 2431.

11. Orchin, M.; Ruplius, W., *Catal. Rev.*, **1972**, *6*, 85.

12. Orchin, M., *Acc. Chem, Res.*, **1981**, *14*, 25.

13. Pino, R.; Piacenti, F.; Bianchi, M., Organic Synthesis via Metal Carbonyls., Volume II; Wonder, I.; Pino. P., Eds.: John Wiley and Sons, New York; **1977**, 43-143.

14. Heck, R.F; Breslow, D.S., *J. Am. Chem. Soc.*, **1961**, *83*, 4023.

15. Roper, M.; Loevenich, H., Catalysis in C_1 Chemistry, Keim, W., Ed., Reidel Publishing Co.,: Dordrecht, **1983**, 105.

16. Chen, M.J.; Rathke, J.W., *Organometallics*, **1987**, *6*, 1833.

17. Wegman, R.W.; Busby, D.C.; Letts, J.B., Industrial Chemicals via C_1 Processes; Fahey, D.R., Ed., *ACS Symposium Series 328*; American Chemical Society, Washington, D.C., **1987**, 125.

18. Pretzer, W.R.; Kobylinski, T.P., *Ann. N.Y. Acad. Sci.*, **1980**, *33*, 58.

19. Keim, W., Industrial Chemistry via C_1 Processes; Fahey, D.R., Ed., *ACS Symposium Series 328*; American Chemical Society, Washington, D.C., **1987**, 1.

20. Fakley, M.E.; Head, R.A., *Appl. Catal.*, **1983**, *5*, 3.

21. Rizkalla, N.; Goloaszewski, A., Industrial Chemicals via C_1 Processes; Fahey, D.R., Ed., *ACS Symposium Series 328*; American Chemical Society, Washington, D.C., **1987**, 136.

22. Gauthier-Lafaye, J.; Perron, R. Methanol and Carbonylation; Editions Technip, Paris, **1987**, 136.

23. Sneeden, R.P.A, Comprehensive Organometallic Chemistry; Wilkinson, G.; Stone, F.G.A.; Able, E.W., Eds., Pergamon Press, Oxford, **1982**; Vol. *8*, Chapter 50.2.

24. Tkatchenko, I., Comprehensive Organometallic Chemistry; Wilkinson, G.; Stone, F.G.A.; Able, E.W., Eds., Pergamon Press, Oxford, **1982**; Vol. *8*, Chapter 50.3.

25. Dumas, H.; Levisalles, J.; Rudler, H., *J. Organomet. Chem.*, **1979**, *177*, 239.

26. Forster, D., *Adv. Organomet. Chem.*, **1979**, *17*, 255.

27. Adamson, G.W.; Daly, J.J.; Forster, D.J., *Organomet. Chem.*, **1974**, *71*, C17.

28. Adams, H.; Bailey, N.A.; Mann, B.E.; Manuel, C.P.; Spencer, C.M.; Kent, A.G., *J. Chem. Soc., Dalton Trans.*, **1988**, 489.

29. Drago, R.S., *Coordination Chem. Rev.*, **1992**, *117*, 185-213.

30. Mimoun, H., Homogeneous Metal-Oxo Complexes; Elsevier, New York, **1985**.

31. Drago, R.S.; Beer, R.H., *Inorganica Chimica Acta*, **1992**, *198-200*, 359-367.

32. Meyer, T.J, "Metal-Oxo Complexes and Oxygen Activation," in Oxygen Complexes and Oxygen Activation by Transition Metal Complexes; Martell, A.E.; Saywer, D.T., Eds., *Proceedings at the Fifth Annual IUCCP Symposium*; Plenum Press, New York, **1988**.

33. Leising, R.A.; Takenchi, K.J., *Inorg. Chem.*, **1987**, *26*, 3833.

34. Lau, T.C.; Che, C.M.; Lee, W.O; Poon, C.K, *J. Chem. Soc., Chem. Commun.*, **1988**, 1406.

35. Schirmann, J.P.; Delavarenne, S.Y., Hydrogen Peroxide in Organic Chemistry; Edition et Documentation Industrielle, Paris, **1979**.

36. Wilson, S., Peroxygen Technology in the Chemical Industry, Internal Publication Solvay Interox Ltd. R&D, New York, **1993**.

37. Einchem Anic Spa, European Patent, EPA 100, 119, **1984**.

38. Bailey, C.; Drago, R.S.; *J. Chem. Soc. Chem. Commun.*, **1987**, 179.

39. Goldstein, A.S.; Drago, R.S.; *J. Chem. Soc. Chem. Commun.*, **1991**, 21.

40. Goldstein, A.S.; Beer, R.H.; Drago, R.S., *J. Am. Chem. Soc.*, **1994**, *116*, 2424-2429.

41. Ahn, K.H.; Groves, J.T., *Inorg. Chem.*, **1987**, *26*, 3833.

42. Dobson, J.C.; Seok, W.K.; Meyer, T.J., *Inorg. Chem.*, **1986**, *25*, 1514.

43. Courthey, J.L.; Swanborough, K.F., *Rev. Pure Appl. Chem.*, **1972**, *47*, 22

44. Lee, D.G.; Van den Engh, M., *Org. Chem.*, **1973**, *58*, 177.

45. Dobson, J.C.; Meyer, T.J., *Inorg. Chem.*, **1988**, *27*, 3283.

46. Robbins, M.H.; Drago, R.S., *J. Chem. Soc., Dalton Trans.*, **1996**, 105-110

47. Parkyns, N.D., *Chem. Brit.*, September **1990**, 841-844.

48. Foulds, G.A.; Gray, B.F., *Fuel Proc. Tech.*, **1995**, *42*, 129-150.

49. Hamiliton, D.E.; Drago, R.S.; Zombeck, A., *J. Am. Chem. Soc.*, **1987**, *109*, 314.

50. Periana, R.A.; Taube, D.J.; Evitt, E.R.; Loffer, D.G.; Wentrch, P.R.; Voso, G.; Moesudai, T. *Science*, **1993**, *259*, 340.

51. Periana, R.A.; Taube, D.J.; Evitt, E.R. *U.S. Patent* **1994**, 5,306,855.

52. Gretz, E.; Oliver, T.F.; Sen, A. *J. Am. Chem. Soc.*, **1987**, *109*, 8109.

53. Kao, L.C.; Hutson, A.C.; Sen, A. *J. Am. Chem. Soc.*, **1991**, *113*, 700.

54. Varagaftik, M.N.; Stolaror, I.P.; Moiseec, I.I. *J. Chem. Soc. Chem. Commun*, **1990**, 1049.

55. Drago, R.S.; Mateus, A.L., *J. Org. Chem.*, **1996**, *61*, 5693-5696.

56. Schneider, H.J.; Muller, W., *J. Org. Chem.*, **1985**, *50*, 4609.

57. Murahashi, S.; Oda, Y.; Komiya, N.; Nasta, T. *Tetr. Lett.*, 35, (43), **1994**, 7953-7956.

58. Schneider, H.J.; Muller, W., *J. Org. Chem.*, **1985**, *50*, 4609.

59. Sheldon, R.A.; Kochi, J.K., Metal Catalyzed Oxidations of Organic Compounds; Academic Press, New York, **1981**.

60. Mimoun, H., Comprehensive Coordination Chemistry; Wilkinson, G. Gillard, R.D.; Mc Cleverty, J.A., Eds., Pergamon Press: Oxford, **1987**; Vol. 6.

61. Hartford, W.H.; Darrin, M., *Chem. Rev.*, **1958**, *58*, 1-61.

62. Stewart, R., Oxidation Mechanisms, Benjamin, New York, **1964**.

63. Rosenzwieg, A.C.; Frederick, C.A.; Lippard, S.J.; Nordlund, P., *Nature*, **1993**, *366*, 537-543.

64. Liu, K.E.; Johnson, C.C.; Newcomb, M.; Lippard, S.J., *J. Am. Chem., Soc.*, **1993**. *115*, 939-947.

65. Cook, G.K.; Meyer, J.M., *J. Am. Chem. Soc.*, **1995**, *117*, 7139-7156.

66. Haber, J., "Studies in Surface Sciences," In *Dioxygen Activation and Homogeneous Catalytic Oxidation*; Simadi, L.I., Ed, Elsevier, New York, **1991**; 66.

67. Roelofs, M.G.; Wasserman, E.; Jensen, J.K., *J. Am. Chem. Soc.*, **1987**, *109*, 4207-4217.

68. Comprehensive Organic Synthesis; Trost, B.M., Ed., Pergamon, New York, **1991** Vol. 7.

69. Cytochrome P-450: Structure, Mechanism and Biochemsity; Ortiz de Montellano, P.R., Ed., Plenum, New York, **1985**.

70. Barton, D.H.R.; Doller, D. *Acc. Chem. Res.*, **1992**, *25*, 504.

71. Barton, D.H.R.; Wang, T.L. *Tetrahedron*, **1994**, *50*, 1011.

72. Shu, L.; Nesheim, J.C.; Kauffmann, K.; Munck, E.; Lipscomb, J.D.; Que, L. *Science*, *275*, **1997**, 515-518.

73. Gonzalez, M.; Drago, R.S.; Gordon, B.W.F. Submitted to *J. Am. Chem. Soc.*, December, **1997**.

74. Beer, R.H., Drago, R.S. *Symposium on Natural Gas Upgrading II*, Co-Chairmen, Huff, G.A.; Scarpiello, D.A, Feb. **1992**, *37*, (1), 239.

75. Che, C.M.; Leung, W.H. *J. Chem. Soc. Chem. Commun.*, **1987**, 1376.

76. Che, C.M.; Tang, W.T.; Wong, W.T.; Lai, T.F. *J. Am. Chem. Soc.*, **1989**, *111*, 9048.

77. Che, C.M.; Yom, V.; Mak, T.C.W. *J. Am. Chem. Soc.*, **1990**, *112*, 2284.

78. Holm, R.H. *Chem. Rev.*, **1987**, *87*, 1401.

79. Griffith, W.P. *Transit. Met. Chem.*, **1990**, *15*, 251.

80. Imoff, V.; Drago, R.S. *Inorg. Chem.*, **1965**, *4*, (3), 6921.

81. Hague, J.P.; Sawyer, D.T. *J. Am. Chem. Soc.*, **1995**, *117*, 5617-5621.

82. Machii, K.; Watanabe, Y.; Morishima, I. *J. Am. Chem. Soc.*, **1995**, *117*, 6691-6697.

83. Leising, R.A.; Kin, J.; Perez, M.A.; Que, L. *J. Am. Chem. Soc.*, **1993**, *115*, 9524-9530.

84. Watanabe, Y.; Groves, J.T. The Enzymes, Sigman, D.S., Ed., Academic Press, San Diego, **1992**; Vol. 20, 405-452.

85. Groves, J.T.; Nemo, T.E.; Meyers, R.S. *J. Am. Chem. Soc.*, **1979**, *101*, 1032-1033.

86. LaMar, G.N.; Van Hecke, G.R. *Inorg. Chem.*, **1970**, *9*, 1547-1549.

87. Goldstein, A.S., Ph.D. Dissertation, University of Florida, **1991**, 63-64.

88. Goldstein, A.S., Ph.D. Dissertation, University of Florida, **1991**, 65-66.

89. Larpent, L. Briffand, T.; Patin, H. *Chem. Soc. Chem. Commun.*, **1990**, 1193.

90. Konig, E.; Watson, K. Chem. *Phys. Lett.*, **1990**, *6*, 457.

91. Ozarowski, A.; McGarvey, B.R.; Sarkar, H.B.; Drake, J.E. *Inorg. Chem.*, **1988**, *27*, 628.

92. Johansson, L.; Molund, M.; Oskarsson, A., *Inorg. Chim. Acta*, **1978**, *31*, 117.

93. Goodwin, H.A.; Kucharski, E.S.; White, A.H., *Aust. J. Chem.*, **1983**, *36*, 1115.

94. Vincent, J.B.; Huffman, J.C.; Christou, G.; Li, Q.; Nanny, M.A.; Hendrickson, D.N.; Fong, R.H.; Fish, R.H., *J. Am. Chem. Soc.*, **1988**, *110*, 6898-6900.

95. Menage, S.; Vincent, , J.-M.; Lambeaux, C.; Chottard, G.; Grand, A.; Fontecave, M., *Inorg. Chem.*, **1993**, *32*, 4766-4773.

96. Kojima, T.; Leising, R.A.; Zang, Y.' Que, L., *J. Am. Chem. Soc.*, **1991**, *113*, 8555-8557.

97. Kim, J.; Harrison, R.G.; Kim, C.; Que, L., *J. Am. Chem. Soc.*, **1996**, *118*, 4373-4379.

98. Kauffmann, K. E.; Bartos, M. J.; Kidwell, C.; Gordon-Wylie, S. W.; Collins, T.J; Clark, R.; Weintraub, S. T.; Münck, E., *J. Inorg. Biochem.*, **1995**, *59*, 317.

BIOGRAPHICAL SKETCH

Michael A. Gonzalez was born in El Paso, Texas, on November 17, 1969, to Wilfredo and Armida Gonzalez. He attended Andress High School in El Paso, Texas, and graduated in June 1987. While in high school, Michael was a member of the National Honor Society, treasurer of the Student Council, and two-time member of the varsity golf team. In the Fall of 1987 he began his college career at the University of Texas El Paso as a pre-medicine major. In his sophomore year, he was awarded a Research Careers for Minority Students (RCMS) academic scholarship, at which time he changed his major to chemistry. After three and one half years of undergraduate research, he graduated in 1992 under the direction of Dr. Leonard W. terHaar. An undergraduate honors thesis "Synthesis and Characterization of Inorganic Polymers" was the result of this research.

In the Fall of 1992 he began graduate school at the University of Florida to attain his doctorate in chemistry. His research focused on the development and application of homogeneous transition metal-oxo catalysts for the activation of alkanes under the direction of Dr. Russell S. Drago. Upon completion of his doctorate he will be employed with the United States Environmental Protection Agency in Cincinnati, Ohio.

I certify that I have read this study and that in my opinion it conforms to acceptable standards of scholarly presentation and is fully adequate, in scope and quality, as a dissertation for the degree of Doctor of Philosophy.

Russell S. Drago, Chair
Graduate Research Professor
of Chemistry

I certify that I have read this study and that in my opinion it conforms to acceptable standards of scholarly presentation and is fully adequate, in scope and quality, as a dissertation for the degree of Doctor of Philosophy.

Daniel R. Talham
Associate Professor of Chemistry

I certify that I have read this study and that in my opinion it conforms to acceptable standards of scholarly presentation and is fully adequate, in scope and quality, as a dissertation for the degree of Doctor of Philosophy.

Rick A. Yost
Professor of Chemistry

I certify that I have read this study and that in my opinion it conforms to acceptable standards of scholarly presentation and is fully adequate, in scope and quality, as a dissertation for the degree of Doctor of Philosophy.

Robert T. Kennedy
Associate Professor of Chemistry

I certify that I have read this study and that in my opinion it conforms to acceptable standards of scholarly presentation and is fully adequate, in scope and quality, as a dissertation for the degree of Doctor of Philosophy.

Michael D. Sacks
Professor of Material Science

This dissertation was submitted to the Graduate Faculty of the Department of Chemistry in the College of Liberal Arts and Sciences and to the Graduate School and was accepted as partial fulfillment of the requirements for the degree of Doctor of Philosophy.

May, 1998

_____

Dean, Graduate School